Journal

LIBRARY

APR 4 1961

FISH AND WILDLIFE SERVICE

JOURNAL

OF THE

TOKYO UNIVERSITY OF FISHERIES

VOL. 47, NO. 1.

CONTENTS

MIYOSHI, H.: The Tsunami caused by the Myojin volcanic explosions (II) 1- 40
KONDO, Y.: The tension test of the netting cord by impact force.. 41- 49
SEKINE, Y., KOZIMA, T. and MOTEGI, S.: Studies on the sterilization of *Clostridium botulinum* by gammaray irradiation 51- 57
HOSHINA, T., SANO, T. and SUNAYAMA, M.: Studies concerning the saprolegniasis of eel 59- 79
TANAKA, K. and NISHIMOTO, J.: Determination of the time required for freezing of whalemeat 81- 92
IWAMOTO, K.: On four species of monostroma in Tokyo bay 93-101
HONDA, K.: On the net and rope after bottom trawl fishings 103-121

THE TOKYO UNIVERSITY OF FISHERIES
SHIBA KAIGANDŌRI 6, MINATO-KU, TOKYO, JAPAN
September, 1960.

JOURNAL OF THE TOKYO UNIVERSITY OF FISHERIES

Editors for this Journal

Toyoki Ono, Professor, Dr.

Hiroshi Niino, Professor, Dr.

Itsuo Kubo, Professor, Dr.

Journal of the Tokyo University of Fisheries Vol. 47, No. 1, 1960

THE TSUNAMIS CAUSED BY THE MYOJIN VOLCANIC EXPLOSIONS (II)

Hisashi Miyoshi

(Received July 7, 1960)

Abstract: From 1952 to 1953, Myojin Sho (Reef) exploded many times. And the self registering wave recorder installed at Yaene on Hachijo Island caught the tsunamis caused by the explosions. We will investigate the several problems on Cauchy-Poisson waves in connection with the analyses of these tsunamis.

These tsunamis began at 30 minutes and stopped at 60 minutes after the large explosions, and then continued again. The existence of these momentary pauses (quiet points) in the wave records, the author et al inferred, comes from the prism effect of Aoga Shima and its island-shelf, which lie between Myojin Sho and the recorder. Concerning this inference, as the investigations about the Cauchy-Poisson waves propagating over the sea of finite depths are yet imperfect, we must only give the qualitative guesses.

Among the caught records, there are those which show the slow damping of waves and the prolonged oscillations of the sea surface, and there are those which show the quick damping and the disappearance of quiet points before the cease of tsunamis. We will think what is spoken by the differences in the rates of waves damping. Let us adopt, for this purpose, the two models whose physical properties seriously resemble each other, (whole energies equal and the distributions of the energies around the origins nearly equal each other,—these are the convenient expressions,) and examine whether one rate of wave damping can differ from another or cannot.

Then, we guess that the quiet points existing in the Cauchy-Poisson waves which started from rather unnatural origins indicated by Burnside et al, result from the mathematical expressions of the origins themselves, expand the shapes of the finite origins which can be expressed by even functions, and make sure to what the positions of the quiet points existing in the analysed Cauchy-Poisson waves correspond. And as the quiet points are frequently covered, we go a step farther into our investigations by adopting a typical model and by examining the degrees of covering effects.

These are, without exception, the theories treating the cases of infinite water depths. We must think about the waves caused by a wide impulse added over the shallow water—for example, the tsunamis caused by the nuclear bomb tests at Bikini. This solution can be integrated. We should solve it to understand the tsunamis from Myojin Sho, where the sea is very shallow around the origin and rather shallow along the course between the origin and the recorder.

We consider, at the biginning of this paper, the relation between the energy of the explosion and that of the tsunami. The most important factor is the efficiency of the tsunami coming inevitably from the elementary dynamics. Concerning this efficiency, we describe, in the appendix of this paper, the case

of the tsunami accompanying the earthquake.

§ 1. Introduction

From 1952 to 1953, the north-eastern part of the underwater caldera lying some 130 km to the south of Hachijo Island, frequently exploded. This reef is called Myojin Sho (Reef) after the name of the fishing boat which discovered its explosion. Corresponding to the large explosions (among many explosions), the beginnings of the tsunamis are found at 30 minutes after the explosions in the recording papers. These papers are rolled in the self registering wave recorder installed at Yaene on Hachijo Island (Fig. 1 and Fig. 4).

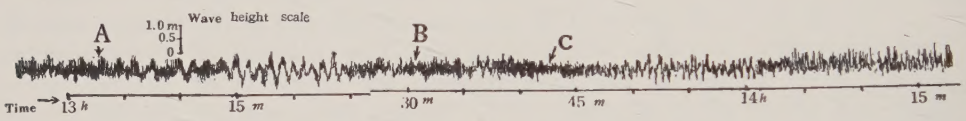

Fig. 1. Record of the tsunami of Sept. 26th, 1952.
A: Beginning of the tsunami (13^h03^m),
B: 1st quiet point, C: 2nd quiet point.

Examining these records, we find the next four facts. (1) The wave height of the highest one is about 1 metre. (2) The wave period at their beginnings is about 95 seconds. (3) After the vertical oscillation of the sea level of some 30 minutes, the 1st quiet points appear (B in Fig. 1). (4) After 40 minutes, the 2nd points appear (C in Fig. 1). There are the data the second quiet points of which are obscure.

The duration of the motion of sea level after the 2nd quiet point is pretty long on Sept. 26th. And the wave periods grow shorter and shorter, until they become about 30 seconds. This manner in which the wave periods decrease is particular to the Cauchy-Poisson wave.

No disturbance occurs in the forms of these caught waves in spite of the convenient shape of the small bay including Yaene to generate the secondary oscillations. This fact seems to demand a reconsideration from the conclusion that the process linking the actual tsunami observed at the bay including several waves to the theory of generation of the tsunami explaining that only one trough follows after one antecedent mountain may be due to this secondary oscillation.

These tsunamis caught at Yaene are guessed to indicate something concerning the circumstances of the explosions. Without exception, there exists a quiet point in every datum showing the waves which does not cease till one hour after the explosion. This fact has supported the idea according to which the horizontal dimensions of the explosions are always 4 km. We doubted this supposition for the next two reasons.

(A) Regardless of the wave height, there exists, without exception, the quiet point one hour after the explosion. This fact compels us to think that the horizontal dimension of a large explosion equals to that of a small one. This is unimaginable. Among the group of the large tsunamis, the largest one

has energy of 3 times as those of the others. As the horizontal dimension can be supposed to be proportional to the fourth root of the tsunami's energy, and as

$$\sqrt[4]{3} \fallingdotseq 1.3 , \qquad (1)$$

this largest tsunami might, roughly speaking, have 30 percent extra horizontal dimension. We must neglect this estimation to adopt the above-mentioned supposition.

(B) Then, the quiet point existing in the tsunami started from one origin corresponds to the trifling character of the mathematical expression of the origin (see § 5), and disappears when we replace the origin with a smooth form becoming to a natural phenomenon.

The appearance of this quiet point seems to indicate, as the present auther et al inferred, that the tsunami came to Yaene along several courses, and that the differences of the distances along these courses were constant. We will study in § 5 about the "general characters of the Cauchy-Poisson waves started from the origins of finite horizontal dimension", which have seldom been investigated.

We will, pervious to that, describe the relation between the energy of the explosion and that of the tsunami.

§ 2. The energy of the explosion and that of the tsunami

We can say statistically that the large energy of the tsunami corresponds to the large energy of the explosion, and must recognize that there is an efficiency, which comes from the elementary dynamics and will be described in Appendix I of this paper. This efficiency links the energy of the tsunami caused by a bottom origin to the energy exchanged between the earth crust and the sea water. The absolute value of this ratio usually proves to be much smaller than 1.

Then we may guess that the tsunami whose damping is rapid might be caused by a wide origin, and that the tsunami whose damping is slow might start from a narrow origin, when the energies of these two tsunamis are exactly alike.

But on the other hand, we should know that the two tsunamis started from the two origins the physical characters of which are nearly equal, differ in their manners of the dampings (see § 4).

Let us return to the subject. Which parts of the mechanical energies of the explosion do change into the apparent energy of the tsunami? In order to answer this question, we must think about the next processes.

(1) Corresponding to the volcanic ejecta and gases at the sea bottom, the elevation of the sea surface appears and causes the tsunami.

(2) These ejecta and gases are thrown up into the high sky, and the sea water pours into the room which has been occupied by them. Then a depression of the sea surface occurs and this depression sends the tsunami falling behind that shown as (1).

(3) When the masses are thrown up from the sea surface, they give the

negative impulses to the surface.

(4) These masses fall to the sea surface and give the positive impulses to water.

The tsunami caused by (3) is of the negligible order comparing to that caused by (4). Because, it is sea water that stops the falling masses, and it is the earth crust (not sea water) that discharges these masses. It is the earth itself that receives the reactions. Then, whether the tsunami caused by (4) is larger than those caused by (1) and (2) or it is smaller will be the matter.

For the purpose to examine this, we should compare the potential energy (assuming it to be zero at the sea surface) of the approximate semi-sphere including all the plumes flied about in different directions, to the potential energy of the hill made by water and the rocks when these plumes were piled on the sea surface. While a considerable part of the former changes into (4), all of the latter means (1) and (2). The former may be larger than the latter beyond comparison. So we may suppose (4) is larger than (1) and (2) as the source of the tsunami. We have only to do the next experiment, in order to conclude that (1) and (2) are negligible comparing to (4).

That is, how much percent of the potential energies of the water masses or the rocks having various densities changes into the energies of the gravity waves (Cauchy-Poisson waves), when they are dropped from the various height above the water surface. The considerable part of the energy, in the same way as in the case of the collision of two semi-elastic bodies, disappears changing into heat or sound. Some part survives as the kinetic energy by which the falling body continues its descent through water. In this paper, we assume that this percentage may not be so small and think (4) is the main source of the tsunami. The mathematical treatment is, therefore, progressed under the assumption that only once the main Cauchy-Poisson wave was radiated from the origin.

Besides these four sources, it is supposed that the explosional waves in water may cause the tsunami. The compressional waves are, however, independent of the gravity waves and do not change into the gravity waves directly, as were indicated in the "generation of the tsunami in compressible water" by the present author or in the results obtained by Pidduck (1912). So, the compressional waves act independently and are absorbed into the crust. (At the water-rock boundary, the absorptive ratio is considerably large.) And a volcanologist inferred, when the explosional waves in water reflect at the sea surface, they rise the water domes which were witnessed from the survey ship. The present author rather thinks the domes might result from the ascending large gas bubble. Because the two talks by the observers who were near the exploding centres, were repeated that the explosions near the Bayonnaise Islands did not accompany the intense compressional waves in water. Generations of the domes or the plumes may, therefore, result from (1) or the initial velocities of the gases and the ejecta. And we need not adopt the domes or the plumes caused by the compressional waves, as the sources of the tsunami.

There are the various intermediate factors between the energy of the explosion and that of the tsunami, which should be investigated one by one.

And the next process of thinking is needed to estimate the whole energy of the tsunami from the energy caught on Hachijo Island.

That is, as will be mentioned in the next paragraph, the tsunami started from Myojin Reef goes along three courses, owing to the existences of Aoga Shima and the shallows around it. These three courses are, (1) along the straight line connecting Myojin Reef and Hachijo Island, (2) along the curve on the right side of Aoga Shima, and (3) along the curve on the left side of Aoga Shima. Consequenty, the energy of almost three times as the other area converges on Hachijo Island. So, we can replace the real bottom topography with a simple mathematical model, can take the effects of the refraction and the diffraction in the estimation, and can calculate the whole energy of the tsunami making a reverse use of the energy caught on Hachijo Island. This calculated whole energy only expresses the energy of the tsunami assumed to have no directivity and be radiated from Myojin Reef uniformly in all directions.

Concerning this problem, as the volcanic activities near the Bayonnaise Islands are considerably frequent, it is desirable to install a self registering wave recorder on Aoga Shima. If it were installed, the above-mentioned mathematical study would be saved and the accuracy would be respected. And the management of the self registering recorder can be prosecuted by the primary school. The data of the tsunami on the isolated island do not receive the effects of the secondary oscillations which develop on the island shelf or in the bay. So, these data are thought to be the raw records of the tsunamis, and are very valuable for investigating the tsunami caused by the earthquake. We advocate its establishment eagerly.

§ 3. Differences of the course distances and the positions of the quiet points

The opinion was published according to which the existence and the position of the quiet point is controlled by the following factor. That is, the origin had a horizontal dimension, so we assume the initial condition of the origin as follows,

$$\left.\begin{array}{ll} y_0=0 & |x|>b \\ y_0=C' & |x|<b \end{array}\right\}. \qquad (2)$$

Here, x-and y-axises are adopted horizontally and upwards (Fig. 2), $x=y=0$ at the sea surface of the origin. Then the Cauchy-Poisson wave started from this origin is, through the application of the stationary phase method, given as follows;

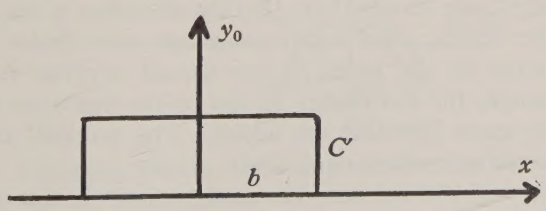

Fig. 2. One model of the explosion.

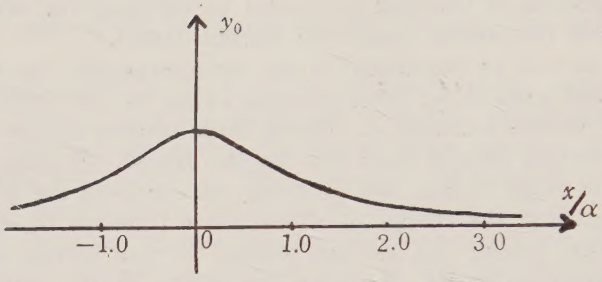

Fig. 3. Another model of the explosion.

$$y=\frac{4C'}{\sqrt{\pi}}\left(\frac{x}{gt^2}\right)^{1/2}\sin\left(\frac{gt^2b}{4x^2}\right)\sin\left(\frac{gt^2}{4x}+\frac{\pi}{4}\right). \qquad (3)$$

Here, g and t are the acceleration of gravity and the time, respectively. We inferred in § 2 that the main source of the tsunami might be the impulse added at the origin. Now, we will adopt, as the representative Cauchy-Poisson wave, the tsunami caused by the elevation of the sea surface at the origin, when we discuss about the problems the conclusions of which have no bearings on whether the origin may be the impulse or the origin may be the elevation. (The rewritings are easy.)

In the right side of (3), $\sin\left(\frac{gt^2}{4x}+\frac{\pi}{4}\right)$ and $\sin\left(\frac{gt^2b}{4x^2}\right)$ represent rapid oscillations the periods of which decrease from some 95 seconds to some 30 seconds, and the slow change of the amplitude, respectively. The positions of the quiet points are naturally obtained by studying of the latter.

Under these assumptions, the position of the quiet point is given as follows;

$$\sin\left(\frac{gt^2b}{4x^2}\right)=0, \text{ so } \frac{gt^2b}{4x^2}=\pi. \qquad (4)$$

Here, x means the distance between Myojin Reef and Hachijo Island, and is some 130 km. t expresses the time from the explosion to the appearance of the lst quiet point, and is about 60 minutes. So, the horizontal dimension of the explosion is given by

$$2b\fallingdotseq 3.2 \text{ km}. \qquad (5)$$

As we mentioned in the introduction, this assumption includes two unreasonablenesses to the one of which we called the attention in (B). Let us explain this in detail. When we assume an elevation of the surface as the source of the tsunami, we should think that the elevation is the most remarkable at the centre of the origin. And when we adopt an impulse added upon the surface as the source of the tsunami, we should suppose the impulse is the intensest at the centre, for the nearer to the centre one approaches, the more masses fall and the more impulses are added. The proposal of the initial condition of (2) is, therefore, rather unnatural.

Then, for example, if we take the next natural initial condition instead of (2),

$$y_0=\frac{C\alpha^2}{\alpha^2+x^2}\,, \tag{6}$$

the Cauchy-Poisson wave started from it is given as follows;

$$y=\sqrt{\pi}\,\frac{C\alpha}{x}\left(\frac{gt^2}{4x}\right)^{1/2}e^{-gt^2\alpha/4x^2}\cdot\sin\left(\frac{gt^2}{4x}+\frac{\pi}{4}\right). \tag{7}$$

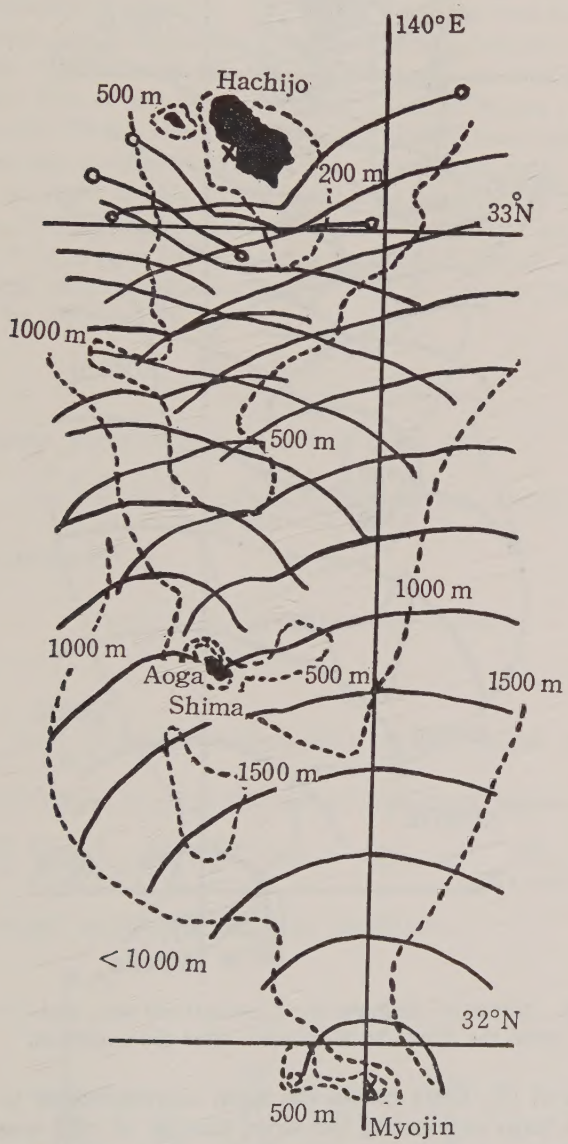

Fig. 4. Refraction diagram for long wave, showing the bottom topography and wave fronts of every two minutes. ○——○ mean the three fronts at 24 minutes after the explosion.

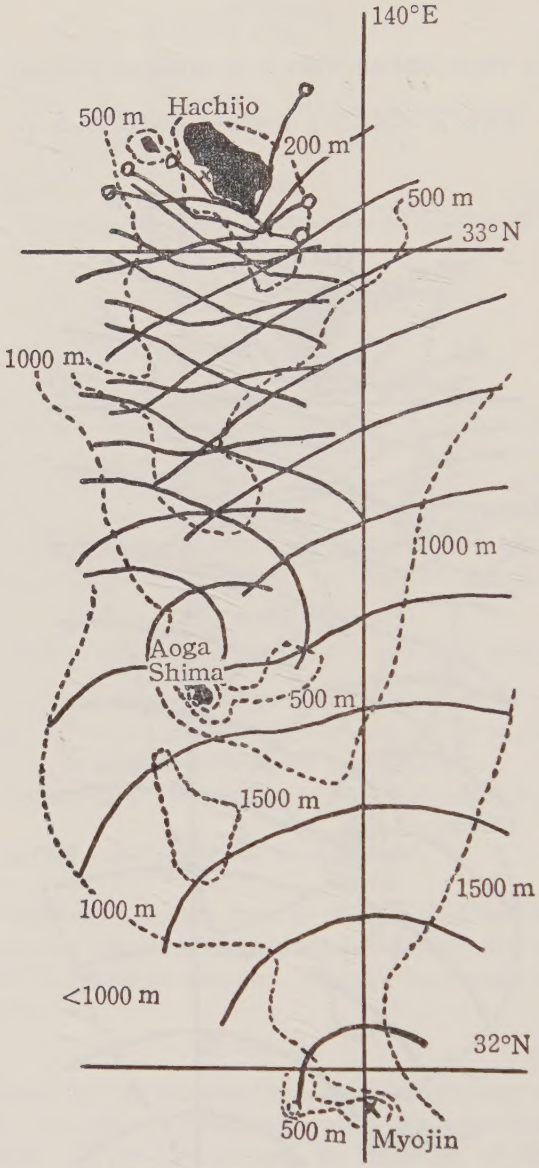

Fig. 5. Refraction diagram for T(period)=60 sec., and ○——○ mean the fronts at 26 minutes after the explosion.

In the right side of (7), there exists the term corresponding to the rapid oscillations. But the term expressing the slow change of the amplitude does not show the reality of the quiet point. This is a trouble. Then, from what does the existence of the quiet point come? Our speculation is to answer this question.

Let us see the bottom topography around the line connecting Myojin Reef

and Hachijo Island. There are Aoga Shima and the prolonged shallows around it in the middle of the line. These shallows usually act a prism-like action on the wave rays.

As the periods of the observed waves range from 95 seconds to 30 seconds, we show the refraction diagrams for long wave and for the wave the period of which is 60 seconds (Fig. 4 and Fig. 5). These figures point the above-mentioned circumstances clearly. That is, all the three rays one of which makes a straight advance along the course Myojin→Hachijo, one of which goes along the curve on the right side of the shallows, and one of which goes along the curve on the left side of the shallows, reach Hachijo Island.

The distances of the three curves along which these three rays go Myojin →Hachijo, differ one another. And all the three rays enter into the bay of Hachijo falling at right angles to the coast. So, on Hachijo Island, the waves are observed as if the tsunamis started from two or three origins had come.

After all it is a question of solving the Cauchy-Poisson wave started from the several natural origins mathematically. Let us assume that the initial condition is given by (8) (Fig. 6).

$$y_0=\sum^{N}\frac{C_n\alpha_n^2}{\alpha_n^2+(x-a_n)^2}=f(x)\,. \tag{8}$$

The Cauchy-Poisson wave started from it is given by

$$y=\frac{1}{\pi}\int_0^{\infty}dm\int_{-\infty}^{\infty}d\lambda\cdot\cos\sqrt{mg}\,t\cdot\cos m(x-\lambda)f(\lambda)\,. \tag{9}$$

And as (8) is represented by

$$y_0=\int_0^{\infty}\sum^{N}\alpha_nC_ne^{-\alpha_nm}\cos m(x-a_n)dm\,, \tag{10}$$

(9) becomes

$$y=\int_0^{\infty}\sum^{N}\alpha_nC_ne^{-\alpha_nm}\cos\sqrt{mg}\,t\cdot\cos m(x-a_n)dm\,. \tag{11}$$

When t and x are large, through the use of stationary phase method, we get

$$y=\sqrt{\pi}\sum^{N}\frac{C_n\alpha_n}{x-a_n}\left\{\frac{gt^2}{4(x-a_n)}\right\}^{1/2}e^{-gt^2\alpha_n/4(x-a_n)^2}\times\sin\left\{\frac{gt^2}{4(x-a_n)}+\frac{\pi}{4}\right\}. \tag{12}$$

Neglecting the small modifications on the amplitude,

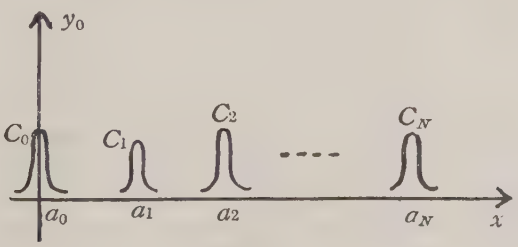

Fig. 6.

$$y=\sqrt{\pi}\sum^{N}\frac{C_n\alpha_n}{x}\left(\frac{gt^2}{4x}\right)^{1/2}e^{-gt^2\alpha_n/4x^2}\cdot\sin\left\{\frac{gt^2}{4(x-a_n)}+\frac{\pi}{4}\right\}. \tag{13}$$

Now, as the substances of the several origins are same, we may put

$$\alpha_0=\alpha_1=\cdots=\alpha_N=\alpha$$

Then (13) becomes

$$\begin{aligned}y&=\sqrt{\pi}\,\frac{\alpha}{x}\left(\frac{gt^2}{4x}\right)^{1/2}e^{-gt^2\alpha/4x^2}\left\{\sin\left(\frac{gt^2}{4x}+\frac{\pi}{4}\right)\sum^{N}C_n\cos\frac{gt^2a_n}{4x^2}\right.\\&\qquad\left.+\cos\left(\frac{gt^2}{4x}+\frac{\pi}{4}\right)\sum^{N}C_n\sin\frac{gt^2a_n}{4x^2}\right\}\\&=\sqrt{\pi}\,\frac{\alpha}{x}\left(\frac{gt^2}{4x}\right)^{1/2}e^{-gt^2\alpha/4x^2}\cdot\sqrt{\left(\sum^{N}C_n\cos\frac{gt^2a_n}{4x^2}\right)^2+\left(\sum^{N}C_n\sin\frac{gt^2a_n}{4x^2}\right)^2}\\&\qquad\times\sin\left\{\frac{gt^2}{4x}+\frac{\pi}{4}+\tan^{-1}\frac{\sum C_n\sin\dfrac{gt^2a_n}{4x^2}}{\sum C_n\cos\dfrac{gt^2a_n}{4x^2}}\right\}.\end{aligned} \tag{14}$$

Glancing the refraction diagrams, we find that the three rays reach Hachijo Island, that the one turning to the left is the first to reach, and that the ones making the straight advance and turning to the right reach Hachijo nearly at the same time. And as the energy of the middle ray diverges, we can think once that the two rays enter into the bay.

Let us put $N=2$, $C_0=C_1=C$, $a_0=0$, $a_1=a$ in (14), and we get

$$\begin{aligned}y&=\sqrt{2\pi}\,\frac{C\alpha}{x}\left(\frac{gt^2}{4x}\right)^{1/2}e^{-gt^2\alpha/4x^2}\sqrt{\left(1+\cos\frac{gt^2a}{4x^2}\right)}\cdot\sin\left(\frac{gt^2}{4x}+\frac{\pi}{4}+\beta\right)\\&=2\sqrt{\pi}\,\frac{C\alpha}{4x}\left(\frac{gt^2}{4x}\right)^{1/2}e^{-gt^2\alpha/4x^2}\cos\frac{gt^2a}{8x^2}\cdot\sin\left(\frac{gt^2}{4x}+\frac{\pi}{4}+\beta\right).\end{aligned} \tag{15}$$

In this operation, we assume that $\alpha\ll a$. But in the actual case of Myojin Reef, α and a may be of the comparable order and the two origins may overlap each other. We may think that the character of the wave is expressed well by (15), under such circumstances.

Looking at (15), we find the same character of Cauchy-Poisson wave, that is, the amplitude changes smoothly including the quiet points, as that started from the initial condition of (2). The term which expresses it is, of course, $\cos\frac{gt^2a}{8x^2}$. The position of the quiet point corresponds to the time given by $\frac{gt^2a}{8x^2}=\frac{\pi}{2}$. Putting $x=130$ km and $t=60$ min., we can get, by a rough estimate, $a=1.6$ km.

Let us, here, study the meaning of the differences of the course distances. For example, the leftmost course is the longest, but the wave along it reaches Hachijo first. Because the mean velocity of the gravity wave along this course is the largest as the sea is the deepest here. So the excess of the distance is compensated. We had better, therefore, remark the differences of the elapsed times

than those of the distances from the origin to the wave recorder. And further, the essences of these factors may become the considerably symbolic ones being modified by the following effect; that is, the differences of the courses may control the forms of the waves along these courses.

In this symbolic meaning, however, the guess that the existences of the quiet points at 60 minutes after the explosions (30 minutes after the beginnings of the tsunamis) indicate that *the difference of the course distances always is* 1.6 *km*, is more convincing than the doctrine that the horizontal dimension of the explosion always is 3.2 km.

And as the actual refraction diagrams show, a little, the character of $N=3$, besides that of $N=2$, let us here analyse the case of $N=3$. If we put $N=3$, $C_0=C_1=C_2=C$, $a_0=0$, $a_1=a$ and $a_2=-a$, (14) becomes

$$y=\sqrt{\pi}\,\frac{C\alpha}{x}\left(\frac{gt^2}{4x}\right)^{1/2}e^{-gt^2\alpha/4x^2}\left(1+2\cos\frac{gt^2a}{4x^2}\right)\sin\left(\frac{gt^2}{4x}+\frac{\pi}{4}\right). \tag{16}$$

This means that the curve including the amplitudes of the rapid oscillations shows the large range and the small range with the time alternately. The second quiet point found (at 10 minutes after the 1st quiet point) in the record on Sept. 26th, 1952 may result from this circumstance.

So far we have studied about the one-dimensional wave propagation. And as the actual waves propagate two-dimensionally, we should here investigate the model of the two-dimensional propagation. Let us take the y-axis upwards, express the horizontal distance from the centre of the origin as r, and assume the initial condition as follows;

$$y_0=f(r)=\frac{C\beta^2}{\beta^2+r^2}. \tag{17}$$

Then the Cauchy-Poisson wave started from this origin is given by

$$y=\int_0^\infty \cos\sqrt{mg}\,t\,J_0(mr)m\,dm\int_0^\infty f(\alpha)J_0(m\alpha)\alpha\,d\alpha$$

From the special formula shown as (5) in p. 425 (Watson), this becomes

$$y=\int_0^\infty \cos\sqrt{mg}\,t\,J_0(mr)mC\beta^2K_0(\beta m)dm. \tag{18}$$

Expanding J_0 in the asymptotic form and using the stationary phase method, we obtain,

$$y=\frac{C\beta^2gt^2}{2\sqrt{2}\,r^3}K_0\left(\frac{gt^2\beta}{4r^2}\right)\cos\frac{gt^2}{4r}. \tag{19}$$

As K_0 is a monotone decreasing positive function, there is not a quiet point in the two-dimensional Cauchy-Poisson wave started from the initial condition of (17). If we superpose the two origins the individual of which is expressed by (17) as in Fig. 7, the resulting Cauchy-Poisson wave is given from the non-oscillatory character of K_0 as follows;

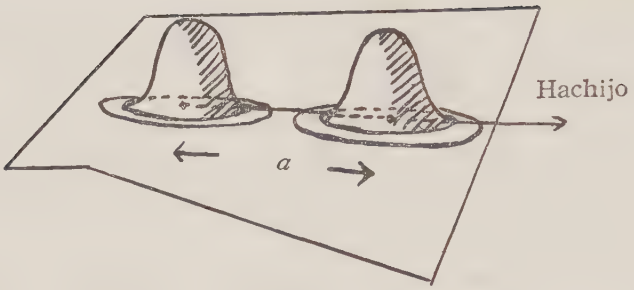

Fig. 7. The model of the two-dimensional wave propagation.

$$y=\frac{C\beta^2 gt^2}{2\sqrt{2}\,r^3}K_0\left(\frac{gt^2\beta}{4r^2}\right)\left\{\cos\frac{gt^2}{4r}+\cos\frac{gt^2}{4(r-a)}\right\}$$
$$=\frac{C\beta^2 gt^2}{\sqrt{2}\,r^3}K_0\left(\frac{gt^2\beta}{4r^2}\right)\cos\frac{gt^2a}{8r^2}\cos\left\{\frac{gt^2}{4r}+\frac{gt^2a}{8r^2}\right\}. \qquad (20)$$

The manner of the amplitude change (position of the quiet point) in (20) is the same one as that of (15). So we might adopt a in the one-dimensional case, as the difference of the course distances.

So far we have assumed the elevation at the origin to be the initial condition. We can get the same theory when the impulse is added at the origin. To prove this theory, the establishment of the wave recording equipment on Aoga Shima is desired eagerly.

Then we should remark that the above-mentioned theory is that of the Cauchy-Poisson wave propagating over the infinitely deep sea. The bottom between Hachijo Island and Myojin Reef is a part of the large ridge where the sea is shallower than 1000 m. This depth exerts naturally an influence upon the wave, the period of which is some one minute. (So the refraction diagrams came into question.) The theory about the Cauchy-Poisson wave propagating over the finite depth water has been, however, very poor.

Generally speaking, no antecedent disturbance appears before the front advancing with the velocity of $\sqrt{gh}$ (g=acceleration of gravity, h=depth of water). This was proved in the paper "Generation of the tsunami in compressible water" by the present author. According to it, after the sufficient elapsed time from the generation of the tsunami, a surface disturbance appears inside the front advancing with the velocity of 1.5 km/sec. (sound velocity in the sea) having nothing to do with the gravity wave. And this disturbance is included in a spheroid made by the rotation of an ellipse round the vertical line at the centre of the origin. The larger the sound velocity becomes, the thinner becomes the spheroid. This spheroid disappears when the sound velocity is infinite. In other words, before the front of the gravity wave of the common tsunami or the Cauchy-Poisson wave advancing with the velocity of $\sqrt{gh}$, no disturbance appears when the liquid is incompressible.*

* When Rayleigh (1909) solved the problem of the Cauchy-Poisson wave propagating

This is proved well in the record caught on Hachijo Island. If the tsunami were the Cauchy-Poisson wave over the infinitely deep water, it would begin as soon as the explosion would happen. But there is a time lag of some 30 minutes between them. This quantity of 30 minutes has been proved in the refraction diagram (Fig. 4). This discrepancy from the theory of infinite depth, is important in the speculation upon the damping of the tsunami (§ 4), and also has an important meaning for another reason. So we should pick it up in this paragraph. If the arrival of the front at Hachijo Island is 30 minutes behind time, isn't the arrival of the quiet point behind time?

The longer the wave length grows, the more remarkable becomes the effect of the finite depth on the gravity wave. So, this effect may be remarkable on the waves near the front, and may not be so marked on those near the quiet point. If the front is 30 minutes behind time, the quiet point may be, therefore, some 15 minutes behind time. This is only a rough estimate.

If we adopted this value of 15 minutes, the quiet point (at 60 minutes after the explosion) would appear at 45 minutes after the explosion in the case of infinite depth. Adopting this value of 45 minutes, we should rewrite $2b$ and a in (3), (15) and (20) as follows;

$$\begin{aligned} 2b&=5.7\ \text{km} \\ a&=2.8\ \text{km}\ . \end{aligned} \tag{21}$$

Once we assumed this delay to be 15 minutes. We want to find the formula showing this delay clearly. But this analysis cannot be succeeded. As the analysis of the Cauchy-Poisson wave is very difficult, we assume the depth (h) is sufficiently large, and the delay of the front is

$$\Delta t' = \frac{x}{\sqrt{gh}}\ . \tag{22}$$

Now the discrepancy of the Cauchy-Poisson wave from that of infinite depth, is

$$\begin{aligned} y_h - y_\infty &= C\alpha \int_0^\infty e^{-\alpha m}(\cos\sqrt{mg\tanh mh}\ t - \cos\sqrt{mg}\ t)\{\cos mx + \cos m(x-a)\}dm \\ &\fallingdotseq 2C\alpha \int_0^\infty e^{-\alpha m}(\cos\sqrt{mg\tanh mh}\ t - \cos\sqrt{mg}\ t)dm\ . \end{aligned} \tag{23}$$

As $\frac{gt^2a}{8x^2} = \frac{\pi}{2}$ near the quiet point, we obtain (putting $mh = X$)

---

over the finite depth water, he got the solution according to which an antecedent disturbance appears before the front of $\sqrt{gh}$. Then, Rayleigh thought "as regards the general question, I do not think that the instantaneous propagation of disturbance should be considered paradoxical. It is to be remembered that in (9) (: $\sigma^2 = gk\tanh kh$) the water is treated as incompressible, i.e. that the velocity of propagation of waves of *expansion* is regarded as infinite." He entitled this paper as "On the Instantaneous Propagation ···". It was his error resulting from the overlook of the imperfection of the Cauchy-Poisson wave analysis. There is, by the way, a theory (1942) that no disturbance appears before the front of $\sqrt{gh}$, when a cylindrical bottom is elevated and the tsunami is generated. This is an accurate mathematical treatise.

$$y_h - y_\infty = \frac{2C\alpha}{h}\int_0^\infty \left(\cos 2x\sqrt{\frac{\pi}{ah}X\tanh X} - \cos 2x\sqrt{\frac{\pi}{ah}X}\right)dX$$
$$= \frac{4C\alpha x^2}{ah^2}\pi\int_0^\infty X(1-\tanh X)dX = \frac{4C\alpha x^2}{ah^2}\pi\cdot A^* . \tag{24}$$

If we assume the delay of the quiet point to be Δt and put $\frac{gt_q^2 a}{8x^2} = \frac{\pi}{2}$,

$$y_\infty(t_q+\Delta t)$$
$$= 2\sqrt{\pi}\,\frac{C\alpha}{x}\left(\frac{\pi x}{a}\right)^{1/2} e^{-\alpha\pi/a}\cdot\cos\left(\frac{\pi}{2}+\frac{2gt_q\Delta t\cdot a}{8x^2}\right)\sin\left(\frac{\pi x}{a}+\frac{\pi}{4}+\frac{\pi}{2}\right)$$
$$= -2\pi^2\frac{C\alpha}{t_n}\frac{1}{\sqrt{ax}}e^{-\alpha\pi/a}\cdot\cos\left(\frac{\pi x}{a}+\frac{\pi}{4}\right)\cdot\Delta t . \tag{25}$$

To satisfy the relation $y_h(t_q+\Delta t)=0$,

$$\frac{4C\alpha x^2}{ah^2}\pi A = 2\pi^2\frac{C\alpha}{t_q}\frac{1}{\sqrt{ax}}e^{-\alpha\pi/a}\cdot\cos\left(\frac{\pi x}{a}+\frac{\pi}{4}\right)\cdot\Delta t$$
$$\therefore\quad \Delta t = \frac{4Ae^{\alpha\pi/a}g^{3/2}}{a\sqrt{\pi x}}\sec\left(\frac{\pi x}{a}+\frac{\pi}{4}\right)\cdot(\Delta t')^4 . \tag{26}$$

This value becomes positive or negative. It is, therefore, a judging by common sense lacking the mathematical proof that the delay of the quiet point may be half the delay of front (30 minutes), when the depth is not so large.

§ 4. Damping of the wave

Examining the records caught by the recorder, we remark the manners of the waves dampings next to the existences of the quiet points. In the record, the wave damping of which is rapid, the tsunami is covered by the swell before the existence of the quiet point (60 minutes after the explosion). The record of the tsunami which began at 00^h42^m on Mar. 20th, 1953, for example, shows this character well. (See Appendix II.)

What do these manners of dampings tell us? Before we answer this question, we should here describe one fact. For example, the two Cauchy-Poisson waves, one of which is started from a uniform impulse (at $|x|<a/2$) and the other of which results from a uniform elevation (at $|x|<a2$), damp in the different manners. In spite of this fact, we treated the Cauchy-Poisson wave under the initial conditions of elevations in this paper. For the next two reasons, it is overhasty to think that the actual wave damping indicates something. Before it, we have questions to solve. Then, the two reasons are (*A*) and (*B*).

(*A*) If the water depth were infinite, the waves would appear on Hachijo Island from the time of explosion ($t=0$) to the time $t=x/\sqrt{gh}\fallingdotseq 30$ min. Where did this energy go? The Cauchy-Poisson wave over a finite depth water is not yet sufficiently solved. So we think by the common sense. In the finite depth

* A is a constant given by $A=\int_0^\infty X(1-\tanh X)dX=0.411$.

case, the energy which should have appeared at t, will appear at $t+\Delta t$. As the gravity wave have not the velocity larger than $\sqrt{gh}$, the energy which should have appeared at $t=0$ in the infinite depth case, will appear at $t=0+x/\sqrt{gh}$. In this case, $\Delta t=x/\sqrt{gh}$. The shorter the wave period becomes, the less remarkable becomes the effect of the water depth upon the wave, and Δt approaches 0.

So, the accumulation of the energy which should have come earlier is remarkable on the left part of the wave record. This fact accelerates the wave damping, and becomes the first barrier to study the exploding centre through the wave record.

(*B*) The second reason arises from the Cauchy-Poisson wave theory of the infinite depth itself. If we prove that the two dampings of the Cauchy-Poisson waves started from the two initial elevations the physical characters of which are nearly equal each other, differ because of the difference of the mathematical expressions of these two elevations, it is very helpless to guess the physical character of the exploding centre through the damping of the caught record of wave. Then we prove this fact about the two examples of the initial elevations.

Let us define the two elevations (I, II) which satisfy the following three conditions, to be alike each other.

1) The whole potential energies of the initial elevations of I and II are equal each other.

2) In the region of $|x|<a/2$, the greater parts of the potential energies* of the twe models are included. And the ratios of these energies to the common whole energy of I and II are nearly equal each other.

3) In the region of $|x|<a$, nearly all the parts of the potential energies* of the two models are included. And the ratios of these energies to the common whole energy of I and II are nearly equal each other.

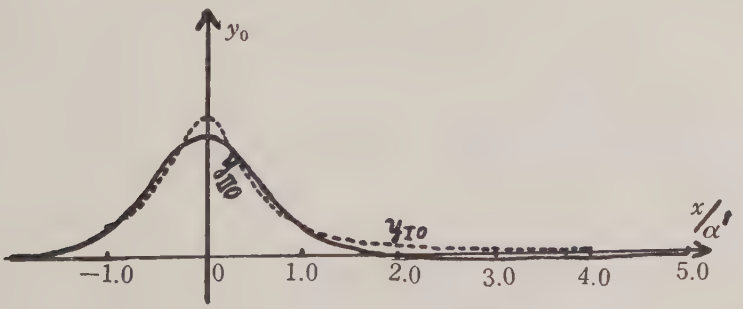

Fig. 8. Two models which are alike each other.

Let us adopt the two models treated by Burnside, as the origins of I and II obeying the above-mentioned three conditions. The initial conditions of these waves are given by

$$y_{I0}=\frac{C}{1+(x/\alpha)^2}\,, \tag{27}$$

* These expressions are not right physically. (See Appendix I.) These are the convenient expressions.

and

$$y_{\text{II}_0}=C'\left\{\frac{1}{1+(x/\alpha')^2}\right\}^{3/4}\cos\left(\frac{3}{2}\tan^{-1}\frac{x}{\alpha'}\right). \tag{28}$$

In order to prove that these two models obey the conditions of 2) and 3), let us calculate the ratio of the potential energy included in $-n\alpha<x<n\alpha$ to the whole energy included in $-\infty<x<\infty$, in the case of I as follows;

$$\frac{\int_0^{n\alpha}\frac{dx}{(\alpha^2+x^2)^2}}{\int_0^{\infty}\frac{dx}{(\alpha^2+x^2)^2}}=\frac{2\tan^{-1}n+\frac{2n}{(n^2+1)}}{\pi}, \tag{29}$$

$$\left.\begin{aligned}&\fallingdotseq 82\% \quad (n=1)\\ &\fallingdotseq 96\% \quad (n=2)\end{aligned}\right\}. \tag{30}$$

Then let us calculate the ratio of the energy included in $-m\alpha'<x<m\alpha'$ in the case of II. Putting $\tan^{-1}x/\alpha'=y$, we get

$$\frac{\int_0^{m\alpha'}\frac{\cos^2\left(\frac{3}{2}\tan^{-1}\frac{x}{\alpha'}\right)}{(\alpha'^2+x^2)\sqrt{\alpha'^2+x^2}}dx}{\int_0^{\infty}\frac{\cos^2\left(\frac{3}{2}\tan^{-1}\frac{x}{\alpha'}\right)}{(\alpha'^2+x^2)\sqrt{\alpha'^2+x^2}}dx}=\frac{m}{\sqrt{1+m^2}}+\frac{m}{(1+m^2)^2}, \tag{31}$$

$$\left.\begin{aligned}&\fallingdotseq 80\% \quad (m=1/2)\\ &\fallingdotseq 96\% \quad (m=1)\end{aligned}\right\}. \tag{32}$$

So, putting $\alpha'=2\alpha$, we can get the two models which obey the conditions of 2) and 3). Then, to satisfy the condition of 1), as

$$\begin{aligned}&\int_{-\infty}^{\infty}\frac{C^2\alpha^4}{(\alpha^2+x^2)^2}dx=\frac{\pi\alpha C^2}{2}\\ &=\int_{-\infty}^{\infty}C'^2\left(\frac{\alpha'^2}{\alpha'^2+x^2}\right)^{3/2}\cos^2\left(\frac{3}{2}\tan^{-1}\frac{x}{\alpha'}\right)dx=C'^2\alpha',\end{aligned} \tag{33}$$

let us put

$$C/C'=2/\sqrt{\pi}, \tag{34}$$

and we have obtained the two models which are alike each other (Fig. 8).

The two Cauchy-Poisson waves started from (27) and (28) are given by the analysis of Burnside as follows;

$$y_{\text{I}}=\sqrt{\pi}\frac{C\alpha}{x}\left(\frac{gt^2}{4x}\right)^{1/2}e^{-gt^2\alpha/4x^2}\sin\left(\frac{gt^2}{4x}+\frac{\pi}{4}\right), \tag{35}$$

and

$$y_{\text{II}}=C'\left(\frac{\alpha'}{x}\right)^{3/2}e^{-gt^2\alpha'/4x^2}\left[\frac{gt^2}{2x}\sin\left(\frac{gt^2}{4x}+\frac{\pi}{4}\right)-\cos\left(\frac{gt^2}{4x}+\frac{\pi}{4}\right)\right]$$

$$\fallingdotseq C'\left(\frac{\alpha'}{x}\right)^{3/2} e^{-gt^2\alpha'/4x^2}\cdot\frac{gt^2}{2x}\sin\left(\frac{gt^2}{4x}+\frac{\pi}{4}\right). \tag{36}$$

Assuming $\alpha'=2\alpha$ and $C/C'=2/\sqrt{\pi}$ we can get the ratio of the two amplitudes of y_{I} and y_{II} as follows;

$$\frac{Amp.(y_{\mathrm{I}})}{Amp.(y_{\mathrm{II}})}=\frac{e^{gt^2\alpha/4x^2}}{\sqrt{gt^2}\sqrt{2\alpha/x}}=\frac{1}{2\sqrt{2}}\frac{e^{T^2}}{T}\left(T=\frac{\sqrt{gt^2\alpha}}{2x}\right). \tag{37}$$

This ratio is so far from being a constant, and changes suddenly with time. So, we know that the two Cauchy-Poisson waves started from the two origins obeying the three conditions, damp in the different manners. We can only guess from a slow damping of the Cauchy-Poisson wave caught on Hachijo Island, that this explosion may be intense and narrow, and from a rapid damping that the explosion may be wide. This factor may be controlled by the explosion depth a little, and by the length (height) and the diameter of the crater decisively.

§ 5. The Cauchy-Poisson waves started from the origins having the finite horizontal dimensions

As is mentioned in § 3, there exists a quiet point in the record of the Cauchy-Poisson wave started from the origin of (2), and there is not a quiet point in the wave started from (6) etc. We should here throw light on the origin of the appearance of the quiet point.

The study in the Cauchy-Poisson wave started from a finite origin is poor Only Burnside studied the Cauchy-Poisson waves resulting from a few models. He developed the difficult mathematical formulas, without knowing the Kelvin's method (stationary phase method) found contemporaneously, so there has been none who has gone a step farther in this problem.

For examples, when we observe the wave spread from a stone thrown into a pond, the ship wave caused by the shocks given by the bow and the stern of the sailing ship, and the tsunami caused by the Myojin volcanic explosion, these are, without exception, the Cauchy-Poisson waves started from the origins having the finite horizontal dimensions. We should, therefore, develop the study of this problem. So, we will spend this paragraph and the next paragraph to the study of the Cauchy-Poisson waves starting from the finite origins and spreading over the infinitely deep water.

If we assume that the initial elevation at the origin is given by an even function of $F(x)$, and put $\varepsilon_0=1$, $\varepsilon_1=\varepsilon_2=\varepsilon_3=\cdots=2$, we get

$$F(x)=\frac{2}{a}\sum_0^\infty \varepsilon_s\cos\frac{2s\pi x}{a}\int_0^{a/2}F(\lambda)\cos\frac{2s\pi\lambda}{a}d\lambda=\frac{2}{a}\sum_0^\infty \varepsilon_s\cos\frac{2s\pi x}{a}\cdot A_s\,. \tag{38}$$

As the initial condition is given by

$$\left.\begin{array}{ll} y_0\propto F(x) & |x|<a/2 \\ =0 & |x|>a/2 \end{array}\right\}, \tag{39}$$

we will express this by an integral as follows;

$$y_0 \propto \frac{2}{\pi a}\int_0^\infty \frac{\sin(x+a/2)m-\sin(x-a/2)m}{m}\cdot F(x)dm\ . \tag{40}$$

Putting (38) in (40), we obtain

$$y_0 \propto \frac{1}{\pi a}\sum_0^\infty \varepsilon_s A_s \int_0^\infty \left[\sin\left\{\left(m+\frac{2s\pi}{a}\right)x+\frac{am}{2}\right\}+\sin\left\{\left(m-\frac{2s\pi}{a}\right)x+\frac{am}{2}\right\}\right.$$
$$\left.-\sin\left\{\left(m+\frac{2s\pi}{a}\right)x-\frac{am}{2}\right\}-\sin\left\{\left(m-\frac{2s\pi}{a}\right)x-\frac{am}{2}\right\}\right]\frac{dm}{m}\ . \tag{41}$$

And then

$$y \propto \sum_0^\infty \varepsilon_s A_s \int_0^\infty \frac{1}{m}\left[\sin\left\{\left(m+\frac{2s\pi}{a}\right)x+\frac{am}{2}\right\}-\sin\left\{\left(m+\frac{2s\pi}{a}\right)x-\frac{am}{2}\right\}\right]$$
$$\times \cos\sqrt{\left(m+\frac{2s\pi}{a}\right)g}\,t$$
$$+\frac{1}{m}\left[\sin\left\{\left(m-\frac{2s\pi}{a}\right)x+\frac{am}{2}\right\}-\sin\left\{\left(m-\frac{2s\pi}{a}\right)x-\frac{am}{2}\right\}\right]$$
$$\times \cos\sqrt{\left|m-\frac{2s\pi}{a}\right|g}\,t\,dm\ . \tag{42}$$

Let us adopt a new variable "m", instead of $\left(m+\frac{2s\pi}{a}\right)$ in the lst integral and of $\left(m-\frac{2s\pi}{a}\right)$ in the 2nd integral, and we get

$$y \propto \sum_0^\infty \varepsilon_s A_s \int_{\frac{2s\pi}{a}}^\infty \frac{1}{m-\frac{2s\pi}{a}}\left[(-1)^s\sin\left(mx+\frac{am}{2}\right)-(-1)^s\sin\left(mx-\frac{am}{2}\right)\right]$$
$$\times \cos\sqrt{mg}\,t\,dm$$
$$+\sum_0^\infty \varepsilon_s A_s \int_{-\frac{2s\pi}{a}}^\infty \frac{1}{m+\frac{2s\pi}{a}}\left[(-1)^s\sin\left(mx+\frac{am}{2}\right)-(-1)^s\sin\left(mx-\frac{am}{2}\right)\right]$$
$$\times \cos\sqrt{|m|g}\cdot t\,dm\ . \tag{43}$$

Then we seperate $\int_0^\infty$ and $\int_{-\frac{2s\pi}{a}}^0$ in the 2nd integral, and adopt a new variable "m" instead of $-m$ in the latter. (43) becomes as follows;

$$y \propto \sum_v^\infty (-1)^s \varepsilon_s A_s \left[\int_0^\infty \frac{1}{m-\frac{2s\pi}{a}}\left\{\sin\left(mx+\frac{am}{2}\right)-\sin\left(mx-\frac{am}{2}\right)\right\}\cos\sqrt{mg}\,t\,dm\right.$$
$$\left.+\int_0^\infty -\frac{1}{m+\frac{2s\pi}{a}}\left\{\sin\left(mx+\frac{am}{2}\right)-\sin\left(mx-\frac{am}{2}\right)\right\}\cos\sqrt{mg}\,t\,dm\right]$$

$$= \sum_0^\infty (-1)^s \varepsilon_s A_s \int_0^\infty \frac{2m}{m^2 - \dfrac{4s^2\pi^2}{a^2}} \left\{ \sin\left(mx + \frac{am}{2}\right) - \sin\left(mx - \frac{am}{2}\right) \right\} \cos\sqrt{mg}\, t \, dm$$

$$= \sum_0^\infty (-1)^s \varepsilon_s A_s \Re \int_0^\infty \frac{m}{m^2 - \dfrac{4s^2\pi^2}{a^2}} \Big[e^{i(mx+am/2+\sqrt{mg}\,t-\pi/2)}$$

$$+ e^{i(mx+am/2-\sqrt{mg}\,t-\pi/2)} - e^{i(mx-am/2+\sqrt{mg}\,t-\pi/2)} - e^{i(mx-am/2-\sqrt{mg}\,t-\pi/2)} \Big] dm \,. \qquad (44)$$

As there is no stationary phase in the 1st or in the 3rd integral, let us adopt only the stationary phases m_2 and m_4, in the 2nd and in the 4th integrals respectively, and (44) becomes as follows:

$$y \propto \sum_0^\infty (-1)^s \sqrt{2\pi}\, \varepsilon_s A_s \left[\frac{gt^2 \cdot \cos\left(\dfrac{gt^2}{4(x+a/2)} + \dfrac{\pi}{4}\right) \cdot m_2^{3/4}}{2(gt^2)^{1/4}(x+a/2)^2 \left\{ \dfrac{g^2t^4}{16(x+a/2)^4} - \dfrac{4s^2\pi^2}{a^2} \right\}} \right.$$

$$\left. - \frac{gt^2 \cdot \cos\left(\dfrac{gt^2}{4(x-a/2)} + \dfrac{\pi}{4}\right) \cdot m_4^{3/4}}{2(gt^2)^{1/4}(x-a/2)^2 \left\{ \dfrac{g^2t^4}{16(x-a/2)^4} - \dfrac{4s^2\pi^2}{a^2} \right\}} \right]$$

$$= \sum_0^\infty (-1)^s \sqrt{2\pi x}\, \varepsilon_s A_s \frac{4\sqrt{2}\, a^2 (gt^2)^{3/2}}{g^2t^4a^2 - 64s^2\pi^2x^4}$$

$$\times \sin\left(\frac{gt^2}{4x} + \frac{\pi}{4}\right) \sin\frac{gt^2a}{8x^2} \,, \qquad (45)$$

as

$$\left(x \pm \frac{a}{2}\right) - \frac{\sqrt{g}\, t}{2\sqrt{m_{2,4}}} = 0$$

$$m_{2,4} = \frac{gt^2}{4(x \pm a/2)^2} \,. \qquad (46)$$

In so far as $A_s \neq 0$, this series takes an indeterminate form for $gt^2a = 8\pi x^2 s$. The general principles showing the conditions of the appearances of the quiet point, are led from (45). These general principles are;

(1) *If there is A_s which is equal to* 0, *there exists a quiet point for* $t^2 = 8\pi x^2 s/ga$. (*The quiet point of the 1st kind.*)

Then let us think over the amplitude of the wave near $gt^2a/8x^2 = s\pi$, it becomes approximately a hyperbola given by $\dfrac{(-1)^s A_s}{gt^2a - 8s\pi x^2}$. According to the sign of A_s, a quiet point appears, therefore, between π and 2π when $A_1A_2 < 0$. (The quiet point of the 2nd kind. See Fig. 9.) And there exists a quiet point of the 2nd kind between π and 3π besides the appearance of the quiet point of the 1st kind at 2π, when $A_2 = 0$ and $A_1A_3 > 0$. Generally,

(2) *If* $A_{i+1} = A_{i+2} = \cdots = A_{i+l} = 0$, *the quiet points of the 1st kind appear for* $gt^2a/8x^2 = (i+1)\pi, = (i+2)\pi, = \cdots, = (i+l)\pi$.

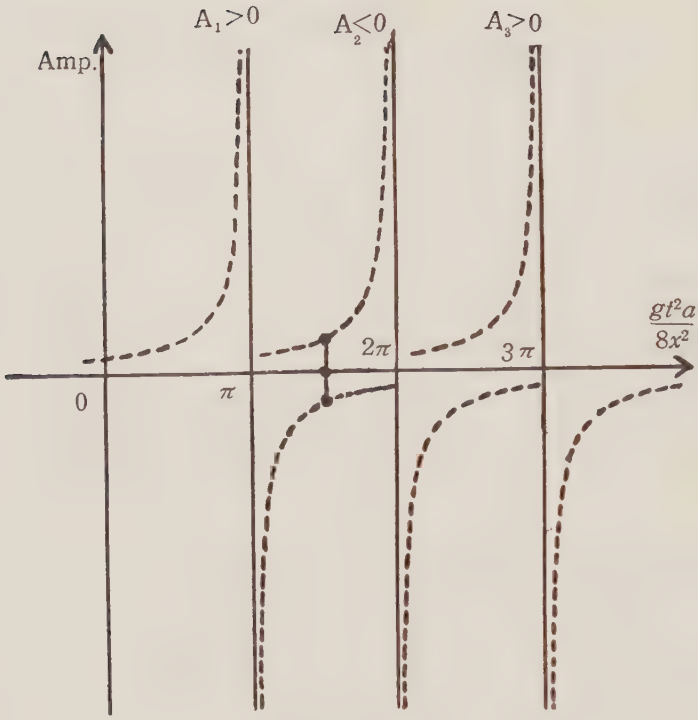

Fig. 9.

There exists a quiet point between $i\pi$ and $(i+l+1)\pi$, when l is even and $A_iA_{i+l+1}<0$.

There exists a quiet point between $i\pi$ and $(i+l+1)\pi$, when l is odd and $A_iA_{i+l+1}>0$. (*The quiet points of the 2nd kind.*)

These are the general principles which is not sometimes established according to the magnitudes of the coefficients. We have, however, obtained the general principles which can be applied to most cases. And we can foretell the positions of the quiet points in the Cauchy-Poisson waves, by the mere expansions of their origins in Fourier series.

And we understand the reason of the appearances of the quiet points corresponding to $t^2=8\pi x^2 s/ga$ $(s=1, 2, \cdots)$, in the wave the origin of which is given by (2). (This wave has been studied by Japanese investigators besides Burnside.) That is, when we expand (2) in Fourier series, we know $A_0\neq 0$, $A_1=A_2=\cdots=0$. This is nothing but the reason. The above-mentioned conclusions are very important, so we will study the Cauchy-Poisson wave started from an impulse of finite horizontal dimension instead of an initial elevation. Let us assume that $F(x)$ is an even function, ϕ and ρ represent the velocity potential and water density respectively, and the initial condition is given by

$$\left.\begin{array}{ll}\rho\phi_0\propto F(x) & |x|<a/2\\ =0 & |x|>a/2\end{array}\right\}, \tag{47}$$

and the caused Cauchy-Poisson wave is given as follows:

$$y\propto -\frac{1}{\pi g\rho}\int_0^\infty \sqrt{mg}\,\sin\sqrt{mg}\,t\,dm\int_{-\infty}^{\infty} F(\alpha)\cos m(x-\alpha)d\alpha\,. \tag{48}$$

$$\therefore\quad y\propto \int_0^\infty \sqrt{mg}\,\sin\sqrt{mg}\,t\,dm\int_{-a/2}^{a/2}\sum \varepsilon_s A_s\cos\frac{2s\pi\alpha}{a}\cos m(x-\alpha)d\alpha\,.$$

Calculating the integrals, we get

$$y\propto \sum(-1)^s\varepsilon_s A_s\int_0^\infty \frac{m\sqrt{mg}}{\frac{4s^2\pi^2}{a^2}-m^2}\left\{\begin{array}{l}\cos(\sqrt{mg}\,t-mx+ma/2)\\ -\cos(\sqrt{mg}\,t+mx-ma/2)\\ -\cos(\sqrt{mg}\,t-mx-ma/2)\\ +\cos(\sqrt{mg}\,t+mx+ma/2)\end{array}\right\}. \tag{49}$$

We have, by replacing cos by $\Re e^t$, using the stationary phase method and neglecting Σ,

$$\int_0^\infty dm\propto\frac{t^4}{(g^2t^4a^2-64\pi^2x^4s^2)\sqrt{x}}\cos\left(\frac{gt^2}{4x}+\frac{\pi}{4}\right)\sin\frac{gt^2a}{8x^2}\,. \tag{50}$$

Comparing to (45), (50) shows us that the damping is slower by the term t/x than that in the case of initial elevation, and that the other circumstances are the same as those in the latter. This result should be taken in the theory of the ship wave which is not resulting from the point source.

Adding to the general principles, when $A_{k+1}=A_{k+2}=\cdots=0$, there is able to appear the quiet point after $(k+1)\pi$, besides the quiet points of the first kind corresponding to $=(k+1)\pi$, $=(k+2)\pi$, $\cdots$.

Fig. 10. A continuous and smooth origin.

Let us examine how much do the real examples coincide with the above-mentioned general principles, by (45).

(A) We will take the case of $\varepsilon_0A_0=\varepsilon_1A_1$, $A_2=A_3=\cdots=0$. That is,

$$\left.\begin{array}{ll} y\propto\left(1+\cos\frac{2\pi}{a}x\right) & |\,x\,|<a/2\\ =0 & |\,x\,|>a/2\end{array}\right\}. \tag{51}$$

This means the continuous and smooth form of the wave origin (Fig. 10). Applying this condition to (45), we get

$$y\propto\left(\frac{x}{gt^2}\right)^{1/2}\frac{64\pi^2x^4}{g^2t^4a^2-64\pi^2x^4}\sin\left(\frac{gt^2}{4x}+\frac{\pi}{4}\right)\sin\frac{gt^2a}{8x^2}\,. \tag{52}$$

For $gt^2a/8x^2=\pi$, y takes an indeterminate form and no quiet point appears.

And for $gt^2a/8x^2=2\pi, 3\pi, \cdots$, the quiet points appear corresponding to the general principle (1).

(B) Then we assume

$$\left.\begin{aligned} y_0 &\propto \cos\frac{\pi}{a}x \quad & |x|<a/2 \\ &=0 & |x|>a/2 \end{aligned}\right\}. \tag{53}$$

This means the continuous and unsmooth form of the origin (Fig. 11). Applying this condition to (45), we obtain

$$y\propto\frac{C\sqrt{\pi}}{a}\left(\frac{gt^2}{x^3}\right)^{1/2}\frac{16a^2x^4}{16\pi^2x^4-g^2t^4a^2}\sin\left(\frac{gt^2}{4x}+\frac{\pi}{4}\right)\cos\frac{gt^2a}{8x^2}. \tag{54}$$

When we expand (53) in Fourier series, A_s becomes $\frac{a}{\pi}\frac{2(-1)^{s+1}}{4s^2-1}$. And we find that $gt^2a/8x^2=s\pi$ is not the quiet point (general principle (1)). The sign of A_s is the opposite of that of A_{s+1}, and we find that the quiet point appears at $(2s+1)\pi/2$ (between $s\pi$ and $(s+1)\pi$), except at $\pi/2$ (general principle (2)). And we become further aware of the fact that the sign of A_0 is the same as that of A_1.

Fig. 11. A continuous and unsmooth origin.

We see that the general principles (1) and (2) led from (45) are very applicable. Let us use the model of (A) in the next paragraph.

§ 6. The degree of the clearness of the quiet points

Supplementing § 5, we will show in this paragraph how much the quiet point is covered when $A_s\neq0$. We said in § 5 that if $A_s\neq0$, the series takes an indeterminate form for $gt^2a/8x^2=s\pi$. This means that the absolute value of the envelope of the amplitude does not become zero, and does not mean that it does not take a minimum value.

If it takes a minimum value which is far smaller than the maximum value, it means actually the appearance of the quiet point. And the conclusions in § 5 have merely a pure theoretical interest. Then we should study the two questions;

(1) Does the absolute value of the indeterminate form take its minimum value near this covered quiet point?

(2) If a minimum value appears, what is its magnitude comparing to its maximum value?

When we expand some functions which become zero for $x=\pm a/2$ and take their maximum values for $x=0$, in the Fourier series, we find that ε_0A_0 and ε_1A_1 are large and are nearly equal each other. So, as a representative case, we adopt a function in which $\varepsilon_0A_0=\varepsilon_1A_1$, and $A_2=A_3=\cdots=0$. This is the example of (A) in § 5.

Putting $\theta=gt^2a/8x^2$ in the amplitude of (52), let us make its derivative

with respect to θ. It is given by

$$\frac{C\sqrt{\pi^3 g}\,a}{4\sqrt{x^3}}\,\frac{\cos\theta(\pi^2-5\theta^2)}{\theta(\pi^2-\theta^2)^2}\left\{\frac{2(\theta\pi^2-\theta^2)}{\pi^2-5\theta^2}-\tan\theta\right\}. \tag{55}$$

(55) takes the forms of the product of 0 and ∞ when $\theta=0$, $=\pi$ and $=\pi/\sqrt{5}$, and does not become 0. Except these points, we should search the points at which (55) becomes 0. These points correspond to the maximum and the minimum values.

To see the outline of { } in (55), we rewrite it as follows;

$$\{\quad\}=\left\{\frac{2}{5}\theta-\frac{4\pi^2}{25}\,\frac{1}{\theta+\pi/\sqrt{5}}-\frac{4\pi^2}{25}\,\frac{1}{\theta-\pi/\sqrt{5}}-\tan\theta\right\}. \tag{56}$$

Thinking that $\pi/\sqrt{5}$ is a little smaller than $\pi/2$, we draw a graph as Fig. 12. There is a root a little larger than $\pi/2$. Then we rewrite (56) as follows.

$$\left\{\left(0.25+\frac{1}{1-0.5066\theta^2}\right)1.6\theta-\tan\theta\right\}. \tag{57}$$

Assuming the three roots are θ_1, θ_2 and θ_3, we look for them by the successive approximations. They are

$$\left.\begin{aligned}\theta_1&=1.91\\ \theta_3&=7.48\end{aligned}\right\}, \tag{58}$$

and θ_2 does not exist.

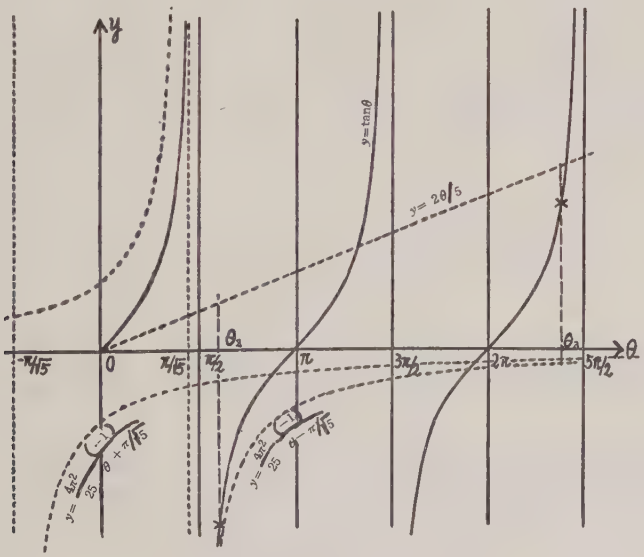

Fig. 12. The graph of (56).

The sign of $\cos\theta$ outside { } changes, but the sign of $\tan\theta$ inside { } changes simultaneously. So the change of the sign of $\cos\theta$ has nothing to do

with the existences of the maximum and the minimum.

The absolute value of the amplitude is 0 for $\theta=0$ and takes its maximum value near $\theta=\pi/2$ (when $\theta_1=1.91$). Near $\theta=\pi$, the absolute value of the amplitude does not take the expected minimum value. When $\theta=2\pi$, the sign of the amplitude changes and a quiet point appears. And near $\theta=5\pi/2$ (when $\theta_3=7.48$), other maximum value of the absolute value appears. So, we found that the quiet point near $\theta=\pi$ is covered perfectly for the initial condition of

$$y_0 \propto \left(1+\cos\frac{2\pi}{a}x\right).$$

And the degree of covering effect upon the quiet points for $\theta=s\pi$ are, from (45), found to be proportional to A_s. And on the other hand, comparing to our example of (A), the actual explosional centre may differ considerably. So we can think that the quiet points corresponding to A_s may be considerably covered, from the example of this paragraph.

The character of the quiet points of the 2nd kind is, that the calm sea condition continues for a long time near these points. It is possible that the actual quiet point may be of this kind.

§ 7. The Cauchy-Poisson wave resulting from a wide impulse and propagating over the shallow depth water

This analysis has been applied by the present author to the tsunami caused by the nuclear bomb test at Bikini (Marshall Islands). Fig. 13 shows the record of the tsunami caused at Bikini and caught at the Japanese coast.

We should treat this wave in order to understand the tsunami started from Myojin Reef where the sea is very shallow around the reef and rather shallow along the course between the reef and the wave recorder.

Thinking about the two-dimensional propagation,* let us assume the initial condition as follows;

$$\left.\begin{array}{ll} \rho\phi_0=P & r<a \\ =0 & r>a \end{array}\right\}_{\text{at } z=0}. \tag{59}$$

z-axis is taken downwards. Putting $c=\sqrt{gh}$ $(h/a\ll 1)$, we get the equation of

$$\phi=\frac{1}{a\rho}\int_0^\infty \cos\frac{m}{a}ct\, J_0\left(m\frac{r}{a}\right)\frac{m}{a}\frac{\cosh\frac{m}{a}(h-z)}{\cosh\frac{m}{a}h}dm\int_0^\infty \rho\phi_0 J_0\left(\frac{m}{a}\alpha\right)\alpha d\alpha\,. \tag{60}$$

Thinking that the initial condition (59) assumes the infinite particle velocity at $r=a$, and avoiding the formula expressing the velocity, we use the equation expressing the surface elevation as $\zeta=\left[\frac{\partial}{\partial z}\int_0^t \phi\, dt\right]_{z=0}$. Then,

* In the recent papers, the propagation in all directions are expressed as the "three dimensional" propagation. As the propagation in the vertical direction is not oscillatory, we obey the classical name.

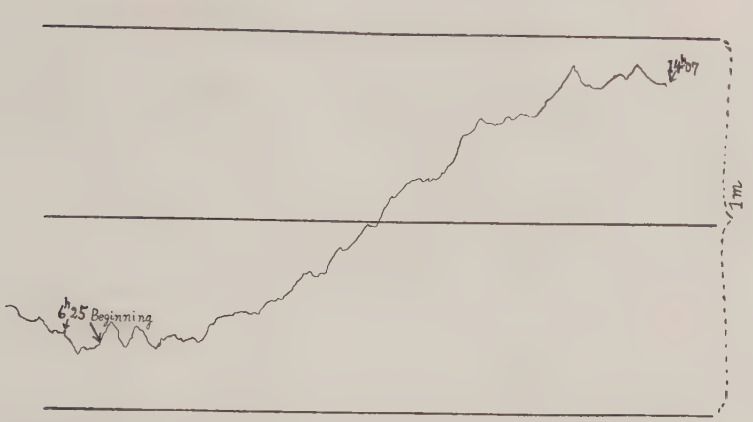

Fig. 13. The tsunami caused at Bikini and caught at the Japanese coast.

$$\zeta=\frac{P}{\rho c}\int_0^\infty \sin\frac{m}{a}ct\,J_0\left(m\frac{r}{a}\right)m\tanh m\frac{h}{a}\,dm\int_0^1 J_0(ms)s\,ds\,. \tag{61}$$

And we use the approximation

$$\tanh\left(m\frac{h}{a}\right)\fallingdotseq m\frac{h}{a}\,, \tag{62}$$

because $\frac{h}{a}\ll 1$.

As $\int_0^1 J_0(ms)sds=\frac{J_1(m)}{m}\propto\sqrt{\frac{1}{m^3}}$ for the large value of m, we can think

$$\zeta\propto\int_0^\infty \sin\frac{m}{a}ct\sqrt{\frac{1}{m}}\cdot m\cdot m\frac{h}{a}\frac{1}{\sqrt{m^3}}dm=\int_0^\infty \sin\frac{m}{a}ct\cdot\frac{h}{a}dm\,. \tag{63}$$

This integral diverges.

But we should look at the approximation (62) again. This approximation means that $m\frac{h}{a}$ is small, and $\tanh m\frac{h}{a}$ does not actually exceed 1 when m becomes large.

So, ζ in (63) is of the next order;

$$\zeta\propto\int_0^\infty \sin\frac{m}{a}ct\frac{dm}{m}\,. \tag{64}$$

This integral proves to converge. Let us remember the formula

$$J_0\left(m\frac{J}{a}\right)\cdot J_0(ms)=\frac{1}{\pi}\int_0^\pi J_0(m\Omega)d\omega$$

$$\Omega=\sqrt{\left(\frac{r}{a}\right)^2+s^2-2\left(\frac{r}{a}\right)s\cos\omega}\,, \tag{65}$$

and rewright (61) as follows;

$$\zeta \propto \int_0^\infty \sin \frac{m}{a} ct \cdot J_0(m\Omega) m^2 dm \,. \tag{66}$$

From the well-known formula of (67) and the convergent character of (62), we may make the second derivatives of the both sides of (67), differentiated with respect to (ct/a).

That is, from

$$\left.\begin{aligned} \int_0^\infty \sin \frac{m}{a} ct \, J_0(m\Omega) dm &= \frac{1}{\sqrt{\left(\frac{ct}{a}\right)^2 - \Omega^2}} \,, & \left(\frac{ct}{a}\right)^2 > \Omega^2 \\ &= 0 \,, & \left(\frac{ct}{a}\right)^2 < \Omega^2 \end{aligned}\right\} , \tag{67}$$

we get

$$\left.\begin{aligned} &\int_0^\infty \sin \frac{m}{a} ct \, J_0(m\Omega) m^2 dm \\ &\quad = \frac{1}{\sqrt{\left\{\left(\frac{ct}{a}\right)^2 - \Omega^2\right\}^3}} - \frac{3\left(\frac{ct}{a}\right)^2}{\sqrt{\left\{\left(\frac{ct}{a}\right)^2 - \Omega^2\right\}^5}} \,, & \left(\frac{ct}{a}\right)^2 > \Omega^2 \\ &\quad = 0 \,, & \left(\frac{ct}{a}\right)^2 < \Omega^2 \end{aligned}\right\} . \tag{68}$$

We can, therefore, solve (61) numerically.

§ 8. Conclusions

The conclusions of the analyses considered in this paper are as follows:

1) There lie Aoga Shima and its island-shelf deviating slightly from the line connecting Myojin Reef and Hachijo Island. We showed the refraction diagrams for long wave and for the wave the period of which is 60 seconds. There are found three rays one of which makes a straight advance along the course Myojin→Hachijo, one of which goes along the curve on the right side of the shelf, and one of which goes along the curve on the left side of the shelf. These three rays reach, without exception, the wave recorder on Hachijo Island, falling at right angles to the coast. The distances of the three curves along which these three rays go Myojin→Hachijo, differ one another. So, on Hachijo Island, the waves are observed as if the tsunamis started from two or three origins had come. We solved the Cauchy-Poisson waves started from the several origins the individuals of which have the continuous forms, mathematically. In spite of the natural form of the individual of these origins, we proved the appearances of the quiet points in the waves in this case. Then, as the analysis of the Cauchy-Poisson wave propagating over the finite depth water is very difficult, we had better avoid the quantitative discussions.

2) In the process of the explosion→generation of the tsunami, there exist many factors. (A) Corresponding to the volcanic ejecta and gases at the sea

bottom, the elevation of the sea surface appears and causes the tsunami. These masses are thrown up into the sky, and a mass deficit appears at the bottom. This corresponds to a mass deficit at the sea surface, which sends the tsunami. (B) These masses fall to the surface and give the positive impulses to the surface. As there is no essential difference of treatments of (A) and (B), we treated the case of (A) as a representative form of the Cauchy-Poisson waves.

Among the many factors, there is the efficiency of the tsunami which comes inevitably from the elementary dynamics. As an important commonsense of geophysics, we will discuss this efficiency in the case of the tsunami caused by the earthquake. The absolute value of this efficiency in the latter case is one several hundredth.

3) There is the differences among the manners of the waves dampings in the many records. Before thinking over this problem, we proved that the two dampings of the Cauchy-Poisson waves started from the two initial elevations the physical characters of which are nearly equal each other, differ because of the difference of the mathematical expressions of these two elevations. We adopted the two models treated by Burnside which satisfy the above-mentioned condition when the horizontal scales are changed. And we found that the two waves damp in the different manners.

We can only guess from a slow damping of the Cauchy-Poisson wave that this explosion may be intense and narrow, and from a rapid damping that the explosion may be wide.

4) In order to throw a light on the origin of the appearance of the quiet point, we analysed generally the Cauchy-Poisson waves resulting from the origins having the finite horizontal dimensions.

If the function expressing the form of the origin is an even function and is expanded in a Fourier series the $(s+1)$th coefficient of which is A_s,

(I) when $A_s=0$, a quiet point appears for $gt^2a/8x^2=s\pi$ (the quiet point of the 1st kind).

(II) When $A_{i+1}=A_{i+2}=\cdots=A_{i+l}=0$, besides the quiet points of the 1st kind corresponding to them, there exists a quiet point of the 2nd kind between $i\pi$ and $(i+l+1)\pi$, in the case l is even and $A_iA_{i+l+1}<0$, or l is odd and $A_iA_{i+l+1}>0$.

These are the two general principles, and will be useful for the analysis of the Cauchy-Poisson wave resulting from a finite origin or the ship wave etc.

5) When $A_s\neq 0$, the quiet point is covered. We examined the degree of this covering effect about a typical form of the origin. The quiet point is, in this case, covered perfectly.

6) The theory of the tsunami caused by the nuclear bomb test is necessary to understand the wave caused by the Myojin volcanic explosion. We introduced the former.

§ 9. Acknowledgement

Dr. Mashito Nakano, Dr. Sanae Unoki and other people on Hachijo Island supplied the tsunami records for the convenience of the present author. He wishes to express his best thanks to them.

§ 10. References

Burnside, W., 1888: On deep-water waves resulting from a limited original disturbances. Proc. Lond. Math. Soc. **20** (22).

Cole, R. S., 1948: Underwater Explosions.

Dietz, R. S. and Sheehy, M. J., 1953: Transpacific Detection by Underwater Sound of Myojin Volcanic Explosions. Journ. Oceanogr. Soc. Japan. **9** (2) pp. 53–83.

Ergin, K., 1952: Energy Ratio of the Seismic Waves Reflected and Refracted at a Rock-Water Boundary. Bull. Seism. Soc. Amer. **42** (4) pp. 349–372.

Lamb, H., 1932: Hydrodynamics.

Mihara, M., 1915: (Manuscript in Japanese).

Miyoshi, H., 1958: Two proposals Concerning Myojinsho Tsunamis. Journ. Oceanogr. Soc. Japan. **14** (2) pp. 65. (In Japanese).

Miyoshi, H., 1959: Generation of the Tsunami and the Compressional Waves. Journ. Oceanogr. Soc. Japan. **15** (1) pp. 24. (In Japanese).

Miyoshi, H., 1954: Generation of the Tsunami in Compressible Water (Part I). Journ. Oceanogr. Soc. Japan. **10** (1) pp. 1–10.

Miyoshi, H., 1955: Generation of the Tsunami in Compressible Water (Part II). Rec. Oceanogr. Wor. Japan. **2** (1) pp. 49–56.

Miyoshi, H., 1954: Efficiency of the Tsunami. Journ. Oceanogr. Soc. Japan. **10** (1) pp. 11–14.

Miyoshi, H. and Akiba, Y., 1954: The Tsunamis Caused by the Myojin Explosions. Journ. Oceanogr. Soc. Japan. **10** (2) pp. 49–59.

Miyoshi, H., 1958: Myojin-Reef and its Tsunami. Kagaku. **28** (2) pp. 90. (In Japanese).

Miyoshi, H., 1958: Some Considerations on Cauchy-Poisson Waves. Kagaku. **28** (10) pp. 527–528. (In Japanese).

Morimoto, R., 1958: Japanese Volcanoes. (In Japanese).

Munk, W. H. and Traylor, M. A., 1947: Refraction of Ocean Waves: A Process Linking Underwater Topography to Beach Erosion. Journ. Geol. **55** (1) pp. 1–26.

Pidduck, F. B., 1912: The Wave-Problem of Cauchy and Poisson for finite Depth and slightly Compressible Fluid. Proc. Roy. Soc. Lond. **86** pp. 396–

Rayleigh, 1909: On the Instantaneous Propagation of Disturbance in a Dispersive Medium. Phil. Mag. **18** (6).

Takahashi, R., 1942: (In Japanese).

The Tokyo University of Fisheries, 1953: Report on the Submarine Eruption of Myojin-Sho. Journ. Tokyo Univ. Fish. **40** (2) pp. 1–43.

Unoki, S. and Nakano, M., 1953: On the Cauchy-Poisson Waves Caused by the Eruption of a Submarine Volcano. (1st paper). Oceanogr. Mag. **4** (4) pp. 119–141.

Unoki, S. and Nakano, M., 1953: On the Cauchy-Poisson Waves Caused by the Eruption of a Submarine Volcano. (2nd paper). Oceanogr. Mag. **5** (1) pp. 1–13.

Unoki, S. and Nakano, M., 1953: On the Cauchy-Poisson Waves Caused by the Eruption of a Submarine Volcano. (III). Pap. Met. Geoph. **4** (3–4) pp. 139–150.

Watson, G. N., 1948: A Treatise on the Theory of Bessel Functions.

Appendix I

Efficiency of the Tsunami

This fact fails easily to be noticed, and forms an important commonsense of geophysics. So we will give a full explanation about it.

When an explosion takes place at the sea-bottom, there follows the mass (vapour etc.) excess. This means the mass deficit of water the volume of which is the same with the mass excess. And this deficit corresponds to the excess of the water mass produced at the sea surface. This water excess at the surface is the "apparent energy" of the tsunami.

And when the explosion calms down, the water mass increases at the bottom comparing to the exploding state. This increase means the mass deficit at the sea surface. This mass deficit is radiated again as the "apparent energy" of the tsunami. These mass excess or deficit at the sea surface, which correspond to the mass deficit or excess at the sea-bottom, become, in this way, the apparent energy of the tsunami. And then, there exists the ratio of the energy of the generated tsunami to the real energy exchanged between the earth crust and the sea water. This ratio should be named the "efficiency of the tsunami", and becomes a complicated factor under the various conditions.

This factor, coming essentially from the elementary dynamics, reduces greatly the absolute value of the energy exchanged between the earth crust and the sea water, and shows this lessened energy on the outside as the energy of the tsunami. In the scope of the classical dynamics, the "energy" only expresses the change which occurs in a specific system, that is, the working ability given to this system or a body through an action of an agency. When a new system (which means the excess or the deficit of the whole mass) takes the place of the original one, the physical quantity named "energy" cannot be applied directly. When the excess or the deficit of sea water happens to the sea surface, for example, we cannot obtain the quantity of energy which has changed in the sea water system but only can get the apparent energy of the tsunami by integrating mgh (potential energy, m: mass, g: acceleration of gravity and h: height from the surface) formally.

In order to explain this fact quantitatively, we had better use the model of the tsunami caused by the earthquake. At the generation of the tsunami, we think the bottom elevation or depression happens suddenly over a wide range, the (positive or negative) water pile of the same shape as the deformed part of the bottom appears upon the sea surface, which is the newborn form of the tsunami.

Let us express the depth of the sea, height of the elevation (or the depression) of the bottom, and the area of the deformed bottom by H, η, and S, and the efficiency is given as follows:

$$e=\frac{\int_S \eta^2 dS}{2H\int_S \eta dS+\int_S \eta^2 dS}\fallingdotseq\frac{\int_S \eta^2 dS}{2H\int_S \eta dS} \qquad (\eta \ll H)\,. \qquad (1)$$

The absolute value of this efficiency is much smaller than 1. It usually becomes one several hundredth. We will think more kinematically by expressing the hydrostatic pressure at the bottom and the volume of the bottom deformation by P and V, the energy exchanged between the crust and the sea water is as follows:

$$\int_V PdV=E_k+E_p+E_b\ . \tag{2}$$

Here, E_k+E_p is the so-called destructive tsunami's energy, and E_b is the term corresponding to the mass excess or deficit of the bottom water. If the hydrostatic pressure during the quasi-static process of the same deformation, is represented as P_q, we can get the following relation;

$$\int_V P_q dV=E_b\ , \tag{3}$$

for, in this case, E_k and E_p vanish. ($\because$ For example, the deformation of $1/N$ height occurs N times, the energy of $1/N^2$ comparing with the original tsunami will be radiated every time. So, the total energy is $1/N^2\times N=1/N\to 0$, $N\to\infty$.)

$$\therefore \int_V (P-P_q)dV=E_k+E_p\ . \tag{4}$$

This has, exclusively, a positive value. And the efficiency is given as

$$e=\frac{\int_V (P-P_q)dV}{\int_V P_q dV}\ . \tag{5}$$

That is, when the bottom is elevated by a quasi-static process, the water column with the upper edge which is being rubbed off triflingly, is lifted. When the bottom is elevated by a sudden process, on the other hand, the water column having a fixed vertical length, is lifted. This slight difference becomes the destructive energy of the tsunami, and the efficiency of the tsunami is one several hundredth of a positive value.

When the bottom is depressed by a quasi-static process, the water column the length of which is growing longer little by little, bears on the crust. When the bottom is depressed by a sudden process, the water column having a fixed vertical length, bears on the crust. In this case, the slight remainder becomes the tsunami's destructive energy. The efficiency is, therefore, also one several hundredth but of a negative value.

The value of (5) takes its maximum absolute value, when the deformation is a sudden one, and tends to zero, when the deformation approaches to the quasi-static one. In the intermediate case, the relative efficiency (the ratio of this efficiency to the one corresponding to the sudden deformation), is a function of the horizontal dimension and the time duration of the deformation, and the water depth, and decreases monotonely with the increase of the time duration.

The above-mentioned rules establish at the tsunami caused by the explo-

sion, and prove to be the most important problems among the many relations of the energies. It is remarkable that the relation between the energy of the explosion of the volcano and that of the caused tsunami is not readily determined by the depth of the explosion, not to speak of the linear relation.

Appendix II

All records (except that on Sept. 26th, 1952—shown as Fig. 1.) of the tsunamis caught on Hachijo Island.

Time: Some 17cm correspond to one hour.

Wave height: 0.72cm correspond to 1m except in the first three data. (In these three figures, each wave height scale is shown.)

A, B, C and D point to the beginning, the 1st quiet point, the 2nd quiet point and the end of the tsunami.

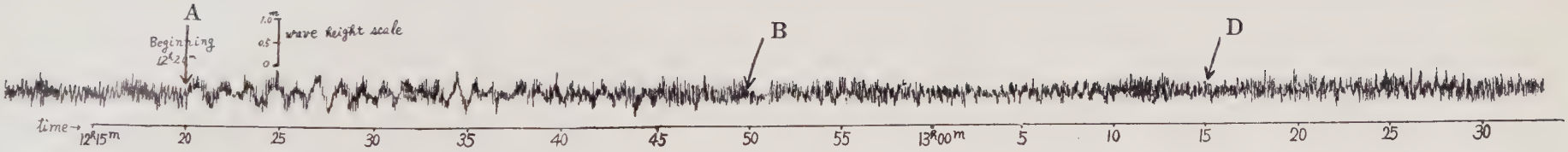

Sept. 16th, 1952, beginning: 12^h20^m,
end: 13^h15^m.

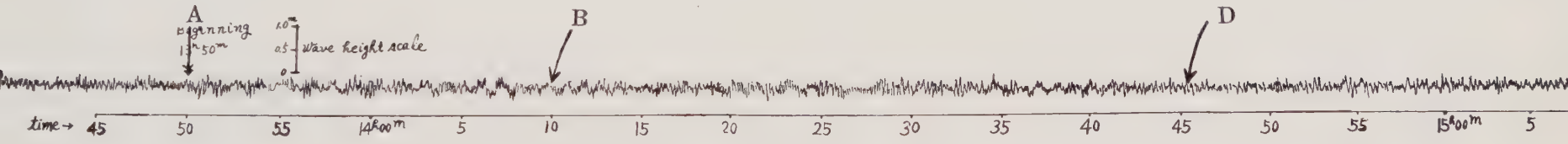

Sept. 23rd, 1952, beginning: 13^h50^m,
end: 14^h45^m.

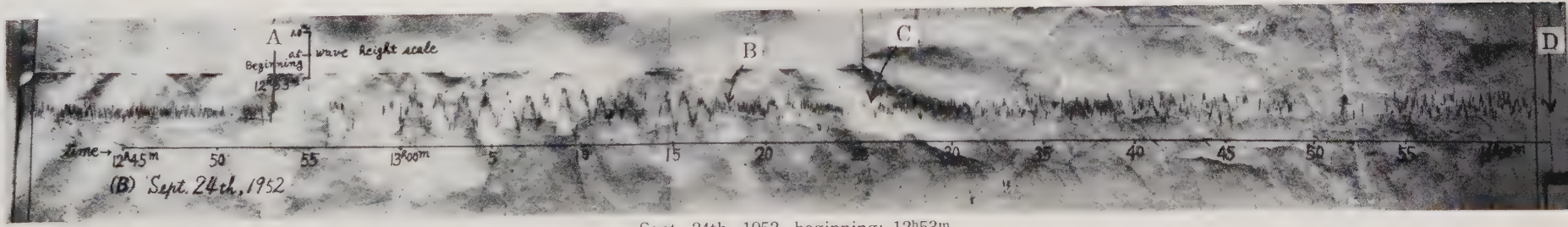

Sept. 24th, 1952, beginning: 12^h53^m,
end: 14^h05^m.

Mar. 11th 1953, beginning: before 08^h56^m,
end: obscure.

Mar. 12th, 1953, beginning: 16^h09^m,
end: obscure.

Mar. 14th, 1953, beginning: 10^h03^m,
end: 10^h52^m.

Mar. 14th, 1953, beginning: 14^h11^m,
end: 14^h22^m.

Mar. 14th, 1953, beginning: 16_h47^m,
end: 17^h05^m.

Mar. 14th, 1953, beginning: 18^h40^m,
end: 19^h00^m.

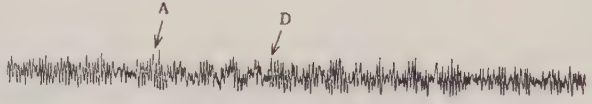

Mar. 14th, 1953, beginning: 21^h05^m,
end: 21^h11^m.

Mar. 15th, 1953, beginning: 03^h49^m,
end: 04^h49^m.

Mar. 15th, 1953, beginning: 13^h08^m,
end: 13^h25^m.

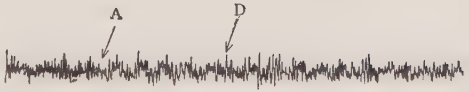

Mar. 15th, 1953, beginning: 15^h16_m,
end: 15^h22^m.

Mar. 15th, 1953, beginning: 17^h15^m,
end: 17^h35^m.

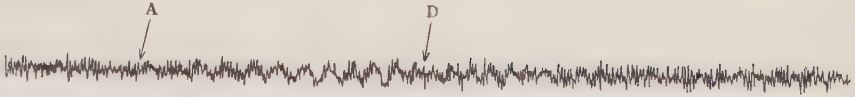

Mar. 15th, 1953, beginning: 18^h42^m,
end: 18^h55^m.

Mar. 15th, 1953, beginning: 22^h09^m,
end: 22^h29^m.

Mar. 16th, 1953, beginning: 00^h24^m,
end: 00^h37^m.

Mar. 16th, 1953, beginning: 00^h49^m,
end: 01^h02^m.

Mar. 16th, 1953, beginning: 03^h47^m,
end: 04^h07^m.

Mar. 16th, 1953, beginning: 07^h34^m,
end: 08^h15^m.

Mar. 16th, 1953, beginning: 09^h37^m,
end: 09^h57^m.

Mar. 16th, 1953, beginning: 11^h23^m,
end: 11^h43^m.

Mar. 16th, 1953, beginning: 13^h43^m,
end: 13^h59^m.

Mar. 16th, 1953, beginning: 18^h46^m,
end: 19^h04^m.

Mar. 17th, 1953, beginning: 02^h24^m,
end: 02^h38^m.

Mar. 17th, 1953, beginning: 04^h40^m,
end: 05^h04^m.

Mar. 17th, 1953, beginning: 13^h36^m,
end: 13^h51^m.

Mar. 17th, 1953, beginning: 16^h45^m,
end: 17^h19^m.

Mar. 17th, 1953, beginning: 20^h18^m,
end: 20^h35^m.

Mar. 17th, 1953, beginning: 22^h51^m,
end: 23^h18^m.

Mar. 18th, 1953, beginning: 01^h15^m,
end: 01^h52^m.

Mar. 18th, 1953, beginning: 03^h44^m,
end: 04^h18^m.

Mar. 18th, 1953, beginning: 04^h56^m,
end: 05^h09^m.

Mar. 18th, 1953, beginning: 11^h06^m,
end: 11^h18^m.

Mar. 18th, 1953, beginning: 14^h07^m,
end: 14^h28^m.

Mar. 18th, 1953, beginning: 16^h25^m,
end: 16^h47^m.

Mar. 18th, 1953, beginning: 19^h27^m,
end: 19^h49^m.

Mar. 18th, 1953, beginning: 21^h39^m,
end: 22^h01^m.

Mar. 18th, 1953, beginning: 22^h15^m,
end: 22^h28^m.

Mar. 19th, 1953, beginning: 02^h05^m,
end: 02^h24^m.

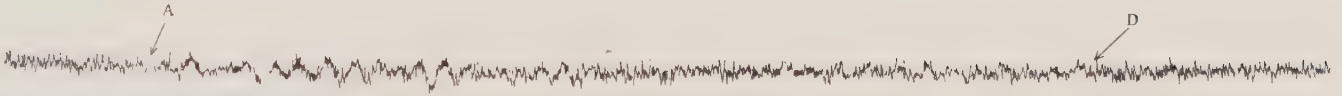

Mar. 19th, 1953, beginning: 05^h06^m,
end: 05^h49^m.

Mar. 19th, 1953, beginning: 09^h35^m,
end: 09^h59^m,

Mar. 19th, 1953, beginning: 13^h16^m,
end: 13^h30^m.

Mar. 19th, 1953, beginning: 16^h33^m,
end: 16^h55^m.

A
B
C
D
Mar. 19th, 1953, beginning: 20h15m,
end: 21h08m.
A
D
Mar. 20th, 1953, beginning: 00h42m,
end: 01h01m.
A
B
C(?)
D
Mar. 22nd, 1953, beginning: 21h08m,
end: 23h06m.

Mar. 23rd, 1953, beginning: 02^h23^m,
end: 03^h13^m.

Mar. 23rd, 1953, beginning: 13^h56^m,
end: 14^h55^m.

Mar. 25th, 1953, beginning: 01^h02^m,
end: 01^h27^m.

Mar. 25th, 1953, beginning: 07^h13^m,
end: 07^h52^m.

Journal of the Tokyo University of Fisheries, Vol. 47, No. 1, 1960

THE TENSION TEST OF THE NETTING CORD BY IMPACT FORCE

Yasushi Kondo

(Received June 25, 1960)

Introduction

The strength of the netting cord is generally expressed in the value of breaking force by applying static loads. It is a wellknown fact however that the netting cord is often easily breakable when a sudden tension is applied to it. From this point of view it appears irrational to assume its tensile strength against impact force through the tensile strength under static loads.

Studies of the tensile strength of the netting cord by applying repeated impact force were conducted by Tauti and Kondo and by a single impact force by Shimidu, Honda and Nagata. These studies were however to find the energy consumed at the instant of break of the netting cord by impact force and no data in its relation to the breaking strength under statical test were available.

In this study the measurement was conducted of the tension of the netting cord by impact force at the instant of its break in order to amend the tests formerly conducted as aforementioned together with a few additional experiments related thereto.

Method of Test

In order to effect impact force on the netting cord an impact tester of the pendulum type was used as shown in Fig. 1. The tester was the same type used in the test of Shimidu and Honda. Supplemental weights were of 4.25 kg and 8.25 kg. The test was conducted at 12 points with the degrees of fall of the pendulum varying from 5° to 70°.

The tester was of a construction with a lever indicating the degrees of rise of the pendulum, moving simultaneously with the pendulum. Inasmuch as the pendulum would have to move against the resistance of the clutches of the indicator, the energy consumed therefor would be an important factor in the test. Therefore, this discrepancy was duly corrected in each test datum through actual measurements of such energy consumed. In addition to that, as a pick-up was installed on the netting cord for the measurement of tension, the obtained data were also corrected to the extent of energy consumed therefor. Others such as the frictional resistance of the pendulum were however ignored as they were negligibly small.

In the measurement of the tension in the netting cord produced by impact an electric resistance strain gauge was used. This pick-up had been made by the writer with the colaboration of other staff and the oscillation of electric current was recorded by means of an electromagnetic oscillograph. It was

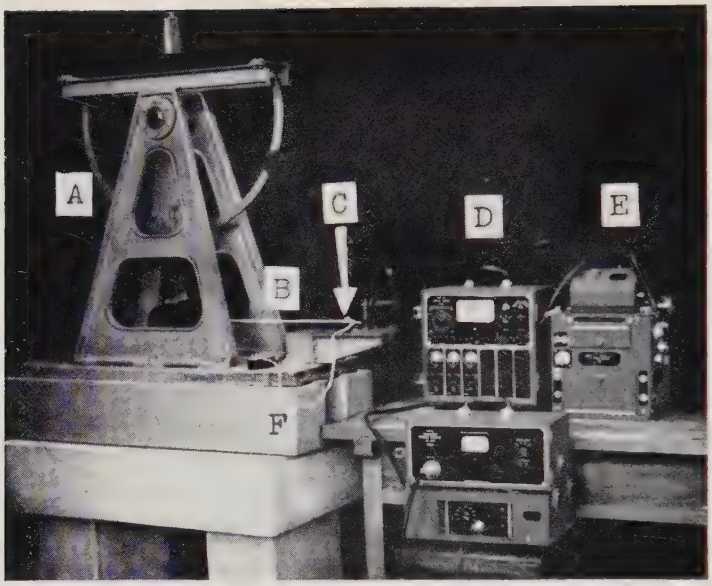

Fig. 1. General view of equipments of impact tensile test.
Note; A: impact tester
B: test piece of netting cord
C: pick-up
D: strainmeter
E: oscillograph
F: leading wire

generally said that the proper oscillation of the pick-up would be better to be more than 10 times the oscillation of phenomena and OKAZAKI held an opinion that the former was desirable to be more than 100 times the latter. But the proper oscillation of the pick-up used was about 1,000 cycles per second and the breaking phenomena of the netting cord was found to be 12/100 sec in the longest and 2/100 sec in the shortest. So it was assumed that no imperfection would appear in the test.

The netting cords used in the test were of cotton $20's$ 3/15, ramie $10's$ 1/2, cremona $20's$ 3/15, amilan 210^D 3/6 and 3/12 and the length of each test piece was 50 cm, and tests were carried out on the cords in dry as well as in wet conditions immersed for 24 hours in fresh water.

Test Results and Observations

(1) Tension produced in the netting cord by impact

a. Effect of impact force:

When the pendulum with a mass m was let fall from a position at a certain degree, the velocity of the pendulum at zero degree would be:

$$V=\sqrt{2gh}\sqrt{1+\frac{I}{Ml^2}}$$

The strength of the impact force would be mv.

Fig. 2 shows the results obtained by measuring the tension produced in the netting cord by an impact force with various weights.

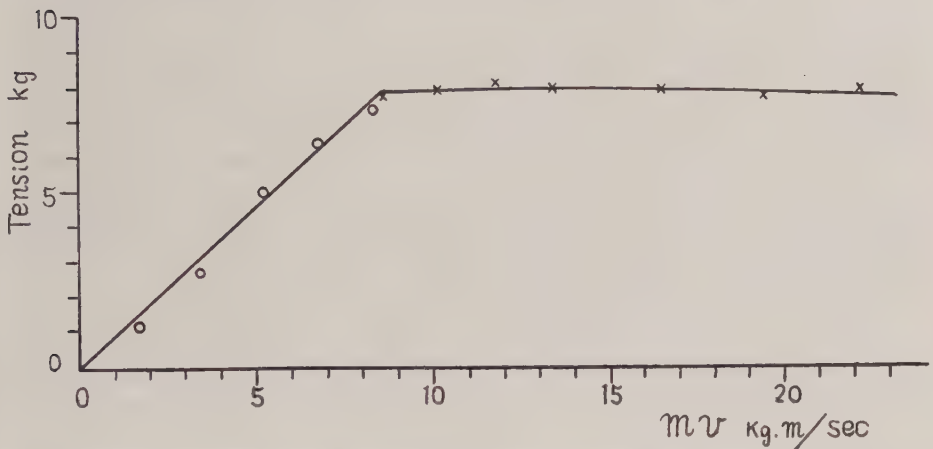

Fig. 2. Relation between impact force and tention of netting cord (cotton, 20's 3/15, dry).
Note; ×: ruptured cord
○: not ruptured cord

In the impact in the extent not causing breakage of the netting cord' the tension produced in it was approximately $T=0.93\,mv$. With mv between the values of 8 and 9 some broke and some not. But above a value of 9 all the cords broke. In such cases the tension in the netting cord was 7.9 kg and constant independent of the value of mv.

b. Tensil strength of various netting cords:

With various materials composing the netting cord; for instance the one made twisting long fibers or the other made by spinning short fibers, were of different structures in their break and it was presumable that each produced different characteristic at the instant of receiving tension by impact. Table 1 shows the results obtained by measuring the tension produced in the netting cord at the instant of break under tension caused by impact.

With the netting cords made by spinning short fibers such as cotton or cremona the tension at the instant of break under slow tension was somewhat smaller than that by impact. Such phenomena were possibly due to the mutual slips taking place among fibers under slow tension and the netting cords might have broken down under far smaller tension than the sum of the strength of each composing fiber. Inasmuch as the tension in the netting cords caused by impact was instant, no mutual slips might have taken place before the break of the fibers.

Table 1. Breaking strength of various netting cords obtained by impact and static test.

Name of cord	Number of hank and yarn	Dry or wet	Static test T_s (kg)	Impact test T_i (kg)	Comparative value T_i/T_s
Cotton	20's, 3/15	D	7.5	7.9	1.06
		W	8.3	8.9	1.08
Ramie	20's, 1/2	D	7.2	7.1	0.99
		W	8.8	9.0	1.02
Cremona	20's, 3/15	D	11.3	12.6	1.12
		W	9.5	10.8	1.14
Amilan	210D, 3/6	D	7.1	6.5	0.92
		W	6.1	5.6	0.92
	210D, 3/12	D	13.2	13.5	1.02
		W	12.0	12.1	1.00

Fig. 3 shows the breaking phenomena of various netting cords by impact transposed from the records of the oscillograph. According to the

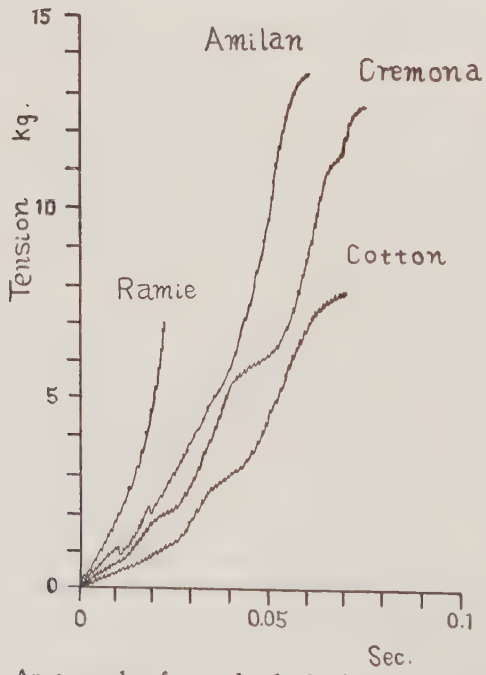

Fig, 3. An example of records obtained with oscillograph.

figure the tensile strength of the netting cords made of cotton and cremona,

respectively, shows increases in a form of stairs. Such phenomena could not be seen in the strees-strain curve under slow tension and it is a tendency only seen in the netting cords of short fibers in tension caused by impact. These phenomena were probably due to the repetition in a discontinuous line of the increase in tensile strength, the shrinkage in diameter (elongation thereby), thereby preventing the mutual slips among fibers which might have taken place otherwise.

In the netting cords made of amilan the fibers of which are seemingly endless there would be not much difference in the break of the cord being caused by the rupture of the fibers themselves no matter whether by slow tension or tension by impact force. Fibers are generally strong against tension along their fibers, but not so against twists. Therefore in the tension by impact the netting cord made of long fibers not being possible to elongate itself in full and naturally the component fibers would receive tension by some greater twist angles by impact force than in the case of slow tension and its tensile strength might have become somewhat smaller. With the netting cord made of ramie showed a similar tendency as the cord of amilan, but as the fiber length of the cord under test was 10 cm, they worked more like long fibers with a thin test cord.

The differences in the tensile strength due to dry and wet conditions of the netting cords were of a similar tendency as in the case under slow tension.

(2) Elongation of the netting cord due to impact

To measure the elongation of the netting cord at the instant of its break by impact force was quite difficult and much accuracy could not be expected from tests. Yet, as the elongation of the netting cord was its important and inherent nature, the measurement was conducted in the following manner.

In the breaking test of the netting cord by means of the impact tester of the pendulum type, the pendulum weight fell from a height of h, that is at degree α and at the instant of passing γ_0 degree, just below the axle of swing it began to pull the netting cord by an impact force. The pendulum swang up to the opposite side pulling the cord and the cord was broken at the point of γ_b degree. Yet the pendulum still continued to swing farther up by its remaining energy and then stopped to swing at γ degree when all the energy had been consumed. The γ degree could be measured by the indicator on the tester, but γ_b degree would not be measured directly. Time required for the pendulum to travel from γ_0 to γ_b degree could however be read from the oscillograph record as shown in Fig. 3. Utilizing this duration of time the number of degree could be determined. The method was to choose several points of $\gamma_1, \gamma_2 \cdots \gamma_n$ degrees which were between γ_0 and γ_b and time recording pick-ups were set up on the scaleplate at each point of such degrees and let the oscillograph record the time at which the pendulum pulling the cord passed the points selected. The speed of the pendulum would fall as it approached γ_b degree, but the result obtained that the speed could be deemed as almost constant when γ_b was within 20°. As the results Fig. 4 could be obtained and thereby to determine γ_b and therefrom the elongation of the netting cord at the

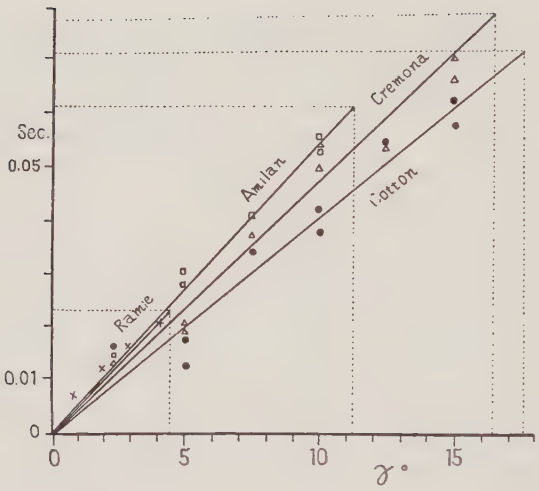

Fig. 4. Relation between swing degree of pendulum and time elapsed (when α is 60°).

instant of its break due to the tension by an impact force. The results are shown in Table 2.

Table 2. Elongation of various netting cords obtained by impact and static test.

Name of cord	Number of hank and yarn	Dry or wet	Static test ε_s (%)	Impact test ε_i (%)	Comparative value $\varepsilon_i/\varepsilon_s$
Cotton	20's, 3/15	D	29	27	0.93
		W	39	—	—
Ramie	10's, 1/2	D	8	7	0.88
		W	9	—	—
Cremona	20's, 3/15	D	28	25	0.89
		W	34	—	—
Amilan	210D, 3/6	D	31	—	—
		W	31	—	—
	210D, 3/12	D	32	17	0.53
		W	31	—	—

As will be seen in the table, the elongation of the netting cord made of short fibers caused by impact force appears comparatively smaller, and the elongation of the netting cord made of amilan still smaller. This phenomenon is to be assumed due to the same reason mentioned in the preceding paragraph.

(3) Breaking energy by impact

a. Effect of impact velocity:

When the netting cord was broken by a single impact whether energy consumed therefor varied by impact velocity or not was another problem. SHIMIDU and NAGATA were negative on that and on the other hand HONDA reported basing on the experiments conducted by his pupils that the breaking energy had varied in proportion to impact velocity. TSUJI through his study on fibers and YAMADA through his study on steel, both stated that in the extent of ordinary impact tests the effect of impact velocity might be neglibible.

Table 3. Influence of impact velocity on cotton netting cord (20′s, 3/15)

Starting angle (°)	V (m/sec)	Tesion (kg)		Energy (kg·m)	
		Dry	Wet	Dry	Wet
40	1.35	7.9	8.9	0.39	0.49
50	1.66	7.9	8.5	0.44	0.50
60	1.96	7.6	9.0	0.38	0.44
70	2.27	8.1	9.1	0.32	0.43

Table 3 show the results of measurement of breaking energy and tensile strength in the test of the netting cord of cotton 20′s 3/15. The effect of impact velocity thereon was not clear.

b. Breaking energy on various netting cords:

Table 4. Energy of various netting cords obtained by impact and static test

Name of cord	Number of hank and yarn	Dry or wet	Static test E_s (kg·m)	Impact test E_i (kg·m)	Comparative value E_i/E_s
Cotton	20′s, 3/15	D	0.27	0.38	1.40
		W	0.30	0.46	1.54
Ramie	10′s, 1/2	D	0.15	0.10	0.67
		W	0.18	0.12	0.67
Cremona	20′s, 3/15	D	0.45	0.46	1.02
		W	0.35	0.59	1.68
Amilan	210D, 3/6	D	0.49	0.39	0.80
		W	0.39	0.46	1.18
	210D, 3/12	D	1.12	0.73	0.65
		W	0.79	0.79	1.00

The breaking energy consumed on various netting cords is shown in Table 4. The energy consumption by impact on the netting cords of cotton or cremona was generally greater than that on statical test. On the other hand, it was comparative small in the case of the netting cord of ramie or amilan.

The breaking energy consumption by impact on wet cords was greater than that on dry cords. Considering this fact together with the value of breaking strength by impact, the elongation of wet netting cords made of synthetic fibers might be expected to be comparatively greater than dry ones of the same fibers.

Summary

Of currently used netting cords there were selected those made of short fibers such as cotton or cremona, those made of long fibers such as amilan and those made of fibers of an intermediate length such as ramie and by using an impact tester of the pendulum type and utilizing electric resistance strain gauge the breaking tests were conducted with the following results:

(1) The tensile strength of the netting cord at its breaking point is constant regardless of the value of impact force and the value of the tensil strength compared with the cases with slow tension was greater in the case of the netting cords made of short fibers and was smaller in the case of the netting cords made of long fibers.

(2) The elongation of the netting cords at the instant of break was smaller in the case of tension produced by impact than that by slow tension

(3) The breaking energy due to impact was in general greater in the case of the netting cords made of short fibers and smaller in the case of those made of long fibers compared with the cases with slow tension.

(4) The netting cord made of ramie showed a nature similar to those of long fibers rather than those of short fibers.

The writer hereby wishes to express his deep appreciation for the thoughtful direction in this experiment rendered by Emeritus Professor Dr. Morisaburo TAUTI of Tokyo University of Fisheries and Dr. Hidetoshi KUSAMA of Tokyo Institute of Technology and also wighes to extend his hearty thanks to Mr. Makoto SUZUKI of Tokyo University of Fisheries for his assistance in the test and to Nippon Gyomo Sengu Kaisha, Ltd. for its generous supply of the test materials.

References

1) M. TAUTI: A study on netting cords, I, III. The strength of the netting cord against the repeated blow. *Jour. Imp. Fish. Inst., Vol.* 23, *P.* 5 (1927), *P.* 130 (1928).

2) Y. KONDO: Influence of the size of cotton yarns composing netting cords on the strength against repeated blows. *Bull. Jap. Soc. Sci. Fish., Vol.* 5 *P.* 171 (1937).

3) H. SIMIDU: Breaking of the netting cord by a single blow. *Bull. Jap. Soc. Sci. Fish., Vol.* 6, *P.* 243 (1938).

4) K. HONDA: On the strength of the netting cord against a single below. *Jour. Tokyo Univ. Fish., Vol.* 38, *P.* 63 (1951).
5) T. NAGATA: On the energy necessary for breaking the netting cord by single blow. *Jour. Tokyo Univ. Fish., Vol.* 40, *P.* 75 (1953).
6) H. KUSAMA and S. KATO: Hippari-sokudo ga amiito hippari-siken kekka ni oyobosu eikyo. *Jour. Fisheries, Vol.* 32, *P.* 123 (1937).
7) H. KUSAMA, Y. KONDO and M. SUZUKI: The distribution of stress on the fishing net *Bull. Jap. Soc. Sci. Fish., Vol.* 21, *P.* 973 (1956).
8) N. OKAZAKI: Kinzoku-zairyo no shogeki-oryoku ni tuite. *Jour. Jap. Soc. Mechanical Engineers., Vol.* 61, *P.* 1451, (1958).
9) M. TAUTI: Studies of netting cords, IV. Strength of cord in relation to the twist. *Jour. Imp. Fish. Inst., Vol.* 25, *P.* 27, (1927).
10) J. M. MATHEW: The textile fibers., (1924) NEW YORK.
11) W. TSUJI: Impact tensile test of single fiber. *Zairyo-siken, Vol.* 1, *P.* 45, (1952).
12) R. YAMADA: Jikkenkogaku-koza, KYORITU-SHA, TOKYO.

Journal of the Tokyo University of Fisheries Vol. 47, No. 1, 1960

STUDIES ON THE STERILIZATION OF *CLOSTRIDIUM BOTULINUM* BY GAMMARAY IRRADIATION

Yutaka Sekine, Tsuneo Kozima* and Sachio Motegi**

(Received June 27, 1960)

Introduction

In the field of food-hygiene, botulism is an important and terrible food-hygiene. Botulism is caused by the toxin of *Clostridium botulinum*, which is produced in food and, if eaten, is expressed by special nervous symptoms and a high mortality rate. Spores of *Cl. botulinum* are widely distributed in the soil, and there exist many opportunities for food to be contaminated by its spores.

Botulism had been overlooked in Japan before 1951, but Nakamura et al.[1] reported the first outbreak of botulism in Japan in 1952. Outbreaks in Japan have almost always proved to be of type E and have been caused by fish products infected with *Cl. botulinum* type E. Dolman et al.[2] pointed out that fish are closely connected with toxin production of *Cl. botulinum* type E and type E botulism is called "fish borne botulism". Fish products are the main protein supply in Japan and the prevention of food-poisoning caused by *Cl. botulinum* type E has an important significance. In this nation fish products are eaten raw occasionally and it is difficult to sterilize fish products by heating. As the spores of *Cl. botulinum*, especially type A and B, have high resistance to heating, sterilization is difficult and is an index to sterilizing of the canned foods. On the other hand, sterilization by means of radiation is termed "cold sterilization" as such rays may kill or inactivate microorganisms without the production of heat. "Cold sterilization" is a very desireble method of sterilizing fish products.

The purpose of this investigation was to study the effect of radiations on the spore suspension and crude toxin of *Cl. botulinum* (type A, B and E), on the toxin produced by radiated spores, and on the spores surviving from imperfect radiation.

Experimental Procedure

a) Preparation of spore suspension and crude toxin

After each type strains were grown separately in liverliver broth at 37°C. for 24 hours, one loop was inoculated to Brain Heart Infusion broth contained 0.5% dextrose on which a layer of sterile liquid paraffin was placed and incubated 10 days at 30°C followed by 10 days at room temperature. They were then centri-

* National Hygienic Laboratory: 2-203, Tamagawa Yoga-machi, Setagayaku, Tokyo, Japan.

** Research Laboratory of Japan Canners Association: 2-2, Marunouchi, Chiyodaku, Tokyo, Japan.

fuged 4,000 r.p.m. for 10 minutes. The supernatant was used for crude toxin and the precipitate were washed twice in M/15 Sörensen phosphate buffer solution of pH 6.0. Then they were resuspended in 10 ml. phosphate buffer solution and were heated for 60 minutes at 60°C. to inactive the vegetative cells. This suspension was used for spore stock solution and preserved in an ice box.

b) Spore counting

The medium used for spore counting was Brain Heart Infusion broth to which was added 0.5% dextrose, 0.1% potassium nitrate and 1.5% agar. The medium was tubed in 10 ml. amounts in special flat tubes and sterilized under steam pressure at 121°C. for 15 minutes. Appropriate dilutions of sample were made in phosphate buffer solution and 1 ml. of the diluted solution was inoculated with spore counting medium. After inoculating about 2 ml. of normal agar with 0.1% sodium thioglycolate was added to each tube of medium. Inoculation was at 37°C. and the counts were determined in 2 or 7 weeks.

c) Toxin production and toxicity test

Toxin production from irradiated spores proceeded in the same manner as the preparation of the crude toxin. Appropriate dilutions of crude toxin were made in gelatin-phosphate diluent and 0.5 ml. of this dilution was injected intraperitoneally into two white mice of 12 to 15 g. weight. The mice were observed for 4 days.

d) Activation of type E toxin

With the type E strain, after the centrifugation of incubated broth, both supernatant (crude toxin) and precipitate (spore) were added to 1/10 volume of 10% trypsin and activated at 37°C. for 120 minutes in the water bath.

e) Radiation

Radiation of type A and B was carried out by using 1,000 curies of gamma rays from radioactive Cobalt-60 in Tokyo University of Fisheries and radiation of type E by using 100 curies of Cobalt-60 in the Scientific Research Institute. The spore suspension was added to the sterilized buffer solution so that each ml. contained the desired spores. One milliliter of the inoculated buffer solution and crude toxin (2 ml. with type E) were added to each sterile glass ampouls (10 mm. diameter, 30 mm. height and 0.25 mm thickness). Ampouls were sealed hermetically and were placed on vertically to radiation source and were radiated at room temperature (9–12°C.).

Results

a) Killing of spores with radiation

The results of the radiation on the spores of *Cl. botulinum* in phosphate buffer are shown in Table 1. Although spores of type A and B could be completely killed with a dose of 600,000 roentgen, type E (VH and Tenno strains) required about 700,000 to 850,000 roentgen. A decrease in spore number was shown as the radiation dose was increased. There existed no marked difference between the three types.

b) Reduction of toxin potency with radiation

Table 2 showed the results of radiation on crude toxin of *Cl. botulinum*.

Potency of toxin of type A and B was not decresaed as the radiation was increased. A radiation of 200,000 roentgen showed only a slight decrease in the toxin potency of type A and B. Complete inactivation of toxin required doses of radiation larger than 200,000 roentgen. But the toxin of type E was destroyed

Table 1. Survival of Cl. botulinum with radiation

a) Type A and B

Radiation dose	Type A		Type B	
	Survival spore		Survival spore	
	Numbers	Per cent	Numbers	Per cent
(*roentgen*)				
0	5,000		7,300	
50,000	1,800	36.0	2,100	28.9
100,000	870	17.4	1,400	19.2
200,000	780	15.6	430	5.8
400,000	100	2.0	26	0.4
600,000	0	0	0	0

b) Type E

Strain	Radiation dose	Survival spore		Strain	Radiation dose	Survival spore	
		Numbers	Per cent			Numbers	Per cent
Tenno	(*roentagen*)			VH	(*roentgen*)		
	0	960			0	7,600	
	33,750	710	74.0		316,800	440	5.8
	49,500	560	58.3		633,600	240	3.2
	58,500	340	35.4		841,600	0	0
	112,500	220	22.9	VH	0	7,200	
	135,000	180	18.8		326,600	460	6.4
	162,000	150	15.6		653,400	20	0.3
	225,000	110	11·4		867,900	0	0
Tenno	0	880					
	79,200	230	26.1				
	118,800	170	20.0				
	237,600	130	14.8				

completely with a dose of 850,000 roentgen. (Table 2–b)

c) Change of potency of toxin produced by irradiated spores

A change of potency of crude toxin was obtained by the cultivation of spores surviving the radiation showed in Table 3. With type A, the potency of the toxin produced from irradiated spores was not changed. But the toxin produced by spores of type B surviving a dose of 400,000 roentgen was complpetely inactivated, and with spores surviving a 50,000 roentgen radiation dose,

Table 2. Destruction of toxin of *Cl. botulinum* by irradiation

a) Type A and B

Radiation dose	Type A				Type B		
	Dilution of crude toxin						
	Original	10×	100×	1,000×	Original	10×	100×
(*roentgen*)							
0	●	●	●	○	●	○	○
	●	●	●	○	●	○	○
50,000	●	●	●	○	●	○	○
	●	●	●	○	●	○	○
100,000	●	●	●	○	●	○	○
	●	●	●	○	●	○	○
200,000	●	●	○	○	○	○	○
	●	●	○	○	○	○	○

b) Type E

Radiation dose	Mouse Intraperitoneal MLD/ml.
(*roentgen*)	
0	8,000
211,000	2,000
316,800	200
633,600	8
841,600	0

the toxin produced showed a decrease of potency. (Table 3–a).

With the type E spores surviving a dose of less than 650,000 roentgen the effect on productive function of toxin could not recognized.

d) Change of numbers of spores surviving repeated radiation

Table 4 shows that results of radiating spores produced by incubating spores surviving radiation. The numbers of type A spores surviving a first radiation dose of 50,000 roentgen was not completely reduced with a second radiation dose of 50,000 roentgen. With type A and B spores surviving a dose of 400,000 roentgen, reduction of spore numbers was not recognized with second radiation dose of less than 200,000 roentgen. When a second radiotion was carried out with a larger dose than 200,000 roentgen, the radiated spores showed a high survival per cent. In other words, when spores survived after insufficient radiation, spores produced from the surviving spores appear to be more resistant to radiation.

Discussion

There are many problems in preserving and sterilizing food by radiation. We obtained the data concerning the destruction of Cl. botulinum in this ex-

Table 3. Toxin production by irradiated spores of *Cl. botulinum*

a) Type A and B

	Radiation dose	Dilution of crude toxin					
		Original	10×	100×	1,000×	10,000×	100,000×
	(*roentgen*)						
Type A	0	●	●	●	●	●	○
		●	●	●	●	●	○
	50,000	●	●	●	●	●	○
		●	●	●	●	●	○
	400,000	●	●	●	●	●	○
		●	●	●	●	●	○
Type B	0	●	●	○	○	○	○
		●	●	○	○	○	○
	50,000	●	○	○			
		●	○	○			
	400,000	○	○	○			
		○	○	○			

b) Type B

		Mouse Intraperitoneal MLD/ml.		
		Supernatant		Preciptitate
Strain	Dose	before activation	after activation	
	(*roentgen*)			
Tenno	0	8	1,600	16,000
	237,600	8	320–2,000	16,000
VH	0	80	800	80,000
	633,600	80	3,200	40,000

periments. Denny et al.[3] reported that *Cl. botulinum* was more resistant to radiation in food than in phosphate buffer solution. In practice the killing of spores of *Cl. botulinum* in food required a large radiation dose.

Morgan and Reed[4] have reported that spores of Cl. botulinum appeared more resistant to radiation than spores of several other food spoilage organisms. When food contaminated by *Cl. botulinum* was sterilized with radiation, it is probable that its spores survived to insufficient dose of radiation. We have not seen the report related to such a case. In the present experiments, toxin produced by spores which had survived radiation was the most radiation resistant, especially was this true with type A. Spores formed by incubation of irradiated spores appeared more resistant to radiation than natural spores. Therefore, in the radiation sterilization of food, it is necessary to use a radiation dose sufficiently large to kill all organisms.

Table 4. Change of numbers of spores surviving repeated radiation

Type	Radiation dose		Survival spores	
	1st radiation	2nd radiation	Numbers	Per cent
A	(*roentgen*)	(*roentgen*)		
	50,000	0	38,000	
		50,000	38,000	100.0
		100,000	26,000	68.4
		200,000	16,000	42.1
		400,000	1,400	3.7
	400,000	0	68,000	
		50,000	68,000	100.0
		100,000	68,000	100.0
		200,000	18,000	26.4
		400,000	6,000	8.8
B	400,000	0	6,000	
		50,000	6,000	100.0
		100,000	6,000	100.0
		200,000	2,000	33.3
		400,000	240	4.0

Summary

The resistance to gamma radiation of *Clostridium botulinum* (type A, B and E strains) spore suspensions and crude toxin was determined by exposure to Cobalt-60. The results are as follows;

1) Spores of type A and B were killed with a dose of 600,000 roentgen, but to destroy type E spores required over 700,000 or 850,000 roentgen.

2) Inactivation of crude toxin required radiation doses larger than 200,000 roentgen. Toxin of type E was destroyed completely with a dose of 850,000 roentgen.

3) Potency of crude toxin produced by irradiated spores of type A was not reduced with a dose of 400,000 roentgen. With type B spores surviving a radiation dose of 400,000 roentgen, the produced toxin was completely inactivated. Toxin produced by spores surviving a dose of 650,000 roentgen was not destroyed.

4) When spores formed by cultivation of irradiated spores were radiated repeatedly, they appeared more resistant to radiation.

In closing, we wish to express our heartful thanks to Dr. I. Okada, Dr. T. Kikuchi, Mr. T. Hirano and Dr. S. Okano for their assistance with the radiation techniques.

Literature

1) NAKAMURA, Y., et al. 1952: Special report on botulism occuring in Hokkaido, Japan. Report of Hokkaido Hygienic Laboratory, Special report. (in Japanese)

2) DOLMAN, C. E., CHANG, H., KERR, D. E. and SHEARER, A. R., 1950: Fish borne and type E botulism, two case due to home pickled herring, Canad. J. Publ. Health, 41, 215-228.
3) DENNY, C. B., BOHRER, C. W., PERKINS, W. E. and TOWNSEND, G. B., 1959: Destruction of Clostridium botulinum by ionizing radiation I. In neutral phosphate at room and freezing temperature, Food Research, 24, 44-50.
4) MORGAN, B. H. and REED, J. M. 1954: Resistance of bacterial spores to gamma irradiation, Food Research, 19, 357-366.

Journal of the Tokyo University of Fisheries Vol. 47, No. 1, 1960

STUDIES ON THE SAPROLEGNIASIS OF EEL

Toshikazu Hoshina, Tokuo Sano and Mariko Sunayama*

(Received June 27, 1960)

As the senior author has informed[8], recently the disease is every year occurrence at spring time in eel-culture ponds in some districts of Japan and there is a great deal of damage to the fish, therefore the adequate control of the disease is desired. The present study was commenced with the view of finding the basic knowledges for the setllement of the problem. Though it is so far from a solution of the problem, we wish to make here a report of the results obtained up to the present.

Before going to the subject, we must acknowledge our indebtedness to Messrs. Yūji Kubota, Chief director of Fish Cultural Fisheries Co-operative Association of Haibara, Shizuoka Pref. and Hiroshi Noguchi, Director of Hamana Branch Station of Shizuoka Prefectural Fisheries Experiment Station for their aids in the supply of materials necessary to the present study.

Further we thank the Ministry of Education for the expense of the present study, partly defrayed by Grant in Aid for Experimental Scientific Research.

1. Characteristics of the disease

The diseased eels, *Anguilla japonica*, allow the infection of a aquatic fungus on the head, especially around the snout, on the caudal part or somewhere on the body surface and a large numbers of them vigourlessly swim near by the surface of water. Some of them heal naturally by falling off the fungus, but numbers of them fall into death within several days. During the epidemic period, eels do not swarm into feeding ground and also they do not at all feed. It is comparatively short, from early March to early May (about 15°C in water temperature). It is characteristic of the present disease to bring as great loss as incomparable to other various diseases on eel. Water temperature increasing nearby 20°C, the condition of the disease rapidly grows less serious and the eels recover. However, the epidemic does not only occure in spring, also, in late autumn, eels being handled.

Fig. 1. Showing the fungus on the affected part. ×ca. 1/2

Anatomical findings on the diseased animals are as follows. At first, the affected parts being covered by a fungus threads (Fig. 1), according to the

* Formerly Ookubo; Faculty of Science, Tôhô University.

lapse of day, hyphae are abundantly sticked by phytoplanktons or muddy particles, becoming dirty. The skin ulcerates or exfoliates, becoming hemorrhagic. Affected ones on head show that, at the result, the jaw bones expose or some of them become blindness. And also, occasionally mouth cavity is affected by the fungus. From these characters, eel culturists in the district call the present disease "Sure".

The aquatic fungus found on the diseased eels is a single species as far as we investigated (May, 1956, April and Dec. '58) and identified with *Saprolegnia parasitica* Coker.

The hyphae penetrate from epidermis to cutis at the site of infection, occasionally through the superficial layer of muscle. The fungus rapidly grows and the affected part is covered up with the hyphae. By and by, the epidermis of the part collapses or ulcerates and the part of lesion is contaminated by aquatic bacteria. Although there is reported a Saprolegniaceous fungus to parasitize fish *per os* by Davis[4], an experiment was undertaken to determine whether the present fungus attacks eel through mouth, by examinating the smear preparations of the tissues of heart, liver, spleen, and kidney of 5 healthy eels and 12 diseased ones (100~200 g in weight), as well as isolating fungus from these organs. The result was negative on all. Accordingly, the present fungus infects directly the fish from the surface. The vegetative life of the fungus is not so long and the hyphae growing closely, they decline rapidly with developing lesion, probably owing to want of nutriments in the part of the influence of bacteria. As Mazilkin (1957) stated the fungus showed the feeble growth under the propagation of bacteria and he succeeded in the control of the fungus by a kind of myxobacteria, and also, the fungus activity was influenced, in our observation. On the other hand, bacteria are found in the debris of the lesion, and the bacteria may help the change for the worse of the disease.

However, Vishinac and Nigrelli (1957) stated that little or no bacterial infection was present in any of the sections of pathological lesions of platyfishes, *Xiphophorus maculatus*, infected artificially with saprolegniaceous fungi and also, the fishes died due to the infection.

Among the eels affected by the foungus, there are many eels showing "Rotseuche" and infecting with bacteria at the same time. Accordingly, it is undeniable that bacteria influence for the present diseased eel. At any rate, it is evident that the fungus takes a great *rôle* in the cause of disease and lethal factor, from the facts that artificially infected fishes with the fungus die and also, water temperature rising over 20°C, the mortality of eel decreases remarkably with the disappearance of the fungus.

From the above-mentioned pathological symptoms, the present disease is similar to so called "Salmon disease"[16].

2. Bacterial examination of the diseased eel

Forty six diseased eels weighing from 9.0 to 137.0 g obtained from some eel culture ponds in Kawajiri district on 26, April of 1958, were used for the

study. Microscopical examinations were carried out on the smear preparations of the tissues of heart, liver, spleen, and kidney of them. As the results are shown in Table 1, various species of bacilli were found in any organ of all individuals.

Table 1. Bacterial examination of the diseased eel.

Nos. of eel examined	Numbers of eel infected with bacteria			
	Heart	Spleen	Kidney	Liver
46	29	36	37	33

3. Some biological studies of *Saprolegnia parasitica* Coker

Formation of sexual reproductive organ: The present species has been considered as sterily one by many authors until the sexual organ is discovered by Kanouse (1932). Culured the fungus on hemp seed for about two weeks at 7–12°C, numerous sexual organs were found (cf. Fig. 2). On observation under microscope, oogonia are apical and intercalary form and they occurred at a

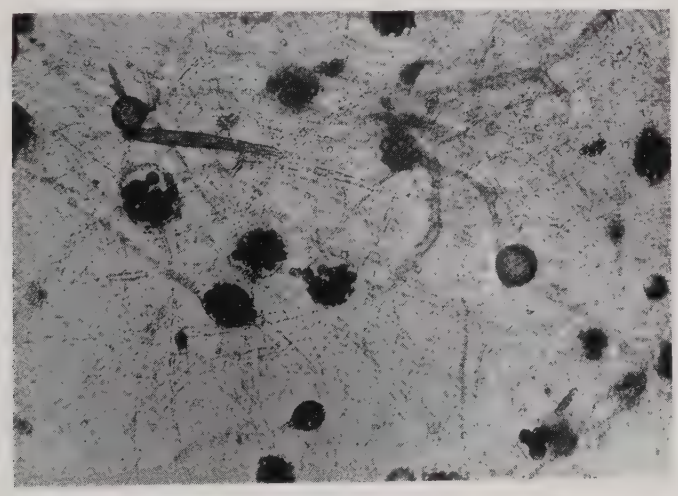

Fig. 2. Showing the oogonia. ×ca. 80

ratio 2.1 of apical to 1.0 of intercalary on 125 oogonia observed. Apical oogonia are mainly spherical, from 48.7 μ to 83.9 μ in diameter. Intercalary ones are oval or pear-shaped, from 53.6–86.6 $\mu \times 39.1$–60.6 μ in dimension. The oogonial wall is rather thin, transparent and smooth. The young oogonia are filled up with obscure, gray or brown granular substances and spherical oil drops. Mature ones contain mostly 2–20 oospores, of 18.2–31.2 μ in diameter, averaging 23.2 μ, but large intercalary ones are filled occasionally with eggs exceeding 30. Eggs with membrane of 0.6–1.3 μ thick, are spherical. In general, antheridia present

on nearly all oogonia, and they are rather androgynous than diclinous. The both organs are seen rarely on single oogonium. Antheridial branches are long and rambling. Mature antheridia are mostly pear-shaped and the fertilizing tubes were often observed in oogonia. Young antheridia are nearly spherical, without fertilizing tubes.

The sexual reproductive organs approximately coincide with the description of KANOUSE (1932).

An attempt was made to test whether the oospores of these oogonia would germinate.

About 60 oospores were separated into the hole object-glass containing steriel water by breaking the wall of oogonia, and they were spreaded out on agar-plate containing 1% yeast extract, on which penicillin G of about 2,000,000 units was administrated. The culture, for 4 days at room temperature (12.0–19.3°C) showed the numerous colonies of the fungus. At the lapse of about 24 hours after germination, the new mycelia considerably elongated and were measured 4.6–8.1 μ in diameter. Oospore may extend outward a germ tube. Under the micro-culture, an oospore just germinating from one point of the surface was observed.

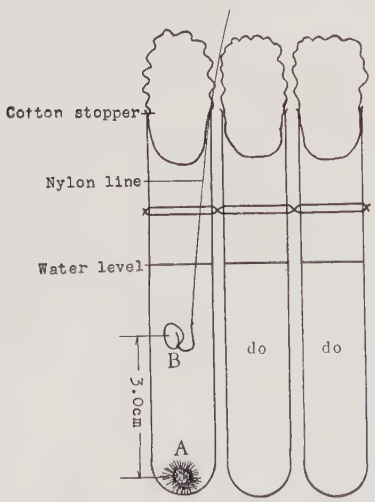

Fig. 3. Showing the set of test tubes.
A, fungus grown on hemp seed, the hyphae ca. 5 mm in length, cultured at room temperature.
B, boiled hemp seed on fish hook, kept at 3 cm. from A.

The micro-culture was made by following method. Oospores were placed on a hole object-glass containing a small amount of agar medium of 1% yeast extract contained penicillin G (about 1000 units per cc.). After that, it was mounted with paraffin.

The pure culture of the fungus was obtained after several subcultures by using antibiotics. This strain was used for the subsequent study.

Relation between the fungus and the water temperature: The present work was attempted to determine the relation between the development of the fungus and the water temperature. A set consisting of three test tubes prepared as shown in Fig. 3, was placed at each definite temperature by using Tauchi's thermostat. The experiment was continued for 17 days and the observation was made two times a day. Found mycelia on B, the development must be due to the zoospore discharged from A, and the detailed observation proved that it was identical A-fungus, too.

The results are summarized in Table 2. Namely, at 0.1°C, the best growth of A occurred after 10 days, but it was only mycelial growth as clear from the table; at 4.1°C, the best growth after the 5th day and B showed the growth of fungus at the same day, it began to decline after 9 days; at 7.2°C, after 2 or 3 days better growth, the maximum on 4 days, fell after 8 days, the fungus

occurred on B after 3 days. At 10.6°C, showed vigourous growth on 3rd day and from 8 days declined, B showed the fungal growth on 4 days; at 13.8°C, A showed remarkable growth from 2 to 4 days, declined after 7 days; the fungus was found on B, 5 days; at 17.9°C, A showed remarkable growth, as well as the preceding from 1 to 3 days, and showed tendency to decline on 6 days, on B the new growth, on the same day; at 21.2°C, A showed somewhat

Table 2. The relation between the fungal development and the water temperature.

Days passed / Hemp seed / Water temperature °C	1		2		3		4		5		6		7		8		9~12		Formation of oogonium
	A	B	A	B	A	B	A	B	A	B	A	B	A	B	A	B	A	B	
0.1													+	−	+	−	##	−	
4.1			+	−	##	−	##	−	###	+									+
7.2	+	−	##	−	##	+	###												+
10.6	+	−	##	−	###	−	##	+											+
13.8	##	−	###	−	###	−	###	−	##	+									+
17.9	###	−	###	−	###	−	##	+											
21.2	##	−	##	−	+	−	+	−											
24.7	##	−	+	−		−													
28.3	+	−		−															
32.3	+	−																	

Remarks: A, hemp seed with the fungus, B, hemp seed without the fungus; +, visible growth, ##, good growth, ###, excellent growth, −, no growth.

inferior growth than the growth at 13.8 or 17.9°C, declined 3 days after and B showed no growth; at 24.7°C, it showed better growth 1 day after, declined the next day, B was as same as the preceding; at 28.2 and 32.3°C, slight growth on 1 day, and fell 2 days after.

The subculture of A at 21.2°C for 5 days, on 1% oatmeal agar-plate, proved live (at room temperature), but each at 24.7, 28.2 and 32.3°C proved dead.

A in each test tube was preserved in 10% formalin after the experiment. Under the microscope, A at 0.1°C showed few ramification, slender, without sporangia, gemmae and oogonia; A at 4.1 and 7.1°C showed moderately thick and branched hyphae, sporangia, gemmae, occasionally empty sporangia and completed oogonia; the hyphae of A at 10.6°C was considerably branched, secondary sporangia, germinating zoospores and numerous oogonia were found; the hyphae at 13.8 and 17.9°C grew as the preceding, numerous secondary sporangia, gemmae and a large number of oogonia were found. A at 21.2°C did not form oogonia. Compared A at 13.8°C with A at 17.9°C, mature oogonia were found more abundantly in the former.

In brief, the fungus produces zoospore at 4.1–17.9°C, and, judging from above mentioned results, the optimum temperature of the fungus to grow may be about 14°C.

Resistance of the fungus against some disinfectants: The study dealing with the resistance of the fungus against various chemicals was made by ARASAKI, *et al*, and also the attempts to the control of fungi by chemicals, *e.g.* formalin, malachite green, common salt and etc. were made by many scientists. The studies on the fungus-static action of some disinfectants mainly were tried by us.

(a) On the action of malachite green, bleaching powder and copper sulphate against the fungus.

Hemp seed A (with fungus grown) and B were put into the test tubes (5 tubes used for every concentration) containing 10 cc. of definite concentration of the disinfectants, as illustrated in Fig. 3, the tubes were observed every day whether the development of the zoospores would occur. The experiments

Table 3. The influence of malachite green, chlorine water and copper sulphate on the fungus (continued on the next page).

Concentration \ Days passed		1		2		3		4~10	
Concentration \ Hemp seed		A	B	A	B	A	B	A	B
Malachite green	1:10,000,000	−	−	−	−	−	−	−	−
	1:20,000,000	−	−	−	−	±	−	±	−
	1:30,000,000	−	−	−	−	−	−	+	−
	1:40,000,000	−	−	−	−	−	−	+	−
	1:50,000,000	±	−	±	−	±	−	+	−
	Control	++	−	++	−	++	+		

Chlorine water* Concentration \ Days passed / Hemp seed	1		2		3		4～7	
	A	B	A	B	A	B	A	B
1:100,000～1:300,000	±	−	±	−	±	−	±	−
1:400,000	±	−	±	−	+	−	+	−
1:500,000	±	−	+	−	+	−	+	−
1:600,000	+	−	+	−	+	−	+	+
1:700,000	+	−	+	−	+	−	+	+
1:800,000	+	−	+	−	+	−	+	+
1:900,000	+	−	++	−	++	−	++	+
1:1,000,000	++	−	++	−	++	−	++	+
Control	++	−	++	+				

Copper sulphate Concentration \ Days passed / Hemp seed	1		2		3		4～5	
	A	B	A	B	A	B	A	B
1:10,000～1:30,000	−	−	−	−	−	−	±	−
1:40,000	±	−	+	−	+	+		
1:50,000	±	−	++	−	++	+		
1:60,000	++	−	++	+				
1:70,000	++	−	++	+				
1:80,000	++	−	++	+				
1:90,000	++	−	++	+				
1:100,000	++	−	++	+				
Control	++	+						

Remarks: ±, invisible growth, +, visible growth, ++, good growth, −, no growth;
A, hemp seed with the fungus, B, hemp seed without the fungus.
* was made from breaching powder, which the active chlorine was determined.

were tried at 10.0–15.5°C. The results obtained are compiled in Table 3.

Malachite green of the concentration of 1:10,000,000 inhibited completely the fungus-growth; although the dilution over 1:20,000,000 a little the growth, it did no the zoospore-formation. The subculture of the fungus on A proved; all in 1:6,000,000 dead; 3 out of 5 in 1:7,000,000 and 4 out of 5 in 1:8,000,000 live; all in the dilution over 1:9,000,000 live. Chlorine water of the concentration of 1:100,000–1:300,000 retarded considerably the growth. B showed the fungus-growth after 4 days in the dilution over 1:600,000. In the case of copper sulphate, the fungus-growth was arrested for 3 days by the concentration of 1:10,000–1:30,000; zoospore-formation was observed in the dilution over 1:40,000.

Table 4. Influence of malachite green against the germination of zoospore.

Concentration \ Days passed / No. of test tube		1	2	3	4	5~7
1:5,000,000~ 1:10,000,000	(1)	−	−	−	−	−
	(2)	−	−	−	−	−
	(3)	−	−	−	−	−
	(4)	−	−	−	−	−
1:20,000,000	(1)	−	−	−	−	−
	(2)	−	−	−	−	−
	(3)	−	−	−	−	−
	(4)	−	−	−	−	−
1:30,000,000	(1)	−	−	−	−	−
	(2)	−	−	−	−	−
	(3)	−	−	−	−	−
	(4)	−	−	−	−	−
1:40,000,000	(1)	−	−	+	+	+
	(2)	−	−	−	+	+
	(3)	−	−	−	−	−
	(4)	−	−	−	−	−
1:50,000,000	(1)	−	−	+	+	+
	(2)	−	−	+	+	+
	(3)	−	−	−	+	+
	(4)	−	−	−	−	+
Control	(1)	+	+	+	+	+
	(2)	+	+	+	+	+
	(3)	+	+	+	+	+
	(4)	+	+	+	+	+

(b) Malachite green and the germination of zoospore.

Zoospores obtained from the fungus grown on hemp seed were suspended in sterilized water (containing about several hundreds of penicillin per cc.), and 1 cc. of the water was added to 9 cc. of malachite green solution, the concentration of which was prepared as the solution becomes a definite concentration by

the procedure. And then, a boiled hemp seed was hung by fish hook. The experiment was continued for a week under the temperature of 11.4–12.6°C. The results are shown in Table 4.

Although the germination was seen in all the control test tubes only a day after, it was not seen in all the tubes of 1:30,000,000. It was seen in the 2 tubes of 1:40,000,000 after 3 days and in the all of 1:50,000,000 after 5 days.

(c) The concentration of malachite green to kill zoospore.

The zoospores (on resting) dipped in the malachite green solution of a definite concentration for a definite time were cultured on the agar-plate of 1% yeast extract (0.2 cc. of the water containing the zoospores was added to 1.8 cc. of malachite green solution; the concentration was determined by the same method as in the preceding experiment; for the culture, the material was smeared on the plate by using a nichrome loop (2 mm.×0.6 mm.); one loop full of the material contained 20~30 spores). The results showed that the spores were killed by the concentration of 1:200,000 in 20 minutes; 1:300,000 in 20 min.; 1:400,000 in 50 min.; 1:500,000 in 70 minutes.

On the germination of zoospore under the condition of free oxygen: Maurizio (1899) ascertained on 5 species of Saprolegniaceous fungi that the growth of them were feeble under insufficient oxygen, but whether the germination of zoospore would occur in free oxygen, it had been studied by any one. The experiment was carried out in following method. Boiled hemp seed and the fungus grown on the seed were put in Petri dish containing 10 cc. of sterile water. The dish was kept in free oxygen. As the control, another Petri dish prepared similarly was placed under the ordinary condition. These cultures were continued for 5 days under room temperature. As Fig. 4 shows, the fungus-growth appeared on the hemp seed in the control dish and it became vigourous day by day. On the contrary, the fungus-growth was not at all seen in the experimental dish. Therefore it is clear that the fungus reproduction is impossible in free oxygen. And, from this fact, it is conjectured that the fungus may not propagate itself in the mud of bottom of eel-culture ponds, being generally insufficient oxygen.

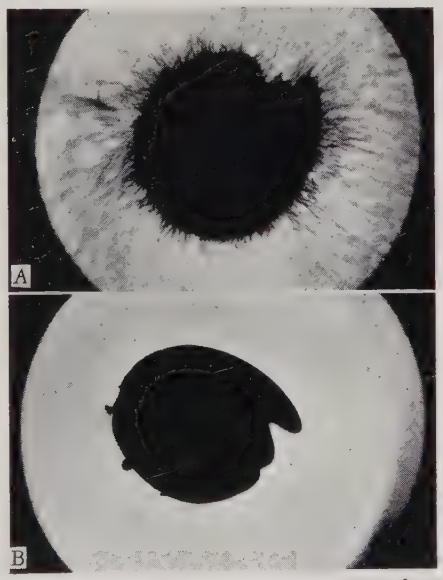

Fig. 4. Showing the fungus-growth.
A, the control hemp seed.
B, the experimental hemp seed.
×ca. 5

On the toxicity of the fungus to eel: The experiments were carried out to make sure whether the fungus possessed a toxic substance to eel, in following methods. 2.1 g. of mycelial mat collected from the fungus grown on hemp

seeds (cultured for 9 days), washed in sterile water, after 2.5 cc. of the water added, was ground by homogenizer and centrifuged. Thus, a milky white liquid containing 20 mg. of the substance per cc. as dry matter was obtained. Two experimental groups each consisting of 4 eels ranging from 87.0 to 94.3 g. in weight, were received intramuscular injection with 0.1 cc. and 0.05 cc. of the liquid, respectively. The fishes of each group were preserved in an aquarium of 9.0–12.0°C for 50 days. The injection caused swelling and hemorrhage at the site is inoculation but it was not lethal for all the fishes.

Next, suspension of dried hyphae was used for the experiment. 6.5 g. of mycelial mat, washed in sterile water, dehydrated in vacuum, was pulverized in mortar. The powder was suspended in sterile water as the liquid contained 20 mg. of the powder per cc. Two groups of eels were injected intermuscularly with 0.1 cc. and 0.05 cc. of the liquid, respectively, and the fishes were observed under the same condition as in the preceding experiment. The fishes showed only swelling and hemorrhage at the site of the inoculation and they survived during the experiment. After the experiment, they were dissected, but any pathological change on viscera was not found.

Further, the following experiment was tried. The pure culture of the fungus was made by using of 1% polypeptone solution at room temperature. The culture showed luxuliant fungus-growth but the liquid was transparent. After 5 days, the liquid was used for the experiment. Two groups, each consisting 5 eels weighing from 41.6 to 60.0g., were received intramuscularly injection with 0.5 cc. and 1.0 cc. of the liquid, respectively. For control eels, the intramuscular injection with 1.0 cc. of polypeptone solution were given. All the fishes survived without any sign of abnormality during the experiment (30 days).

Judging from these results, it is thought that the present fungus may not possess in itself a toxic substance or excrete a toxic metabolite.

The reason that the fishes parasitized aquatic fungi are fatal, is still obscure. The more detailed pathological study is required to make clear this point.

4. Aquatic fungi in eel-culture ponds

Though there are not a few studies on the aquatic fungi in Japan, the saprolegniaceous flora in fish-culture ponds are not studied at all. It may be not worthless for accomplishment of the object to make clear the fungus flora in eel-culture ponds. Therefore, the present work was attempted.

Nine ponds (A–I) in Kawajiri district were appointed an object of the study. The outline of these ponds is as follows:

A, Area, 5,700 sq. m.; Bottom, clayey mud; Loss of eel due to the disease, slight, about 65 kg.
B, 1,280 sq. m.; 〃 , sanded and clayey mud; 〃 , about 2,000 kg.
C, 6,100 sq. m.; 〃 , clayey mud; 〃 , 660 kg.
D, 5,100 sq. m.; 〃 , sanded mud; 〃 , about 3,000 kg.
E, 4,300 sq. m.; 〃 , clayey mud; 〃 , practically no loss.
F, 3,500 sq. m.; 〃 , clayey mud; 〃 , do.

G, 4,400 sq. m.; 〃 , sanded mud; 〃 , do.
H, 4,300 sq. m., 〃 , sanded and clayey mud; 〃 , more than 550 kg.
I, 4,200 sq. m.; 〃 , sanded and clayey mud; 〃 , 316 kg.

The location of each pond is shown in Fig. 5.

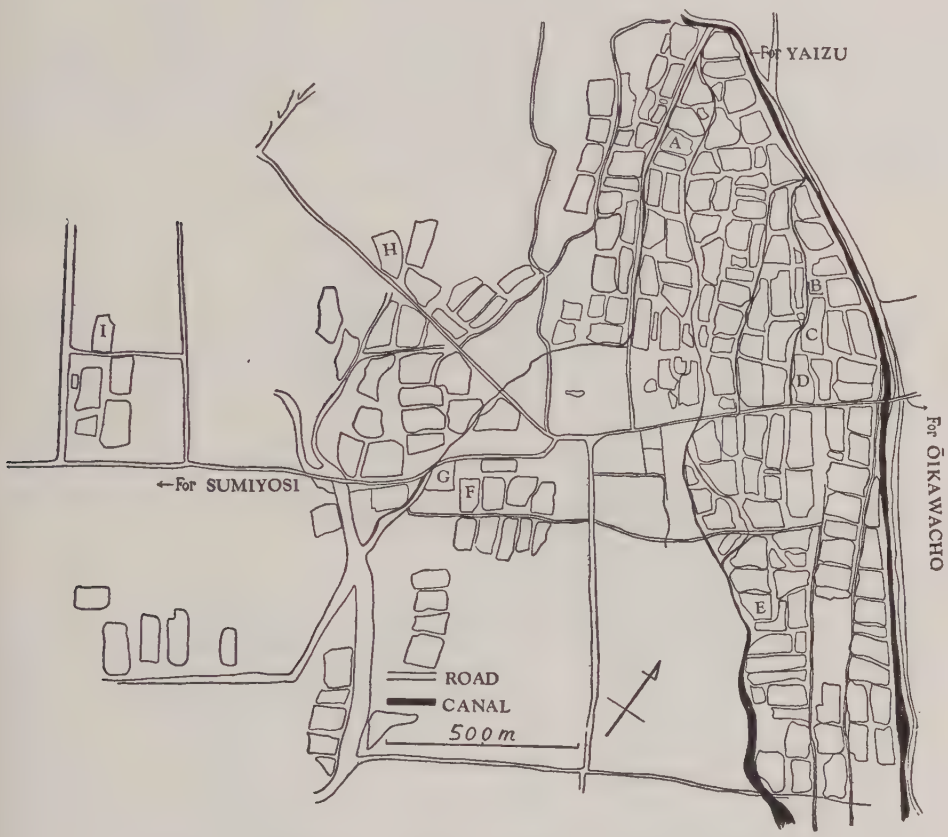

Fig. 5. Showing the eel-culture ponds in Kawajiri district, Shizuoka Prefecture.

The mud collected from each pond and transported (packed in ice) to our laboratory was employed for the isolation of water fungi. For obtaining the fungus cultures, 10 g. of the mud was placed into a Petri dish, and suitable amount of sterile water and boiled hemp seeds were added. The cultures were made by using ten Petri dishes per pond. Five to seven days after, if the fungi became visible, they were transferred into other Petri dishes to maintain the cultures and identified. The experiments were carried out once a month from April, '58 to May, '59 excepting May and July to October in '58.

From the above-mentioned experiments, thirteen species of saprolegniaceous fungi were detected in all. They are as following.

1) *Saprolegnia ferax* (Gruith) in Am. Sci. Nat., **3**, 214, Pl. 22, (1950); Coker, Saproleg., 40, Pls., 11, 12, (1923) et North Amer. Fl. **2**, 22, (1937). Syn. *Conferva ferax* Gruith in Nova Acta Acad. Leop. Carol. **10**, (2), 455, (1821); *Saprolegnia*

Thureti deBary in Abh. Senck. Nat. Ges. **12**, 326, (1881); Migula Krypt. Fl. III Pilze **1**, 66, Pl. 2, figs. 4–7, (1936); Kobayashi et Ookubo in Sci. Research. Ozegahara Moor, 568, (1954).

2) *S. diclina* Humprey in Trans. Amer. Phil. Soc., **17**, 109, Pl. 17, figs. 50–53, (1892); Coker, Saproleg.; Nagai, in Jour. Fac. Agr. Hokkaido Imp. Univ., **32**, 4, Pl. 1, figs. 12–21, (1931). Syn. *Saprolegnia dioica* deBary (not Pringsheim nor Schroeter) in Bot., 2 et 46, 619, Pl. 10, figs. 12, 13, (1888); Fischer in Rabenn. Krypt. Fl. 1 (4), 335, (1892); Schroeter in Engl. et Prantl., Natül. Pflanzenfam., **1**, (1), 98, (1897); von Minden, in Krypt. Fl. Mark Brand, **5**, 512, (1915); Ookubo in Nagaoa, **4**, 53, fig. 42, (1954).

3) *S. delica* Coker, Saproleg., 30, (1923) et in Nort. Amer. Fl. **2** (1), 21, (1937).

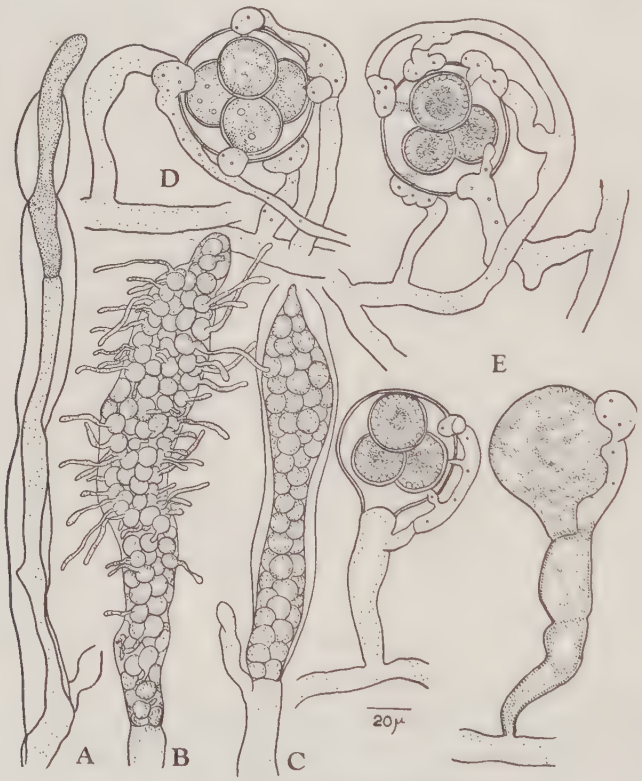

Fig. 6. *Saprolegnia delica.*
A, zoosporangium; B, zoosporangium, the spores sprouting through the wall; C, zoosporangium; D, oogonium with antheridia (androgynous and diclinous); E, oogonium with androgynous antheridium.

Main hyphae more or less 20 μ in diameter. Zoosporangia apical or on lateral branches; zoospores sprouting occasionally in the zoosporangium as Aplanes-type. Oogonia spherical, growing on apex of main hyphae or on lateral branches; the wall smooth and hyaline, 40–60 μ in diameter, bearing 2–7 eggs.

Eggs spherical, centric, 25–28 μ in diameter. Antheridial branches androgynous or diclinous, well developed and attaching on the oogonium (cf. Fig. 6, A–E).

4) *S. parasitica* Coker in Saproleg., 57, Pl. 18, (1923). Syn. *Isoachlya parasitica* Nagai, in Journ. Fac. Hokkaido Imp. Univ., **32**, 12, Pl. 2, figs. 27–34, (1931).

5) *Pythiopsis cymosa* deBary in Bot. Zeit., 46, 632, Pl. 9, fig. 1, (1888); Berlese et DeToni in Sacc. Syll. Fung., 9, 346, (1891); Fischer, Rabenn, Krypt. Fl., **1** (4), 328, (1892); Humpherey, in Trans. Amer. Phil. Soc., **17**, 113. Pl, figs. 60–68, (1892); Schroeter, in Engl. u. Prantl., Natül. Pflanzenfam., **1**, 97, (1897); von Minden, in Krypt. Fl. Mark Brand, **5**, 563, Textfigs. 3a, b, (1915); Coker, Saproleg., 18, Pl. 1, (1923); Nagai, in Jour. Fac. Agr. Hokkaido Imp. Univ., **32**, Pl. 1, figs. 1–11, (1931).

Hyphae slender, 15–22 μ broad, tapering distally. Sporangia globular or clavate; spores 8–10 μ in diameter. Oogonia spherical, oblong or pear-shaped; the wall smooth, without pits, 15–30 μ in diameter, containing one egg. Oospores eccentric, 15–18 μ in diameter. Antheridial branches short, clavate, occuring one or two on each oogonium (cf. Fig. 7, A–E).

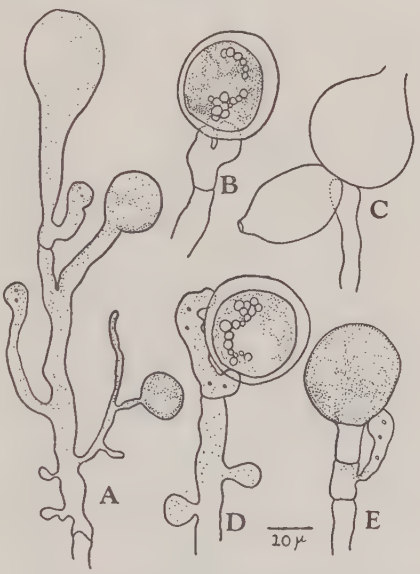

Fig. 7. *Pythiopsis cymosa.*
A, immature oogonia; B, D, E, oogonium with antheridium; C, zoosporangia.

6) *Isoachlya* sp.

Hyphae slender, with a few ramifications, 29–35 μ broad at the proximal part and 10 μ or more at the distal part. The young threads showing dark brown colour. Secondary zoosporangia lateral growth or rarely, regrowing from primary one. Zoospores 8–10 μ in diameter, escape from apical pore of the zoosporangium. Oogonia apical or lateral growth, globose, 30–45 μ in diameter, containing several numbers of eggs. Oospores spherical, light yellow, 10–15 μ in diameter. Antheridia androgynous, generally short and not branched, clavate, attaching to oogonia. (cf. Fig. 8, A–H).

The present species is similar to *Isoachlya terrestris*, but it is distinguishable one from the other by the differences in oospore. The oospore of the present species without a large eccentric oil globe and smaller than that of *Isoachlya terresris*.

7) *Achlya racemosa* Hildebrand, in Jahrb. Wiss. Bot., 6, 249, Pl. 7, (1867); Coker, Saproleg., 106, Pl. 14, 31, (1923); Nagai, in Journ. Fac. Agr. Hokkaido Imp. Univ., **32**, 13, Pl. 3, figs. 9–14, (1931); Schrot, in Engl. Natül. Pflanzen fam. 1, 99, fig. 78a, A-C, (1897); Coker et Matthews in North Amer. Fl. **2** (1), 32, (1937); Ito, Myc. Fl. Japan, **1**, 81, fig. 33, (1936); Kobayashi et Ookubo, in Sci.

Research Ozegahara Moor, 565, fig. 5, (1954).

8) *A. proliferoides* Coker, Saproleg., 115, Pl. figs. 1–10, (1923) et in North Amer. Fl. **2**, 37, (1937); Kobayashi et Ookubo, Jap. Jour. Bot., **27**, 110, fig. 7, (1952).

9) *A. Oryzae* Ito et Nagai, in Jour. Fac. Agr. Hokkaido Imp. Univ., **32** (1), 17 Pl. 4, figs. 3–11, (1931); Ito, Myc. Fl. Jap., **1**, 84, fig. 34, (1936); Ito, in Jap. Jour. Bot. **18**, 127, (1942); Kobayashi et Ookubo, Jap. Jour. Bot., **27**, 106, fig. 9, (1952).

10) *Aphanomyces stellatus* deBary, Jahab. Wiss. Bot., **2**, 178, (1859). Nagai, in Jour. Fac. Agr. Hokkaido Imp. Univ., **32**, 13, Pl. 7, figs. 18–22, (1931).

Hyphae branched moderately, slender, 5–7 μ in diameter. Sporangia long,

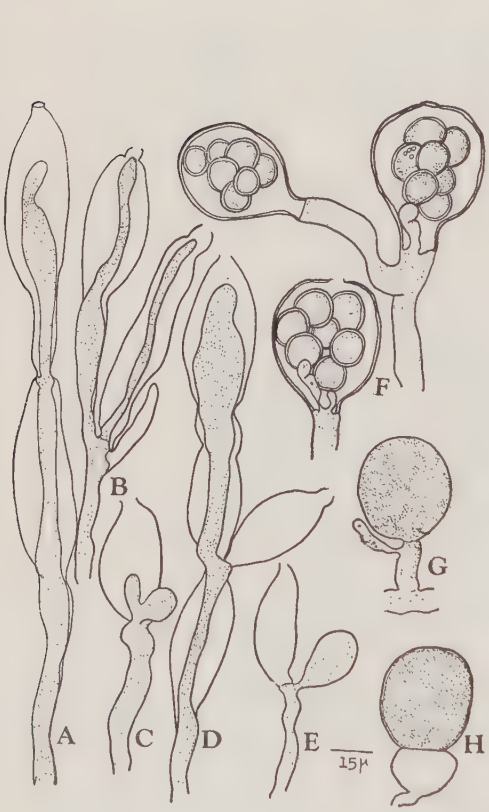

Fig. 8. *Isoachlya* sp.
A, B, C, D, E. zoosporangium; F, G, oogonium and antheridium; H, oogonium.

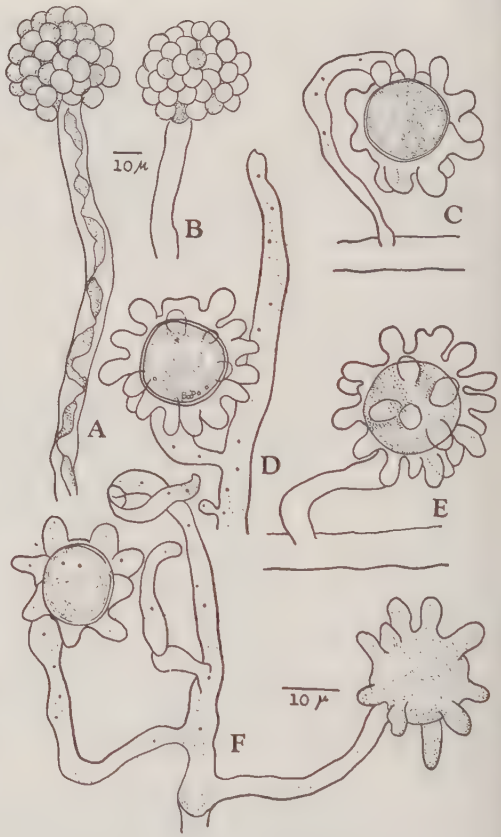

Fig. 9. *Aphanomyces stellatus.*
A, B, zoosporangium and escaped zoospores; C, D, E, oogonium; F, oogonium and antheridium.

as broad as hyphae and apical. Zoospores in the zoosporangium irregular, rod-shaped, agglomerate forming a mass near by apical pore of the sporangium, and after a resting period swim out, about 8 μ in diameter. Oogonia spherical

or subspherical 20–32 μ including papillae, with lateral branches and numerous blunt papillae, the former long or short; the later 5 μ in length each, containing one oospore. Oospores 16–25 μ in diameter, with thin membrane without pits. Antheridial branches short tuberous arising from main hyphae or oogonial stalks, adhering by side to the wall of oogonia (cf. Fig. 9, A–F).

11) *Brevilegnia* sp.

Hyphae little branched; main hyphae 15–20 μ in diameter. Zoosporangia apical; thin-walled, hyaline; the wall disappearing at maturity of zoospores and and the zoospores going on liberation. Oogonia terminal on main branches or on lateral branches, 25–30 μ in diameter, containing one or two eggs with a oil drop being 20–30 μ in diameter. Antheridia arising from directly beneath the oogonium, attached to the sides of oogonium (cf. Fig. 10, A–E).

12) *Apodoachlya brachynema* (Hildebrand) Pringsheim, Berichte Deutsch. Bot. Gesell., **1**, 289, (1883). Syn. *Leptomitus brachynema* Hildebrand in Jahrb. Wiss. Bot., **6**, 261, Pl. 16, figs. 12–23, (1867–68).

Hyphae cylindrical, constricted, 5–8×60–140 μ in size. Sporangia apical,

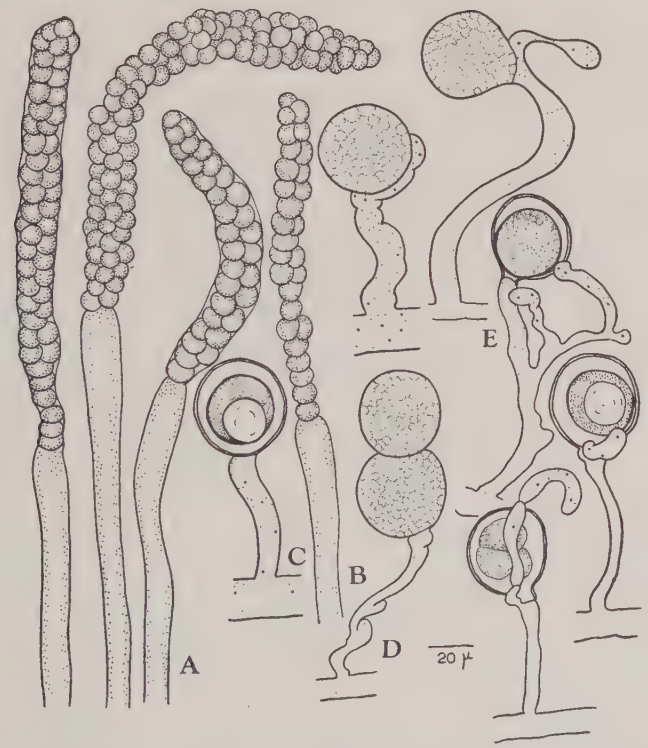

Fig. 10. *Brevilegnia* sp.
A, B. zoosporangium; C, D, oogonium; E, oogonium and antheridium.

Table 5. Showing isolation of aquatic fungi from each pond.

Pond / Date	A	B	C	D	E	F	G	H	I	Averaged percentage
April 25, '58	0%	0%		0%	(4), (6) 40%	0%	(10) 40%			13.3
May 5, '58	0%	(1) 20%	(4), (7) 20%	(13) 50%	(13) 20%	0%			(11), (13) 20%	17.1
Nov. 15, '58	(12) 30%	(3) 40%	(3), (8) 60%	0%	(12) 20%			(12) 20%	(8), (12) 60%	32.8
Dec. 20, '58	(5), (12) 100%	(2) 20%		(7) 20%	0%	(4), (6) 70%		(12), (14) 30%	(3), (11), (12) 40%	40.0
Jan. 24, '59	(12) 100%	(12) 70%	(2) 50%	(9) 70%	(12) 70%	(4) 90%		(9) 100%	(2) 50%	75.0
Feb. 23, '59	(12) 90%	0%	(4), (12) 100%	(9), (12) 100%	0%	0%		(7) 30%	(8) 50%	46.3
March 28, '59	0%	(7) 20%	(12) 30%	(12) 30%	(2) 30%	0%		0%	0%	13.3
May 20, '59	(12) 30%	(1) 20%	(9) 30%	(9) 20%	(7) 40%	0%		(12) 20%	0%	20.0
Averaged percentage	48.8	22.5	48.3	36.3	26.3	22.9		33.0	31.4	

Remarks: The percentage indicates the ratio of Petri dishes, in which the fungi grew, to the total (This was determined as rate of detection of the fungi).

(1) *Saprolegnia ferax*; (2) *Saproleg. diclina*; (3) *Saproleg. delica*; (4) *Saproleg. parasitica*; (5) *Pythiopsis cymosa*; (6) *Isoachlya* sp.; (7) *Achlya racemosa*; (8) *Achlya proliferoides*; (9) *Achlya Oryzae*; (10) *Aphanomyces stellatus*; (11) *Brevilegnia* sp.; (12) *Apodoachlya brachynema*; (13) *Pythium violae*.

pyriform or similar to the hyphae, 20–27× 20–45 μ in dimension. Oogonia apical or on lateral branches having 3–4 constrictions, spherical or pyriform, 20–30 μ in diameter, and in which an eccentric egg involved; the wall smooth, unpitted, 2 μ in thickness. Suboosporangial cells generally spherical, occurring near by oogonium (cf. Fig. 11, A–E).

13) *Pythium violae* Chesters et Hickman, in Trans. Brit. Mycol. Soc., **27**, 60, (1944).

The detailed results are compiled in Table 5 and the average rate of detection in each pond throughout a year and that of each month throughout all the ponds are shown in Textfig. 12.

It seems that the average rate of detection does not make a remarkable difference among the ponds. On the contrary it varys in season. It was easy to detect saprolegniaceous fungi in cold season.

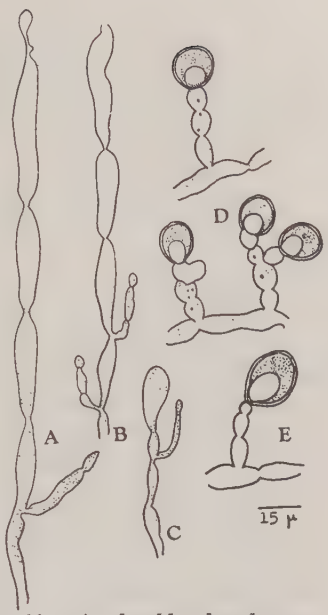

Fig. 11. *Apodoachlya brachynema*. A, hypha; B, sporangium; C. young sporangium; D, E, oogonium.

Recently, Suzuki (1960) has reported an interesting work dealing with the aquatic fungi in Arakawa River. He stated that the zoospore of aquatic fungi showed considerable variations in amount, with one maximum occurring in winter and minimum in summer.

Compared the fungus flora of the eel-culture ponds with the flora of inland waters developed in moor of highland, which are acidic dystrophic type and filling with brown water characteristic of peat moss, such as Hakkôda or Ozegahara, it shows that the species are comparatively poor but the individuals belonging to certain species are numerous.

Table 6 shows the saprolegniales which were identified up to the present in Japanese inland waters.

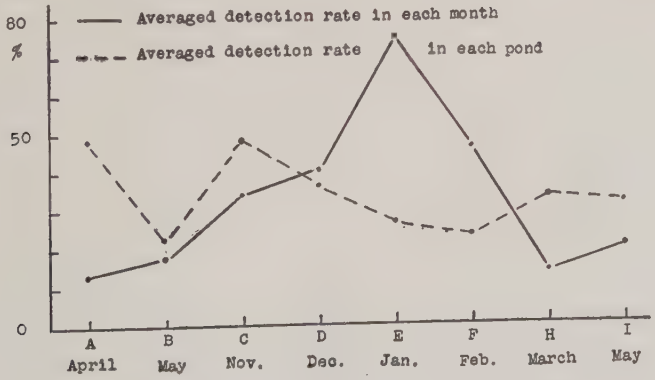

Fig. 12. Detection rate of aquatic fungi in eel-culture pond.

Table 6. Saprolegniales in some inland waters in Japan.

Species \ Locality	Ozegahara	Hakkôda	Lake Kasumigaura	Eel-culture pond
Allomyces arbusculus	+	−	−	−
Gonapodia prolifera	+	+	−	−
Gonapodia polymorpha	+	+	−	−
Aplanes Braunii	+	+	−	−
Aplanes Ozeensis	+	−	−	−
Aplanes sp.	+	−	−	−
Leptolegnia caudata	+	+	−	−
Saprolegnia ferax	+	+	+	+
Saprolegnia asterophora	+	−	−	−
Saprolegnia diclina	−	+	−	+
Saprolegnia stagnalis	+	−	−	−
Saprolegnia delica	−	+	−	+
Saprolegnia litoralis	−	−	+	−
Saprolegnia parasitica	−	+	−	+
Pythiopsis cymosa	−	−	−	+
Pythiopsis sp.	−	−	+	−
Isoachlya monilifera	+	−	−	−
Isoachlya sp.	−	−	−	+
Achlya racemosa	+	+	−	+
Achlya apiculata	−	+	−	−
Achlya oblongata	−	+	−	−
Achlya americana	+	+	−	−
Achlya Radiosa	−	−	+	−
Achlya klebsiana	−	+	−	−
Achlya proliferoides	+	+	−	+
Achlya conspicua	+	+	−	−
Achlya imperfecta	+	−	−	−
Achlya oligacanta	−	+	−	−
Achlya Oryzae	+	+	−	+
Aphanomyces lavis	+	−	−	−
Aphanomyces stellatus	−	−	−	+
Dictyuchus monosporus	+	+	+	−
Brevilegnia sp.	−	−	−	+
Apodoachlya brachynema	−	−	−	+
Apodoachlya pyrifera	−	−	+	−
Pythium violae	−	−	−	+
Pythium sp.	−	−	+	−
Pythiomorpha oryzae	+	−	−	−
Total	20 species	18 species	7 species	13 species

As Table 6 shows, of 13 species of the aquatic fungi found in the eel-culture ponds, 6 species were found out in the ponds alone. It is interesting expressly that such *Apodoachlya* sp. and *Brevilegnia* sp. were found in the ponds.

5. An attempt to infect eel with some aquatic fungi isolated from eel-culture ponds

The present work was undertaken to ascertain whether certain species of saprolegniaceous fungi isolated from the eel-culture ponds would infect eel. Among the fungi, seven species, viz. *Achlya Orezae*, *A. racemosa*, *Aphanomyces stellatus*, *Apodoachlya brachynema*, *Saprolegnia parasitica*, *S. ferax* and *Brevilegnia* sp. were tested because they were showing the active growth on the culture medium. Small eels, *Anguilla japonica*, collected from the pond of Hamana Branch Station of Shizuoka Prefectural Fisheries Experiment Station, measuring about 6–7 cm. in body length were used for the experiment.

Twenty eels were kept in a glass vessel containing 2 liters of well water, which proved previously free from saprolegniaceous fungi and the fungus cultured on hemp seeds and enclosed in a glass tube (2 cm.×4 cm.; the both ends covered by a gauze) was added in the vessel. Same number of eels was kept in a similar vessel as control. The fungus was renewed every 3 days and the experiment continued for 25 days. The water temperature showed about 18°C during the experiment. The fishes were feed with brine-shrimps.

The results obtained are shown in Table 7. As Table 7 shows, among the seven species tested, four species, viz. *Achlya racemosa*, *Aphanomyces stellatus*, *Saprolegnia parasitica* and *S. ferax* infected eel. But the infected fish was only one in three heads.

Table 7. The infection experiment with the aguatic fungi isolated from eel-culture ponds to eel.

Fungus / Group / Days passed	1		2		3		4		5		6		7	
	A	B	A	B	A	B	A	B	A	B	A	B	A	B
Start of Exp. May 31, '59	20	20	20	20	20	20	20	20	20	20	20	20	20	20
〜 10	17	15	18	18	16	17	19	20	17 (2)	20	18	20	20	18
〜 17	12	12	16	16 (1)	12 (3)	14	19	19	13 (1)	15	15	18	19	17
〜 25	8	7	13	14	9	11	9	8	3	5	7 (2)	13	16	9

Remark: 1. *Achlya Oryzae*; 2. *Achlya racemosa*; 3. *Aphanomyces stellatus*; 4. *Apodoachlya brachynema*; 5. *Saprolegnia parasitica*; 6. *Saprolegnia ferax*; 7. *Brevilegnia* sp.

A, experimental group; B, control group.

The numeral in each colum indicates the number of survived fish by the time and that of parenthesized shows numbers of the fish parasitized by the fungus.

This may be attributable to that all the fishes used were uninjured and considerable large numbers of the fishes died during the experiment. The dead fishes were removed each time and placed in Petri dishes for several days but any fungus-growth was not observed. The cultures were made from the infected fishes to confirm the species and it was proved that the species was identical to the species used respectively as the source of infection. The infected fishes died within 7 to 10 days with the progress of the affected part. As the infection with *Achlya racemosa* occurred on only one fish, it seems that the species is most hardly infectious to eel. Hoffman (1947) reported that the species did not attack the fishes used in his experiments (two species of sunfish and three species of minnow).

An attempt to infect platyfish, with the saprolegniaceous fungi occurring as parasite of aquatic animals had been made by Vishniac and Nigrelli (1957). According to the authors, 16 species belonging to 7 genera out of 17 species of the fungi parasitized the fish. And the authors stated, "although the family Saprolegniaceae is primarily saprophytic in nature, the potentiality of parasitic existence is a familial characteristic." Juding from the results of our study, *Aphanomyces stellatus* and *Saprolegnia ferax* as well as *S. parasitica*, may trouble the eels in culture ponds.

Summary

Saprolegnia parasitica Coker caused heavy mortality of eels in the culture ponds at spring every year, though the mortality might not be based uniquely on the fungus. The fungus parasitized especially the head and the caudal part. The affected parts showed remarkable pathological lesions and were contaminated with bacteria. The diseased fishes aften were infected with bacilli, especially in the viscera of moribund ones.

The present fungus formed oogonia on hemp seed after 2 weeks at 4.1–13.8°C. Apical oogonia are 48.7–83.9 μ in diameter; intercalary ones, 53.6–86.6 $\mu \times$ 39.1–60.6 μ in size. Oogonia were filled with 2–20 oospores of 18.2–31.2 μ in diameter. Antheridia are mostly pear-shaped. These oospores germinated easily on agar-plate of 1% yeast extract.

The optimum temperature of the fungus-growth was about 14°C. The fungus at higher temperature more than 24.7°C died within several days.

The fungus-growth was inhibited completely by malachite green of the concentration of 1:10,000,000. The germination of the zoospore was inhibited completely by the solution of 1:30,000,000, but the concentration of 1:300,000–1:500,000 was required to kill the zoospore in a short time, 20–70 minutes.

The development of fungus is impossible under free oxygen.

The fungus might not possess a toxic substunce, and also excrete a toxic metabolite for eels.

Thirteen species belonging to 7 genera of saprolegniaceous fungi were found in eel-culture ponds of Kawajiri district, Shizuoka Pref. by the investigation from April, 1958 to May, '59. It seems that the fungal flora of the eel-culture ponds is poor in variety, however, it abounds in population numbers

belonging to a few species. The fungi were detected easily in cold season.

An attempt to infect with 7 species of the fungus was carried out and the results showed that 4 species, viz. *Achlya racemosa*, *Aphanomyces stellatus*, *Saprolegnia parasitica* and *S. ferax* infected the fish.

Literature

1. Arasaki, S., K. Nozawa and M. Miyake, 1958. On the pathogenitic water mold.—I (in Japanese). Bull. Japanese Soc. Sci. Fish., Vol. 23, pp. 534–538.
2. ———, 1958. ——————— II (in Japanese). Ibid., Vol. 23, pp. 593–598.
3. Bessey, C. E., 1950. Morphology and taxonomy of fungi. The Blakiston Co., Toronto.
4. Davis, H. S., 1953. Culture and disease of game fishes. Univ. California Press, Berkely & Los Angels.
5. Gilman, J. C., 1950. Soil fungi. Iowa State College Press.
6. Hoffman, G. L., 1949. Isolation of *Saprolegnia* and *Achlya* with penicillin-streptomycin, and attempts to infect fish. Prog. Fish.-Cult., Vol. 11, pp. 171–174.
7. Hoshina, T. and M. Ookubo, 1956. On a fungi-disease of eel. Jour. Tokyo Univ. Fish., Vol. 42, pp. 1–13.
8. Hoshina, T., 1959. Fungus disease of eel (in Japanese). The Aquiculture, Vol. 7, 161–166.
9. Hoshina, T., T. Sano and M. Sunayama, 1958. Studies on the control of the aquatic fungi occurring on the egg of pond smelt *Hypomesus olidus* (In Japanese). Report Fish. Promot. Station Ibaraki Pref., No. 3, pp. 35–44.
10. Kanouse, B. B., 1932. A physiological and morphological study of *Saprolegnia parastica* Mycologia, Vol. 24, pp. 431–452.
11. Maurizio, A., 1899. Beiträge zur Biologie der Saprolegnieen. Zeitschri. f. Fisch., 7 Jahrb., pp. 1–66.
12. МАЗИЛКИН, И. А., 1957. Биологический метод борьбы с Сапролегнией. Труд. Совеща. По Рыбовод, 81–88 Стр.
13. Sparrow, F. K., 1943. Aquatec phycomycetes. Univ. Michigan Press.
14. Suzuki, S., 1960. Ecological studies on the aquatic fungi in the Arakawa River (in Japanese). Japanese Jour. Limno., Vol. 21, pp. 17–24.
15. Vishniac, H. S. and R. F. Nigrelli, 1957. The ability of the Saprolegniaceae to parasitize platyfish. Zoologica, Vol. 42, pp. 131–134.
16. Williamson, I. J. F., 1929. A study of bacterial infection in fish and certain other lower vertebrates. Fish. Board Scot., Salmon Fish., No. 11, 128.

Journal of the Tokyo University of Fisheries Vol. 47, No. 1, 1960

DETERMINATION OF THE TIME REQUIRED FOR FREEZING OF WHALEMEAT

Kazuo Tanaka and Jun-ichi Nishimoto*

(Received June 27, 1960)

Introduction

In Japan, yearly about 80,000 tons of frozen whalemeat are produced in the Antarctic Ocean by Japanese whaling expeditions. Reduction of freezing-time of the meat and increasing of capacity of the freezer are important problems given to us. Under such circumstances the authors induced a formula, determining the time required for freezing of whalemeat, and carried out calculations to obtain some proper values.

Induction of Basic Formula

1. Freezing of Whalemeat.

The whales caught in the Antarctic waters are cut to a rectangular shape of meat, then taken in a metal tray and frozen by a freezer on board a refrigerator mother-ship.

2. Induction of Formula to Determine the Time Required for Freezing of Whalemeat.

Plank applied the theory of heat transmission for determination of the

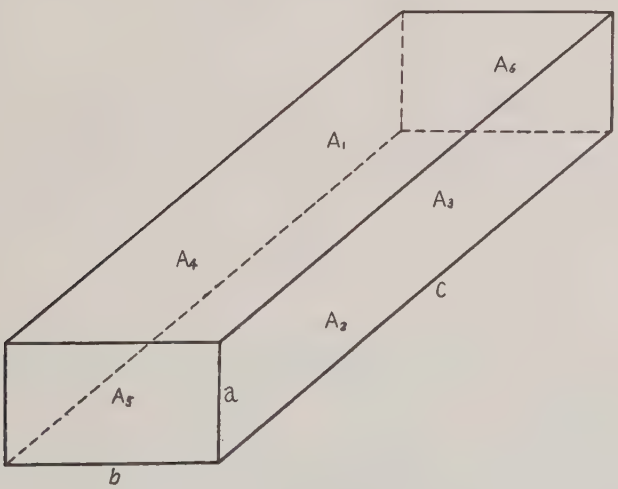

Fig. 1. Rectangular body.

* The Faculty of Fisheries, Kagoshima University.

freezing-time of foods cylindrical in shape. According to the same method of Plank, and regarding a whalemeat as a rectangular body, the authors induce a formula determining the time required for freezing of whalemeat.

In referring to figure 1, we let a, b, c: total height, total width, and total length of a rectangular shape of the meat respectively m, and $a \leqq b \leqq c$.

$A_1, A_2, A_3, A_4, A_5, A_6$: each surface of the meat to radiate its heat m^2.

γ_1, γ_2 : specific weight of the meat in unfrozen and frozen state respectively Kg/m^3.

c_1, c_2 : specific heat of the meat in unfrozen and frozen state respectively Kcal/Kg °C.

f : latent heat of freezing of the meat Kcal/Kg.

λ_1, λ_2 : thermal conductivity of the meat in unfrozen and frozen state respectively Kcal/mh °C.

θ_a, θ_b : initial and final temperature of the meat respectively °C.

θ_f : freezing point of the meat °C.

r : freezing percentage of the meat.

θ_e : temperature of the cooling medium °C.

α : heat transmission coefficient at the surface of the meat Kcal/m^2h °C.

q : freezing-heat-quantity of unit weight of the meat Kcal/Kg.

Q : freezing-heat-quantity of the meat Kcal.

t : freezing-time of the meat h.

Then, if we assume that the freezing of meat proceeds uniformly from each surface to the center, and put a_0, b_0, c_0, for height, width and length of unfrozen parts of the meat m, thickness of frozen part $\delta_0 m$ is all equally given by

$$\delta_0 = \frac{a-a_0}{2} = \frac{b-b_0}{2} = \frac{c-c_0}{2}$$

1) in freezing the meat has not any insulated surfaces and radiates its heat through the whole surfaces A_1, A_2, A_3, A_4, A_5 and A_6.

On the one hand, the freezing-heat-quantity dQ Kcal taken away from the thin meat layer of which thickness is $d\delta_0$ m is given by

$$dQ = \{c_1(\theta_a-\theta_f)+c_1(1-r)(\theta_f-\theta_b)+fr+c_2r(\theta_f-\theta_b)\}\times\gamma_2\times 2(a_0b_0+b_0c_0+c_0a_0)d\delta_0$$

As $d\delta_0 = -(da_0)/2$ is derived from the above relation, this equation is transformed into

$$dQ = -\{c_1(\theta_a-\theta_b)-(c_1-c_2)r(\theta_f-\theta_b)+fr\}\gamma_2(a_0b_0+b_0c_0+c_0a_0)da_0$$

On the other hand, this dQ Kcal is expressed by heat transmission from the inner part of the meat to the cooling medium through the surface of the meat during dt h as follows.

$$dQ = 2(\theta_f-\theta_e)dt \Bigg/ \frac{1}{2\lambda_2\sqrt{2\{(a-b)^2+(b-c)^2+(c-a)^2\}}} \times \left[\ln\frac{2(a_0+b_0+c_0)+\sqrt{2\{(a-b)^2+(b-c^2)+(c-a)^2\}}}{2(a+b+c)+\sqrt{2\{(a-b)^2+(b-c)^2+(c-a)^2\}}}\right.$$

$$-\ln\frac{2(a_0+b_0+c_0)-\sqrt{2\{(a-b)^2+(b-c)^2+(c-a)^2\}}}{2(a+b+c)-\sqrt{2\{(a-b)^2+(b-c)^2+(c-a)^2\}}}\Bigg]+\frac{1}{\alpha(ab+bc+ca)}$$

Let each right term of these equations is equal and to carry out integration, and the freezing-time of the meat rectangular in shape which has not any insulated surfces canbe obtained as follows.

$$t=\frac{r_2}{24\lambda_2}\Bigg[\frac{1}{9}\{3a(2\overline{b+c}-a)-\overline{(a-b)^2+(b-c)^2+(c-a)^2}\}\ln\frac{ab+bc+ca}{(c-a)(b-a)}$$
$$+\frac{2(2a-\overline{b+c})(2b-\overline{c+a})(2c-\overline{a+b})}{\sqrt{2\{(a-b)^2+(b-c)^2+(c-a)^2\}}}\times\ln\frac{2bc-a(2a-\sqrt{2\{(a-b)^2+(b-c)^2+(c-a)^2\}})}{2bc-a(2a+\sqrt{2\{(a-b)^2+(b-c)^2+(c-a)^2\}})}$$
$$+\frac{4\lambda_2}{\alpha}\frac{3abc}{ab+bc+ca}\Bigg]\frac{q}{\theta_f-\theta_e}$$

here $q=c_1(\theta_a-\theta_b)-(c_1-c_2)r(\theta_f-\theta_b)+fr$.

When the differences between c, b and a are not so large, as we can expand logarithmic terms and carry out some abbreviation in this equation, it is simplified as follows.

$$t=\frac{r_2}{24\lambda_2}\frac{3abc}{ab+bc+ca}\left(\frac{3abc}{ab+bc+ca}+\frac{4\lambda_2}{\alpha}\right)\frac{q}{\theta_f-\theta_e}$$

Putting $3abc/(ab+bc+ca)=D$, the equation is transformed into

$$t=\frac{r_2}{24\lambda_2}D\left(D+\frac{4\lambda_2}{\alpha}\right)\frac{q}{\theta_f-\theta_e}$$

2) in freezing the meat has two insulated surfaces opposited A_6 and A_5 at both ends of length c and radiates its heat through the residual four surfaces opposited each A_1, A_2, A_3 and A_4 at both ends of width b and height a.

We put $c\to\infty$ at the original equation in case 1), following result can be obtained.

$$t=\frac{r_2}{16\lambda_2}\Bigg[\left\{ab-\frac{(b-a)^2}{2}\ln\frac{b+a}{b-a}\right\}+\frac{4\lambda_2}{\alpha}\frac{2ab}{a+b}\Bigg]\frac{q}{\theta_f-\theta_e}$$

Again, when the difference between b and a is not so large, as we can expand logarithmic term and carry out some abbreviation in this equation, it is simplified as follows.

$$t=\frac{r_2}{16\lambda_2}\frac{2ab}{a+b}\left(\frac{2ab}{a+b}+\frac{4\lambda_2}{\alpha}\right)\frac{q}{\theta_f-\theta_e}$$

Putting $2ab/(a+b)=D$, the equation is transformed into

$$t=\frac{r_2}{16\lambda_2}D\left(D+\frac{4\lambda_2}{\alpha}\right)\frac{q}{\theta_f-\theta_e}$$

3) in freezing the meat has four insulated surfaces opposited each A_6, A_5, A_4 and A_3 at both ends of length c and width b and radiates its heat through the residual two surfaces opposited A_1 and A_2 at both ends of height a.

We put $b\to\infty$ at the original equation in case 2), following result can be

obtained.

$$t=\frac{r_2}{8\lambda_2}a\left(a+\frac{4\lambda_2}{\alpha}\right)\frac{q}{\theta_f-\theta_e}$$

Putting $a=D$ also, the equation is transformed into

$$t=\frac{r_2}{8\lambda_2}D\left(D+\frac{4\lambda_2}{\alpha}\right)\frac{q}{\theta_f-\theta_e}$$

4) in freezing the mest has five insulated surfaces each A_6, A_5, A_4, A_3 and A_2 and radiates its heat through the residual one surface A_1.

We put $a=2a$ at the original equation in case 3), following result can be obtained.

$$t=\frac{r_2}{2\lambda_2}a\left(a+\frac{2\lambda_2}{\alpha}\right)\frac{q}{\theta_f-\theta_e}$$

Putting $a=D$ also, the equation is transformed into

$$t=\frac{r_2}{2\lambda_2}D\left(D+\frac{2\lambda_2}{\alpha}\right)\frac{q}{\theta_f-\theta_e}$$

Through these solutions, we can obtain the following general formula to determine the time required for freezing of a rectangular body in shape as a whalemeat.

$$t=\frac{r_2}{\mu\lambda_2}D\left(D+\frac{4\lambda_2}{\alpha}\right)\frac{q}{\theta_f-\theta_e}$$

here $$q=c_1(\theta_a-\theta_b)-(c_1-c_2)r(\theta_f-\theta_b)+fr$$

freezing percentage of the meat r is approximately given by

$$r=1-\frac{\theta_f}{\theta_b}$$

and μ: constant, D: mean (equivalent) thickness of the meat m. The value of D changes relating to the value of μ as follows.

$$\mu=24\,,\qquad D=\frac{3abc}{ab+bc+ca}$$

$$\mu=16\,,\qquad D=\frac{2ab}{a+b}$$

$$\mu=8\,,\qquad D=a$$

$$\mu=2\,,\qquad D=a \quad \text{and} \quad 4\lambda_2\rightarrow 2\lambda_2$$

In connection therewith, formula determining the time required for freezing of a food cylindrical or spherical in shape can be induced as follows.

In referring to Fig. 2, we let B, H: diameter of the base and height of the food regarded as a cylindrical body in shape respectively m.

1) in freezing there are not any insulated surfaces in the food and the food radiates its heat through the whole surfaces.

We put $a=b=B, c=H$ at the original equation in case 1), following result

can be obtained.

$$t=\frac{r_2}{24\lambda_2}D\left(D+\frac{4\lambda_2}{\alpha}\right)\frac{q}{\theta_f-\theta_e}$$

here $D=\dfrac{3BH}{B+2H}$ in case of $B\leqq H$

$D=\dfrac{3BH}{2B+H}$ in case of $B\geqq H$

2) in freezing the base area of the food is insulated and the food radiates its heat through the side area.

We put $a=b=B$ at the original equation in case 2), following result can be obtained.

$$t=\frac{r_2}{16\lambda_2}D\left(D+\frac{4\lambda_2}{\alpha}\right)\frac{q}{\theta_f-\theta_e}$$

here $D=B$

This equation is induced by Plank firstly.

3) in freezing the side area of the food is insulated and the food radiates its heat through the base area.

We put $a=H$ at the original equation in case 3), following result can be obtained.

$$t=\frac{r_2}{8\lambda_2}D\left(D+\frac{4\lambda_2}{\alpha}\right)\frac{q}{\theta_f-\theta_e}$$

here $D=H$

Through these solutions, we can obtain the following general formulas to determine the time required for freezing of a cylindrical body in shape.

$$t=\frac{r_2}{\mu\lambda_2}D\left(D+\frac{4\lambda_2}{\alpha}\right)\frac{q}{\theta_f-\theta_e}$$

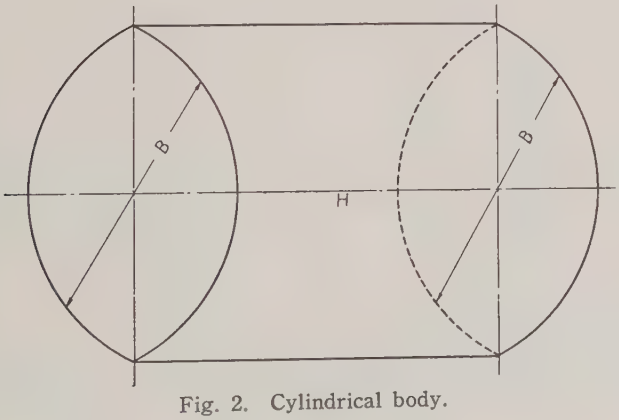

Fig. 2. Cylindrical body.

here $$q=c_1(\theta_a-\theta_b)-(c_1-c_2)r(\theta_f-\theta_b)+fr$$

freezing percentage of the food r is approximately given by

$$r=1-\frac{\theta_f}{\theta_b}$$

and μ: constant, D: mean (equivalent) diameter of the food m. The value of D changes relating of the value of μ as follows.

$$\mu=24\,,\qquad D=\frac{3BH}{B+2H}\qquad \text{in case of } B\leqq H$$

$$D=\frac{3BH}{2B+H}\qquad \text{in case of } B\geqq H$$

$$\mu=16\,,\qquad D=B$$

$$\mu=8\,,\qquad D=H$$

In referring to Fig. 3, we let B: diameter of the food regarded as a spherical body in shape m.

We put $a=b=c=B$ at the original equation in case 1), following result can be obtained.

$$t=\frac{r_2}{24\lambda_2}D\left(D+\frac{4\lambda_2}{\alpha}\right)\frac{q}{\theta_f-\theta_e}$$

here $$D=B$$

and $$q=c_1(\theta_a-\theta_b)-(c_1-c_2)r(\theta_f-\theta_b)+fr$$

freezing percentage of the food r is approximately given by

$$r=1-\frac{\theta_f}{\theta_b}$$

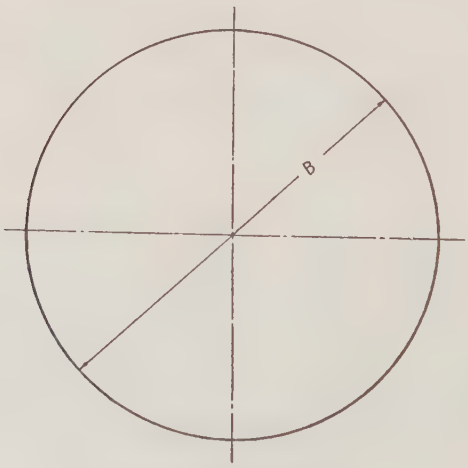

Fig. 3. Spherical body.

and μ: constant, D: mean (equivalent) diameter of the food m. The value of D is determined relating to the value of μ as follows.

$$\mu=24\,, \qquad D=B$$

Then, if we put W is weight of the meat or food, the freezing-heat-quantity Q Kcal taken away from the meat or food is given by in all cases

$$Q=Wq=W\{c_1(\theta_a-\theta_b)-(c_1-c_2)r(\theta_f-\theta_b)+fr\}$$

here

$$r=1-\frac{\theta_f}{\theta_b}$$

Calculation of Values of Some Physical Constants of Whalemeat

As these formulas include some physical constants of whalemeat, we must decide these values to calculate freezing-time of the meatthrough these formulas. If we take X, Y and Z as moisture, fat and solid matter contents of the meat, and γ_{w1}, γ_{w2} as specific weight, c_{w1}, c_{w2} as specific heat, λ_{w1}, λ_{w2} as thermal conductivity of water and ice respectively, f_w as latent heat of freezing of water, as well as γ_f, c_f, λ_f and γ_s, c_s, λ_s are specific weight, specific heat and thermal conductivity of fat and solid matter of the meat respectively, the physical constants of the whalemeat can be expressed as follows.

as for specific weight of the meat

in unfrozen state $\gamma_1=\gamma_{w1}X+\gamma_fY+\gamma_sZ$

in frozen state $\gamma_2=\gamma_{w2}X+\gamma_fY+\gamma_sZ$

as for specific heat of the meat

in unfrozen state $c_1=c_{w1}X+c_fY+c_sZ$

in frozen state $c_2=c_{w2}X+c_fY+c_sZ$

as for latent heat of freezing of the meat $f=f_wX$

as for thermal conductivity of the meat

in unfrozen state $\lambda_1=\lambda_{w1}X+\lambda_fY+\lambda_sZ$

in frozen state $\lambda_2=\lambda_{w2}X+\lambda_fY+\lambda_sZ$

But in case of thermal conductivity of the meat, these equations give only that

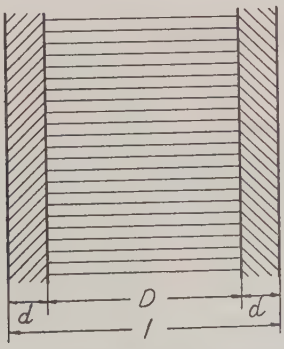

Fig. 4. The meat which become in fat layers both sides of muscle.

d : thickness of fat layer.

D: thickness of muscle (water+solid matter) layer.

then $\dfrac{1}{\lambda}=\dfrac{2d}{\lambda_f}+\dfrac{D}{(\lambda_wX+\lambda_sZ)/1-Y}$

here $2d+D=1$

$2d=Y$

$D=1-Y$

therefore $\lambda=\dfrac{(\lambda_wX+\lambda_sZ)\lambda_f}{(\lambda_wX+\lambda_sZ)Y+\lambda_f(1-Y)^2}$

of mixed substances. When the meat is in layers which become in fat layers both sides of muscle, in referring to Fig. 4, thermal conductivity of the meat

is given by

in unfrozen state $$\lambda_1=\frac{(\lambda_{w1}X+\lambda_s Z)\lambda_f}{(\lambda_{w1}X+\lambda_s Z)Y+\lambda_f(1-Y)^2}$$

in frozen state $$\lambda_2=\frac{(\lambda_{w2}X+\lambda_s Z)\lambda_f}{(\lambda_{w2}X+\lambda_s Z)Y+\lambda_f(1-Y)^2}$$

The constituents of the lean meat of fin-whales caught in the Antarctic waters are about moisture content : $X=0.727$, fat content : $Y=0.03$, solid matter content : $Z=0.243$ (protein 0.233+ash 0.01), and the values of physical constants of those matters are roughly

$\gamma_{w1}=1000$, $\gamma_{w2}=920$, $c_{w1}=1$, $c_{w2}=0.5$, $\lambda_{w1}=0.5$, $\lambda_{w2}=2$, $f=80$, $\gamma_f=920$, $c_f=0.5$, $\lambda_f=0.1$, $\gamma_s=1300$, $c_s=0.35$, $\lambda_s=2$.

Therefore, the values of physical constants of whalemeat can be obtained as follows.

specific weight in unfrozen state	$\gamma_1=1071$ Kg/m³.
specific weight in frozen state	$\gamma_2=1012$ Kg/m³.
specific heat in unfrozen state	$c_1=0.83$ Kcal/Kg °C.
specific heat in frozen state	$c_2=0.46$ Kcal/Kg °C.
latent heat of freezing	$f=58.16$ Kcal/Kg.
thermal conductivity in unfrozen state	$\lambda_1=0.71$ Kcal/mh °C.
thermal conductivity in frozen state	$\lambda_2=1.27$ Kcal/mh °C.
Further, the freezing point of whalemeat	$\theta_f=-1.03$ °C.

and the freezing percentage of whalemeat is appoximately given by

$$r=1-\frac{-1.03}{\theta_b}$$

Comparison of Experimental Results and Calculated Values of Freezing-Time of Whalemeat

The freezing-curves of lean meat of fin-whales were experimentally taken in the Antarctic Ocean on the one hand, calculations of the freezing-time of whalemeat were carried out by using above formulas and the values of physical constant of whalemeat on the other hand.

Three types of freezer were used and three types of freezing-curve were obtained there.

1. An air type freezer.

In Fig. 5 and 6, the meat taken in a metal tray was put on a wooden box in the cold room and frozen under a still air, therefore cooling medium was a cold still air, and the meat radiated its heat through the whole surfaces, so $\mu=24$, $D=3abc/(ab+bc+ca)$ and $\alpha=6+4v$, here v: air velocity m/sec will be used in calculations.

Then, in Fig. 5, the freezing-curve shows that the raw meat having a rectangular shape of $a\times b\times c=0.139\times 0.345\times 0.594$ m in size, $W=30.800$Kg in weight and initial temperature of the meat $\theta_a=18.0$ °C was frozen at final temperature of the meat $\theta_b=-8.2$ °C (freezing percentage of the meat $r=0.8744$) for time $t=35$ h under average temperature of a cold still air $\theta_c=-18.5$ °C. While

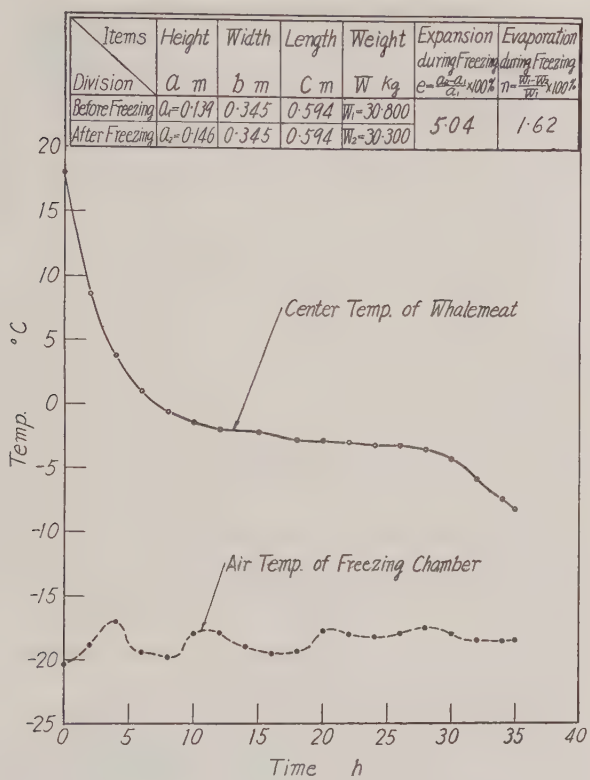

Fig. 5. Freezing-curve by still air type freezing of whalemeat.

the freezing-time of the meat t from the calculation is 37.50 h under mean thickness of the meat $D=0.255$ m and heat transmission coefficient at the surface of the meat $\alpha=6$ Kcal/m²h °C because of air velocity $v=0$ m/sec.

Also, in Fig. 6, the freezing-curve shows that the raw meat having a rectangular shape of $a\times b\times c=0.130\times0.297\times0.388$ m in size, $W=16.200$ Kg in weight and initial temperatue of the meat $\theta_a=4.0$ °C was frozen at final temperature of the meat $\theta_b=-7.0$ °C (freezing percentage of the meat $r=0.8529$) for time $t=23$ h under average temperature of a cold still air $\theta_e=-20.8$ °C. While the freezing-time of the meat t from the calculation is 22.44 h under mean thickness of the meat $D=0.220$ m and heat transmission coefficient at the surface of the meat $\alpha=6$ Kcal/m²h °C because of air velocity $v=0$ m/sec.

2. An air-sharp type freezer.

In Fig. 7 and 8, the meat as above was put on a cooling coils with ammonia evaporating within them and frozen under a still air, therefore cooling mediums are a cold still air and an evaporating ammonia through the pipe coils, and the meat radiates its heat through the whole surfaces. But we took into consideration that cooling medium was a cold still air only, so

$\mu=24$, $D=3abc/(ab+bc+ca)$ and $\alpha=10+4v$, here v: air velocity m/sec will be used in calculation.

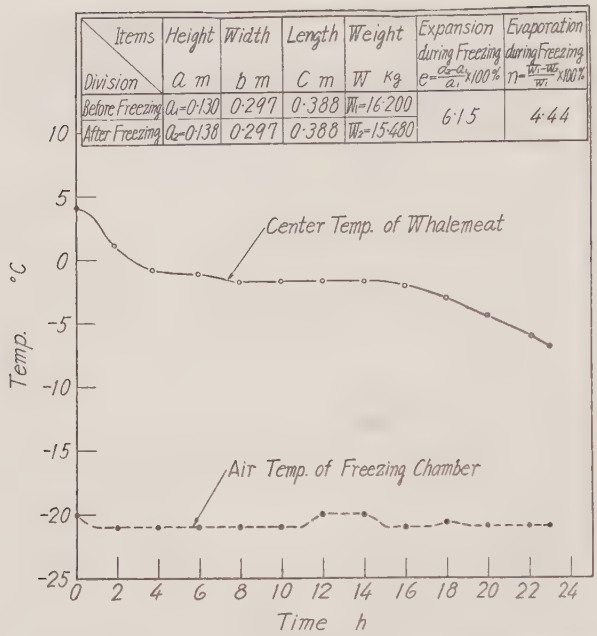

Fig. 6. Freezing-curve by still air type freezing of whalemeat.

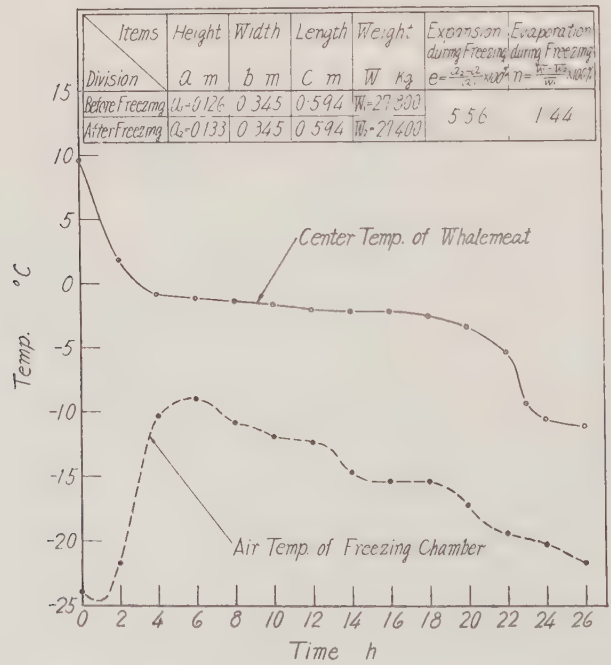

Fig. 7. Freezing-curve by still air-sharp type freezing of whalemeat.

Then, in Fig 7, the freezing-curve shows that the raw meat having a rectangular shape of $a \times b \times c = 0.126 \times 0.345 \times 0.594$ m in size, $W = 27.800$ Kg in weight and initial temperature of the meat $\theta_a = 9.6$ °C was frozen at final temperature of the meat $\theta_b = -11.1$ °C (freezing percentage of the meat $r = 0.9072$) for time $t = 26$ h under average temperature of a cold still air $\theta_e = -15.8$ °C. While the freezing-time of the meat t from the calculation is 26.88 h under mean thickness of the meat $D = 0.240$ m and heat transmission coefficient at the surface of the meat $\alpha = 10$ Kcal/m²h °C because of air velocity $v = 0$ m/sec.

Also, in Fig. 8, the freezing-curve shows that the raw meat having a rectangular of $a \times b \times c = 0.126 \times 0.297 \times 0.388$ m in size, $W = 15.700$ Kg in weight and initial temperature of the meat $\theta_a = 11.0$ °C was frozen at final temperature of the meat $\theta_b = -16.0$ °C (freezing percentage of the meat $r = 0.9356$) for time $t = 16$ h under average temperature of a cold still air $\theta_e = -23.4$ °C. While the freezing-time of the meat t from the calculation is 16.61 h under mean thickness of the meat $D = 0.216$ m and heat transmission coefficient at the surface of the meat $\alpha = 10$ Kcal/m²h °C because of air velocity $v = 0$ m/sec.

3. A multiplate type freezer.

In Fig. 9, the meat as above was inserted between cold metal plates with cold $CaCl_2$ brine circulating within them and frozen, therefore cooling medium is $CaCl_2$-brine through the plates, and the meat radiates its heat through the two

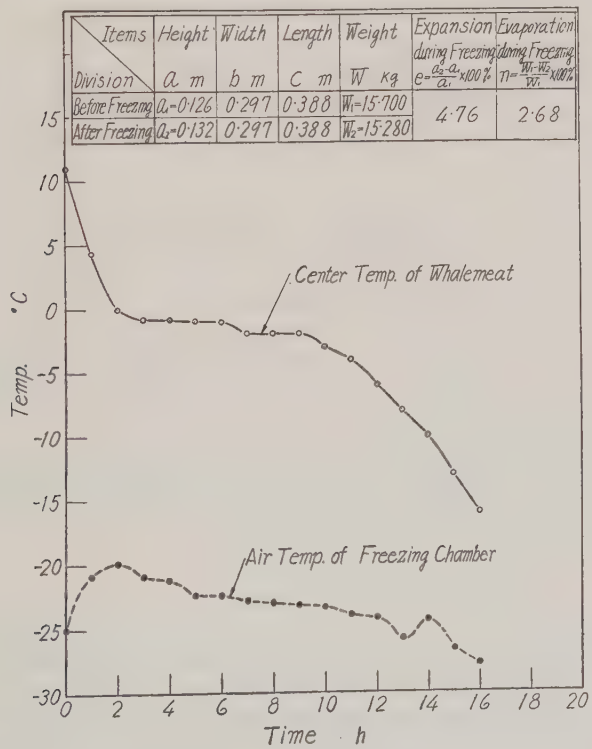

Fig. 8. Freezing-curve by still air-sharp type freezing of whalemeat.

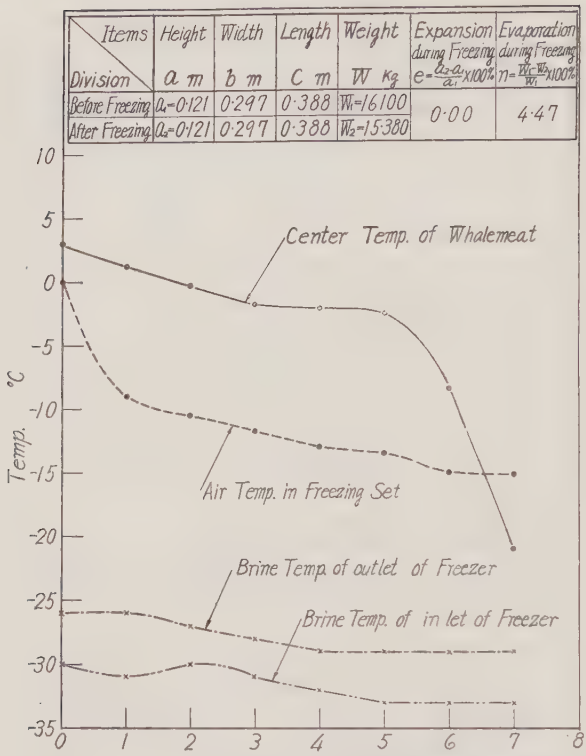

Fig. 9. Freezing-curve by double contact pressure type freezing of whalemeat.

surfaces opposited, so

$\mu=8$, $D=a$ and $\alpha=40$ will be used in calculation.

Then, in Fig. 9, the freezing-curve shows that the raw meat having a rectangular shape of $a\times b\times c=0.121\times 0.297\times 0.388$ m in size, $W=16.100$ Kg in weight and initial temperature of the meat $\theta_a=3.0$ °C was frozen at final temperature of the meat $\theta_b=-21.0$ °C (freezing percentage of the meat $r=0.9510$) for time $t=7$ h under average temperature of a cold $CaCl_2$-brine $\theta_e=-29.5$ °C. While the freezing-time of the meat t from the calculation is 7.17 h under mean thickness of the meat $D=0.121$ m.

If the calculated freezing-times using above formula are compared to those that from the freezing-curves obtained in the Antarctic Ocean, it can be recognized these values are much agreed with each other.

Conclusion

To determine the time required for freezing of foods rectangular in shape as a whalemeat, formulas and values of physical constants induced here are quite effective. Though the brine immersion type freezing of whalemeat has not been used in the Japanese whaling expeditions, if we intend to adapt the formula to such freezing system, $\mu=24$, $D=3abc/(ab+bc+ca)$ and $\alpha=30+50\sqrt{v}$ here v: brine velocity m/sec will be used in calculation.

Journal of the Tokyo University of Fisheries Vol. 47, No. 1, 1960

ON FOUR SPECIES OF MONOSTROMA IN TOKYO BAY*

Kozo Iwamoto

(With five Figures in the Text and four Plates)
(Received Jun. 27, 1960)

Some species belonging to *Ulvaceae* grow in *Porphyra* cultivating grounds and they have attracted our attention as harmful algae in *Porphyra* cultivation or as useful algae in some cases. And the investigations on these green algae are very few, whereas there are many reports on *Porphyra* or *Porphyra* cultivation. So there is only vague knowledge now on these algae.

The writer is engaged in the taxonomical and ecological studies of *Ulvaceae* which grow in *Porphyra* cultivating grounds since several years ago. Some informations which were gained by now on four species of *Monostroma* growing in Tokyo Bay are described in the present paper, among which *Monostroma tubiforme* and *M. crassissimum* are described as new species.

Here the writer expresses his thanks to all those who have aided him during the course of the present study. Especially he wishes to express his hearty thanks to Prof. S. Ueda, who gave him many facilities and kind guidance. Thanks are also due to Dr. M. Katada, Mr. A. Miura, Mr. S. Ito, and Mr. Y. Iwahashi, who collected the materials and gave valuable suggestions for him. Thanks are also expresses to Dr. Y. Nakamura and Mr. M. Tatewaki, who gave the specimens of *Monostroma zostericola* collected at Muroran, Hokkaido, and to Dr. S. Arasaki who gave valuable suggestions. And the writer expresses his cordial gratitude to Prof. Y. Yamada, Hokkaido University, for his revising the manuscript.

The writer shall be very happy if the present paper is beneficial for the fishermen and the investigators in spite of that the present paper is a very incomplete one.

1. *Monostroma tubiforme* spec. nov.

Fig. 1; Fig. 2, A; Fig. 3, A; Fig. 5, I a–e; Pl. I.

Frons initio minute tubulosa, deinde fissens ad illam apicem et evadens formae tubae, demum membrana radiata cum margine plano vel undato, ad 2 cm. alta; in conspecto superficiali cellulis multiangularibus, inaequariter ordinatis arctius, cellulis emittentibus rhizoidea et cellulis ordinariis misto ad bases, hae minoribus quam illis; in conspecto transversali membrana 17–22 μ crassa, cellulis quadratis, 10–13 μ altis, multis rhizoideis emissis ex celluis vix perforantibus deorsum in strato pellucido et emittentibus extra.

Frond tubulose at the beginning, afterwards trumpet-like, at last radial with even or undulate margin in general appearance; up to 2 cm. high; in surface view cells polygonal rather irregularly closely set, cells issuing the rhizoids mingled with normal vegetative ones near the base, and the former

* Dedicated to Prof. Hajime Matsuura and Prof. Yukio Yamada celebrating their Sexagenary birthdays.

distinctly cornered and larger than the latter, the normal vegetative ones cornered also near the base, becoming round towards the upper portion; in cross view membrane 17–22 μ thick, lower and upper portions of which not distinctly varying in thickness, cells quadrate, 10–13 μ high, and many rhizoids issued from the larger cells hardly perforating downwards in hyaline layer of membrane, soon shooting out. Swarmers 5.5–6×8–13 μ in size with two cilia and an eyespot, and with positive phototaxis.

Jap. name: *Rappa-hitoe* (nov.).

Hab.: Growing on stones, bamboos and wood works in littoral belt from October to next spring or whole year according to Dr. S. ARASAKI. Shinagawa and Haneda.

Probably the present species grows in water of the lowest salinity compared with other species of *Monostroma*. The writer found several plants of the present species on the wood works and on the stones at the mouth of creek at Shinagawa at the end of October in 1959. At that time the largest individual among them had reached to 1 cm. in height, on the other hand, however, the microscopic ones were found also. In December many individuals different in size were found, among them the large one reached to 2 cm. in height, and they produced many swarmers with two cilia and an eyespot. Many microscopic individuals were found also at the same time. These sporiferous and microscopic ones were always found to next March.

Fig. 1. A young tubular frond of *M. tubiforme*. ×230.

A remarkable characteristic of the present species appears in its microscopic stage, that is, in the present plants the writer has not found any discs as are recognized in many other species of *Monostroma*, viz., *M. angicava*, *M. zostericola*, *M. grevillei* at the beginning of development to the leafy plants. It suggests that the initial spores of the present species develop to the erect siphonous fronds with poor discs or without the discs. And then these siphonous fronds split at their tips during their microscopic size and become trumpet-like in external appearance. At this time the cells constituting the lowermost portion of the frond are very large and the cells abruptly become small towards the upper.

Still the basal part of the trumpet-like frond is made of only a few seriations of cells after the frond considerably developed, however, the upper portion splitted at the tip takes such an extension as its outer side faces to the substratum. Simultaneously the rhizoids are issued from many cells surrounding the base and these rhizoids penetrate downwards for some distance in the hyaline layer and some of them severally shoot out on the way to the base, then the frond is firmly attached to the substratum. So the general appearance of the basal part of the grown frond is almost the same as those of the other species which produce the discs at the beginning of the development.

From the descriptions mentioned above two very interesting characteristics will be found in the new species, that is, the one is the discs may not be produced at the beginning of the development to the leafy plants, the other is some of the rhizoids issued from the lower cells severally shoot out on the way to the base. It is judged by the writer that both these characteristics are inevitably correlated to attach the fronds to the substratum.

In the culture investigation of the swarmers in natural sea water, most of them directly develop to the few celled masses as the case of *M. wittrockii* figured by Bornet et Thuret (1880) or the 2- or 3-celled erect fronds without any rhizoids, and the writer was not able to observe any fronds developing to *Enteromorpha*-like fronds. The fact that there is a large variation in size was recognized among the swarmers produced in an individual, however, the writer was not able to confirm whether the swarmers escaped from the different individuals or from an individual conjugate each other or not. But from October to next March the microscopic *Enteromorpha*-like and trumpet-like fronds were found abundantly in nature, especially after the beginning of December the sporiferous individuals were always found with the microscopic ones, and in their bases any discs have not been found. It is supposed from these observations that the swarmers escaped from the leafy plants of this species directly (parthenogenetically) develop again to the leafy plants or the zoospores, which are produced in the zygocysts resulted from the rapid growth of the zygotes produced by the conjugation of the swarmers mentioned above, develop to the leafy ones. The parthenogenetic development of gametes and the rapid growth of zygotes were observed in *M. wittrockii* by Moewus. Bornet and Bliding observed also the parthenogenetic development in the same species. The writer has not observed yet the habit of this species in the period from April to October.

Miyake and Kunieda (1931) observed that a few zygotes directly developed to 2- or 3-celled sporelings without discs in a certain *Monostroma* species collected in the vicinity of Misaki situated near the mouth of Tokyo Bay.

The new species was collected also from the bamboo bars for *Porphyra* cultivation at Haneda on January in 1960.

Mr. G. Nagura figured and described the same developing form in his *Monostroma*, which was collected in Aichi Prefecture and referred to *M. nitidum* by him in 1920. Nagura's plant, however, seems to reach larger size and thicker membrane than the present one and the present one differs from *M. nitidum* by the arrangement of cells, their shape and their size. The present one is rather near to *M. orbiculatum* in the shape of cells and their arrangement, but the former differs from the latter by having the thinner membrane.

The present plants very well agree with the dimensions of the leafy plants of *M. wittrockii* mentioned by Bornet (1880) and Kylin (1949). That the sporiferous plants and microscopic ones are always found from December to next spring may be explainable by the habit of *M. wittrockii* investigated by Bornet, Bliding and Moewus. But these investigators have not shown that the young fronds of this species take such trumpet-like form as the new species does. And the young frond shown by Bliding (1935) differs undebtedly from that

of the new one.

NAGURA's plants are named *Bekkō-nori* or *Bekkō-awo* in the state of merchandise for food. Nowaday the plants named *Bekkō* in Tokyo Bay and in Ise Bay differ from NAGURA's plants in their developing form, the former belong to *M. latissimum* described in this paper.

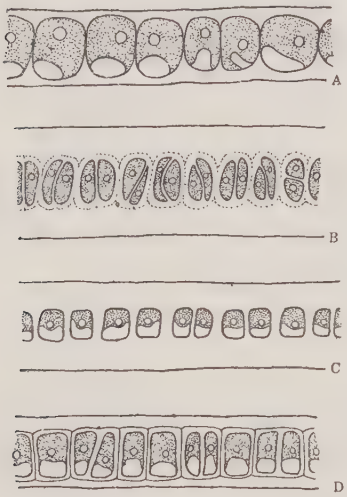

Fig. 2. Four cross views of the upper portions of the fronds. ×450.
A. *Monostroma tubiforme* (living material).
B. *M. crassissimum* (fixed material).
C. *M. latissimum* (〃).
D. *M. grevillei* (〃).

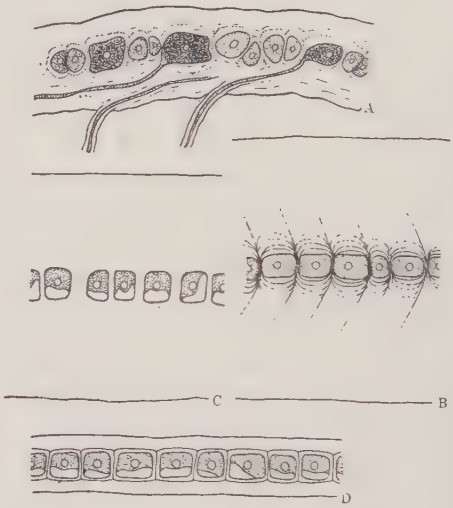

Fig. 3. Four cross views of the fronds. ×450.
A. A lowermost portion of *M. tubiforme*, showing three rhizoids shot out severally.
B. A lowermost portion of young *M. crassissimum*.
C. A lower portion of *M. latissimum*.
D. A lower portion of *M. grevillei*.

2. *Monostroma crassissimum* spec. nov.

Fig. 2, B; Fig. 3, B; Fig. 4; Pl. II.

Frons ad 20 cm. alta, plicata, margine lacerato, nitida; membrana 70–80 μ crassa in basem, 30 μ crassa in parte media, 90–140 μ crassa in parte marginis; in conspecto superficiali cellulis semiorbicularibus irregulariter ordinatis arctius appositis, ternis vel quaternis, in conspecto transversali membranae cellulis horizontariter quadratis, 7–8 μ altis; monostromatico in parte inferiore, in parte media et in parte superiore cellulis ovalibus vel verticaliter ovalibus, irregulariter composita monostromatico cellularum, in parte marginis irregulariter distromatico cellularum, interdum cavis interioribus inter stromaticis cellularum.

Frond up to 20 cm. high, plicate, with lacerate margin, glossy; membrane 70–80 μ thick near the base, 30 μ thick in the middle, 90–140 μ thick in the marginal portion; cells semicircular in outline, irregularly arranged in twos to fours in surface view; in cross view cells horizontally quadrate, 7–8 μ high,

arranged to one layer in the lower portion, in the middle to the upper portion the shape of cells becoming oval or vertically oval, height of which increased, the single arrangement becoming irregularly by transitioning of cells to both sides, in the upper to the marginal portions the arrangement becoming irregular two layers, and sometimes inner cavities produced here and there in the hyaline space between two layers. Swarmers unknown, propagated by gemmation?

Jap. name: *Atsuba-hitoe* (nov.).

Hab.: On bamboos or wood works in littoral belt from autumn to next spring. Kisarazu and Matsugashima.

The new species evidently differs from *M. latissimum* by the remarkably thickened membrane in full grown in late of winter to spring. But in early winter both these young plants are hardly distinguished in external appearance because the former's thickness of membrane is not increased yet. If the difference is constrained between both these young ones in external appearance, it may be able to say that the young plants of the new species apt to lacerate along their margin. But clear difference between the both ones is shown in their section views. That is, in *M. latissimum* the membrane attains 70 μ in thickness in the lower portion, where the cells are almost quadrate with rounded angles, slightly taller than the width and about 10 μ in the height and they are arranged to one layer. And towards the upper portion of the frond the thickness of membrane gradually decreased, however, the shape and size of cells are not variable. On the other hand in the new species the membrane is about 80 μ in thickness in the lower portion, where the cells are rather horizontally quadrate and 7–8 μ in height, and they are arranged to one layer, the thickness of membrane decreases towards the middle portion to about 30 μ and the cells are transformed to oval or vertically oval, and the thickness of membrane gradually increases again towards the upper and the cells attain to 15 μ in height, and they are arranged to one layer in twos to fours. And it is interesting that the planes bordering the cells are not always perpendicular to the frond surface, sometimes are oblique or horizontal. These

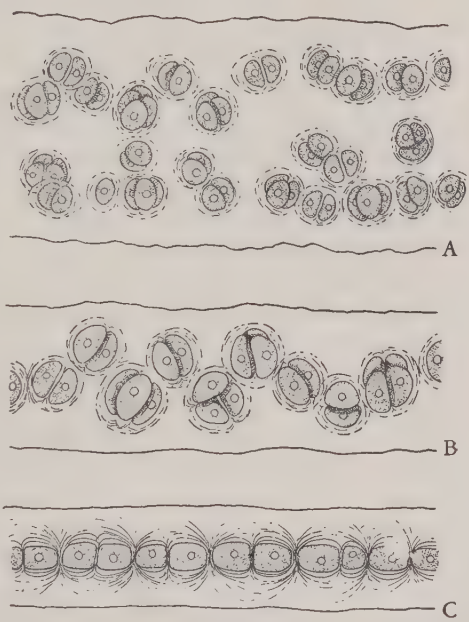

Fig. 4. Three cross views of a full grown *M. crassissimum*.

A. An uppermost portion, showing the cells arranged irregularly to two layers. ×225.

B. A middle portion, showing the irregular arranged cell layer. ×450.

C. A lower portion. ×450.

oblique or horizontal directions of the bordering planes may show signs of the irregular arrangement of cells in grown frond in which the cells are arranged to the irregular two layers in the upper to marginal portion and the thickness of membrane attains to above 100 μ.

According to the appearance of the arrangement of the cells issuing the rhizoids and the normal cells in the basal part, it seems the present species is a near relative of *M. orbiculatum* and *M. nitidum*, however, remarkable increase of the thickness of membrane and the conspicuous disorder of cell layer are very peculiar, so the writer puts the present one as a new species. The developing form to leafy plants has not been observed.

3. *Monostroma latissimum* (KUETZING) WITTROCK

Fig. 2, C; Fig. 3, C; Fig. 5, II a–e; Pl. III, C; Pl. IV, A–C.

1866, pp. 33–37, Pl. 1, Fig. 4; KJELLMAN, 1883, pp. 294, 295; HAUCK, 1885, p. 424; DE TONI, 1889, p. 102; COLLINS, 1901, p. 211; SETCHEL and GARDNER, 1920, p. 241; KYLIN, 1949, p. 14; SEGI and GOTO, 1959, pp. 57, 58.

Ulva latissima KUETZING, 1843, p. 296.

Jap. name: *Hiroha-no-hitoegusa*.

Hab.: From autumn to spring in upper littoral belt. Kisarazu and Matsugashima.

The leafy plants of the present species occur in the middle of autumn, the writer considers that the present one is the most dominant species among *Monostroma* growing in Tokyo Bay. The present one strongly resembles the young plant of *M. crassissimum* in external appearance, but both plants are distinguishable in their cross views as mentioned above.

In the present species the most peculiar characteristic is found in the developing form to the leafy plant. The discs as are produced in many other species are samely produced at the beginning of the development, and the erect shoots issued from the discs, however, do not exhibit any forms of the tube or sack, are always spherical leafy plants composed of a single layer of cells from the first. In proportion to the growth of the leafy plant, the base connecting to the disc extends towards both directions as draw an arch on the disc. Such extension finally draw a circle, so it is hard to distinguish in considerably grown plant that the erect shoot issued from the disc is leafy and not showing any tubular or saccate fronds. The present plants found in Tokyo Bay differ from the plants identified to *M. latissimum* in Ise Bay by their small size, not plicated margin and not having perforation in their fronds. But the former agrees well with the latter in the shape and size of cells and their arrangement, and the thickness of membrane.

The writer has not observed any floating plants in Tokyo Bay, and grown plants of this species living in the state of floating has been mentioned by COLLINS and by SETCHELL and GARDNER. So the writer refer the present plants to *M. latissimum* with some hesitation because of the detail of the developing form of *M. latissimum* by WITTROCK, COLLINS, and SETCHELL and GARDNER has not been clearly investigated yet. But the other characteristics of the present plants agree with those described in this species by several investigators.

4. *Monostroma grevillei* (Thuret) Wittrock

Fig. 2, D; Fig. 3, D; Fig. 5, III a–e; Pl. III, A, B; Pl. IV, D, E.

1866, pp. 57–63, Pl. 4, Fig. 14; Kjellman, 1883, pp. 298, 299; Hauck, 1885, p. 424; De Toni, 1889, p. 103; Rosenvinge, 1893. pp, 946–949, Fig. 50; Collins, 1901, p. 209; Setchell and Gardner, 1920, pp. 236, 237; Yamada, 1935, p. 9; Kylin, 1949, pp. 14, 15, Fig. 8; Iwamoto, 1960, pp. 8–11, Photos 5–7, Fig. 2.

Enteromorpha grevillei Thuret, 1854, p. 25.

Ulva lactuca Harvey, 1846–'51, Pl. 243; Kuetzing, 1956, Pl. 12.

Jap. name: *Usu-hitoegusa*.

Hab. Growing on shells and stones in upper sublittoral belt or in tide pool from the end of December to next March. Haneda and Kisarazu.

The present species occurs in later season than that in which other three species occur in Tokyo Bay, and it is found for the first time on the barnacles, the shells and the stones, which are always covered with sea water, at the end of December. They grow largely to next spring. At the beginning of the development to the leafy plants the discs are produced on the substratum, the discs shoot out the saccate plants. A few of them inhabiting in still water are grow to 4–5 cm. in the height just as the state of sac, but the others are splitted at their tips when they attain 2–3 cm. height. It is able to acknowledge as far as the plants which were observed at Kisarazu and at Haneda the saccata plants growing in still water may persist for sometime as mentioned by Collins. It is an important characteristic in the present species to persist in the state

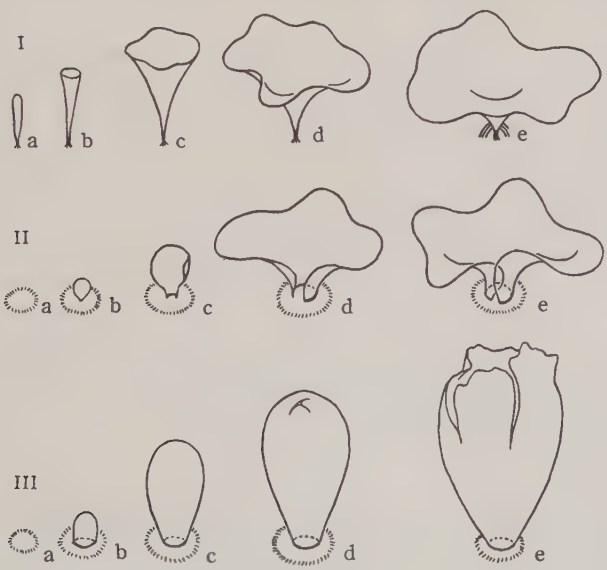

Fig. 5. Shematic figures showing three developing forms of *Monostroma* growing in Tokyo Bay.

I a–e. *M. tubiforme*.

II a–e. *M. latissimum*.

III a–e. *M. grevillei*.

of the saccate plant, however, another characteristics are present also, that is, the large linear cells, which contain 2 or 3 pyrenoids, constitute the basal parts of the fronds. These linear cells have not been found in the other *Monostroma* described in this paper, and have not been found in *M. zostericola* collected at Muroran, Hokkaido, which has a similar developing process and observed to compare the developing form to the leafy plant with those of the various species growing in Tokyo Bay.

References

BLIDING, C. 1935 Sexualität und Entwicklung bei einigen marinen *Chlorophyceen*. Svensk Bot. Tidskr., 29.

BORNET, E. et THURET, G. 1880 Notes Algologiques Recueil d'Observations sur les Algues. Fasc. II.

CARTER, N. 1926 An investigation into the cytology and biology of the *Ulvaceae*. Ann. of Bot., Vol. 40.

COLLINS, F. S. 1909 The green algae of North America. Trufts College Studies, Vol. 2, No. 3.

DE TONI, D. B. 1889 Sylloge Algarum. Vol. 1.

HARVEY, W. H. 1846–'51 Phycologia britannica.

HAUCK, F. 1885 Die Meeresalgen Deutschlands und Oesterreichs. Rabenhorst,s Kryptogamenflora, Vol. 2.

KJELLMAN, F. R. 1883 The Algae of the Arctic Sea. Kongl. Sv. Vet.-Akad. Handl., Vol. 20.

KUNIEDA, H. 1934 On the life-history of *Monostroma*. Proceed. Imp. Acad., Vol. 10.

KUETZING, F. T. 1843 Phycologia Generalis.

——— 1956 Tabulae Phycologicae, Vol. 6.

KYLIN, H. 1949 Die *Chlorophyceen* der schwedischen Westkuste. Lunds Univ. Arsskr. N. R. Avd., Vol. 45, No. 4.

MIYAKE, K. and KUNIEDA, H. 1931 On the conjugation of the gametes and the development of the zoospores in *Ulvaceae*. Journ. Coll. Agr., Imp. Univ., Vol. 11, No. 3.

MOEWUS, F. 1938 Die Sexualität und der Generationswechsel der *Ulvaceen* und Untersuchungen ueber die Parthenogenese der Gameten. Archiv f. Protistenk., Vol. 91, No. 357.

NAGURA, K. 1921 Kaiso chosa hokoku. Rep. Aichi Pref. Exp. Stat. Fish., Vol. 24, No. 1.

ROSENVINGE, L. K. 1893 Groenlands Havalger. Meddelelser om Groenland, Vol. 3.

REINKE, J. 1878 Ueber *Monostroma bullosum* THUR. und *Tetraspora lubrica* KUETZ. Jahrb. Wissensch. Botanik, Vol. 11.

SEGI, T. and GOTO, W. 1959 On *Monostroma* and its culture. Bull. Jap. Soc. Phycology, Vol. 4, No. 2.

SETCHELL, W. A. and GARDNER, N. L. 1920 The Mar. Alg. of the Pac. Coast of North America. II. *Chlorophyceae*. Univ. Calif. Publ., Bot., Vol. 8, No. 2.

THURET, G. 1854 Notes sur la synonymie des *Ulva lactuca* et *Ulva latissima*. Mem. Soc. Sc. Nat., Vol. 2.

TOKIDA, J. 1939 Ueberblick ueber die Forschungen von dem Lebenszyklus bei den *Ulvaceae*. Bot. and Zoology, Vol. 7, No. 7.

WITTROCK, V. B. 1866 Försök till en monographi öfver algslägtet *Monostroma*. Akad. Afhandling.

YAMADA, Y. 1935 Marine Alg. from Urup, the Middle Kuriles. Sci. Pap. of the Inst. Algolog. Res., Fac. Sci., Hokkaido Univ., Vol. 1, No. 1.

——— and KANDA, T. 1941 On the culture exp. of *Monostroma zostericola* and *Ent. nana var. minima*. Ibid., Vol. 2, No. 2.

——— and SAITO, E. 1938 On some culture exp. with swarmers of certain species belonging to the *Ulvaceae*. Ibid., Vol., 2, No. 1.

Plate I

Monostroma tubiforme spec. nov.

A. An Enteromorpha-like young frond. ×180.
B. A young frond splitted at the tip. ×180.
C. A trumpet-like frond. ×90.
D. Two dried specimens. ×2/3.
E. A surface view of the basal portion showing the cells issuing the rhizoids and ordinary vegetative cells. ×220.
F. A surface view of the upper portion. ×220.
G. A surface view of more magnified upper portion. ×720.
H. A surface view of the ripe cells and swarmers produced in the cells. ×720.

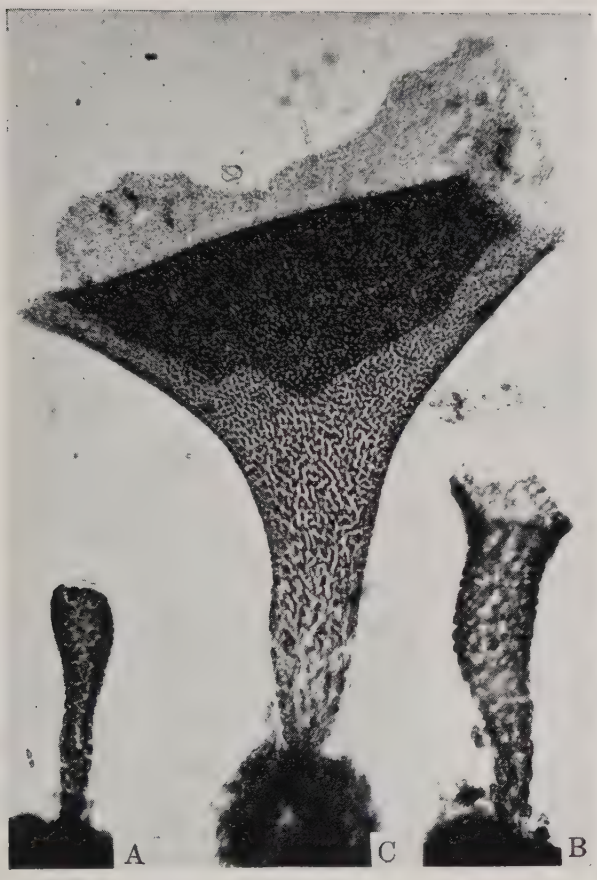
A
C
B

D

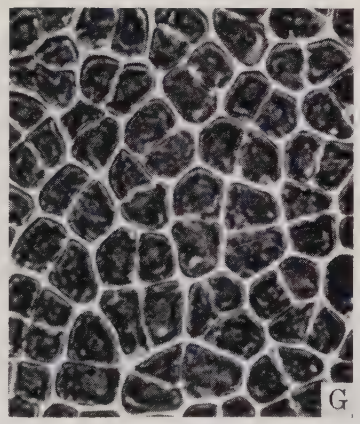
G

E

F

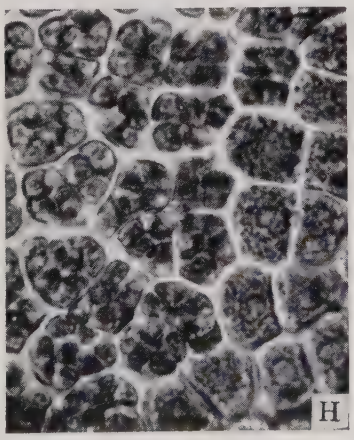
H

Plate II

Monostroma crassissimum spec. nov.

A. A dried specimen. ×3/5.
B. A surface view of the upper portion of the fairly grown frond, showing the irregular arrangement of cells. ×320.
C. A surface view of the marginal portion of the young frond. ×320.
D. A surface view of the basal cells issuing the rhizoids, and showing some ordinary vegetative cells. ×320.
E. A cross view of the basal portion, showing the basal cells issuming rhizoids and ordinary vegtative cells. ×320.
F. A cross view of the upper portion of the full grown frond, showing irregular arrangement of the cells. ×320.

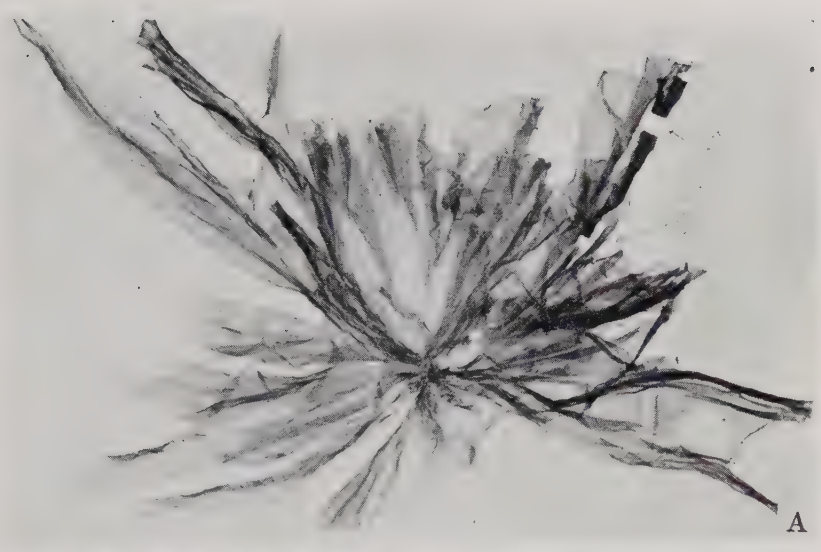
A

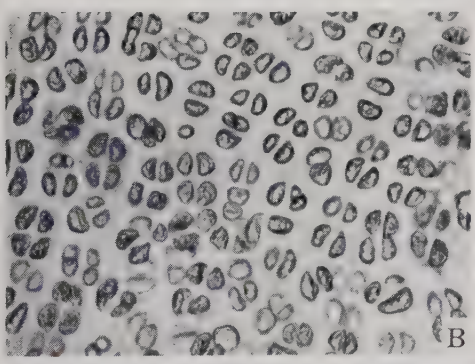
B

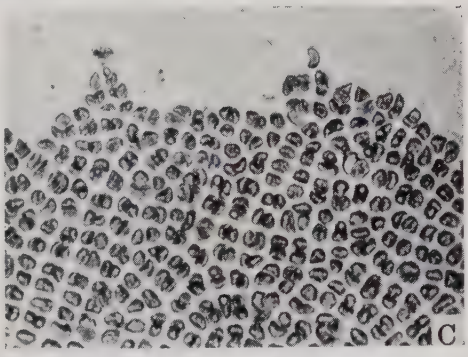
C

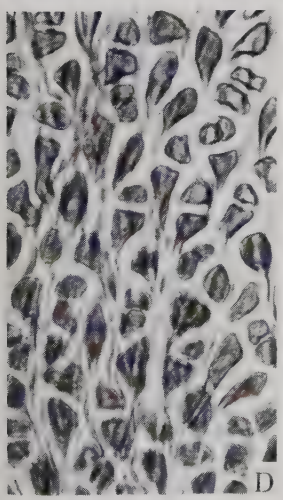
D

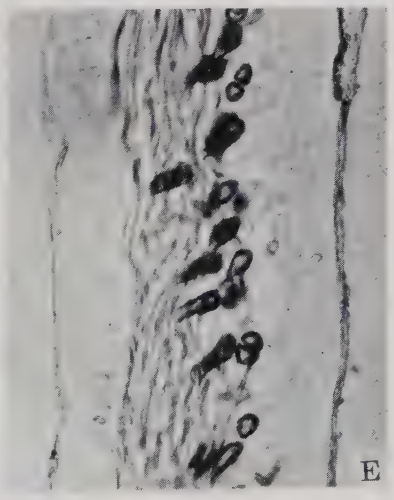
E

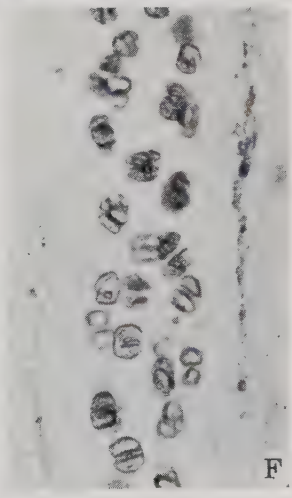
F

Plate III

A, B. *Monostroma grevillei* (THUR.) WITTROCK

A. A photograph showing various grades of the young saccate fronds. ×2/5.

B. A dried specimen. ×1/4.

C. *Monostroma latissimum* (KUETZ.) WITTROCK

C. Two dried specimens. ×1/2.

A

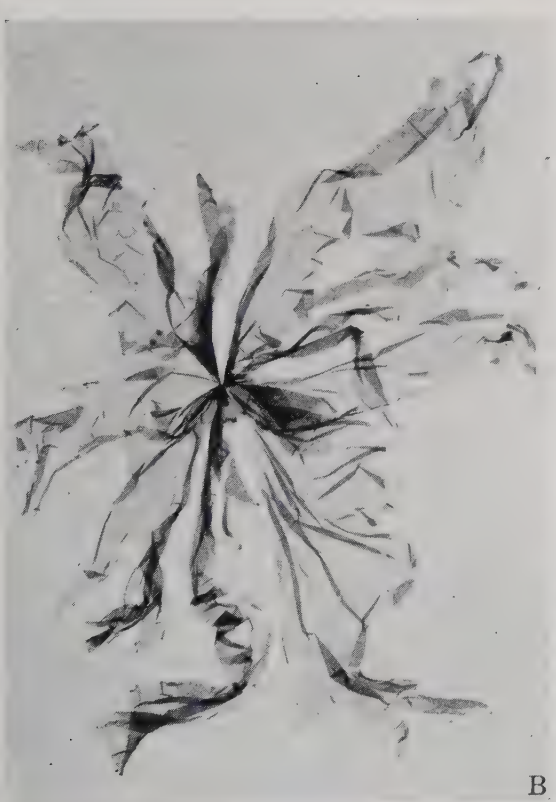

B

C

Plate IV

A-C. *Monostroma latissimum* (KUETZ.) WITTROCK

A. A sphaerical young frond composed of one layer of cells. ×180.

B. A surface view of the basal portion, showing the cells issuing rhizoid and ordinary vegetative cells. ×220.

C. A surface view of the marginal portion of the frond. ×320.

D, E. *Monostroma grevillei* (THUR.) WITTROCK

D. A surface view of the basal portion, showing most cells issuing rhizoids and containing two or three pyrenoids. ×220.

E. A surface view of the marginal portion. ×220.

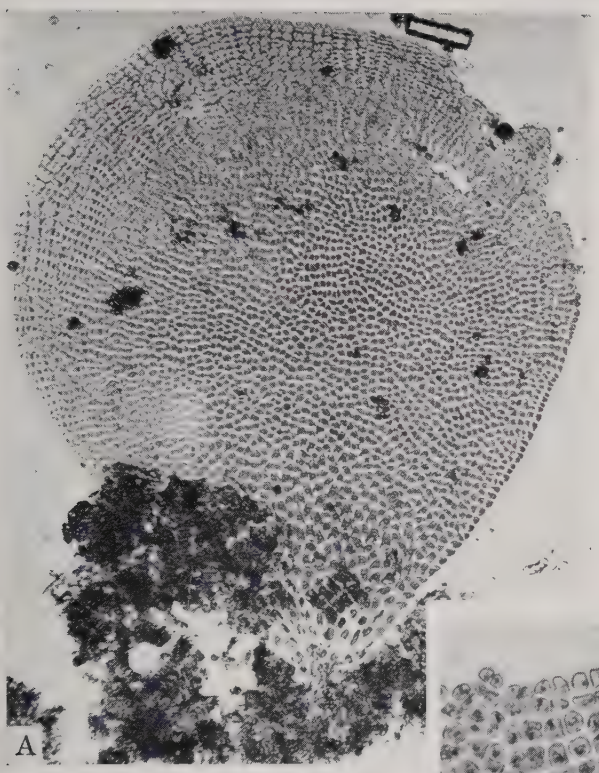
A

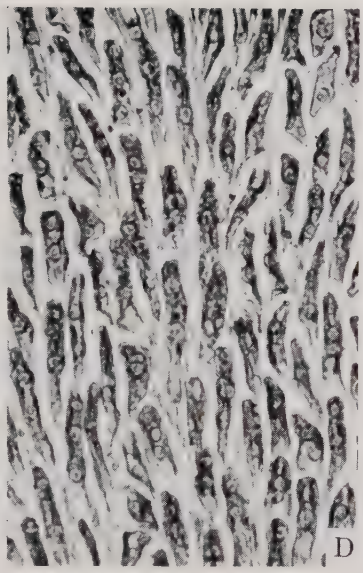
D

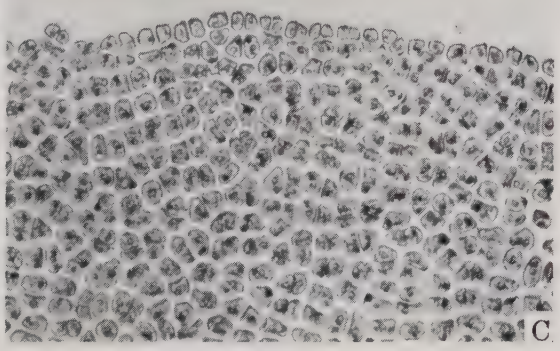
C

B

E

Journal of the Tokyo University of Fisheries Vol. 47, No. 1, 1960

ON THE NET AND ROPE DISUSED AFTER BOTTOM TRAWL FISHINGS

Katuji Honda

(Received June 27, 1960)

Introduction

When the design of the fishing gear is commenced, it is important matter to make clear the properties of materials disused after the fishings. Consequently, the present study has done.

Various conditions effected in bottom trawl net operation were investigated on fishing boats belonging to many fishing ports, while samples of net and rope disused after their usage in bottom trawl fisheries were collected from various fishing boats, and examined of this properties in order to formulate the foundamental knowledges about the design of the gear taking into account of the peculiarities in the disposition of the gear as well as the circumstances in which the gear is used.

I. Investigations on the measure of net and rope disused and the weakening factors of net and rope during the operation

On the net and rope used, (1) the measure of disuse and (2) the weakening factors during their usage were invesigated on the bottom trawl fisheries in Table 1 with fishing bases in Figure 1.

As the results obtained are expressed in Table 2, in the (1), the judgement from the degree of wear is first of all and next the increment of breaking accident during the operation, period or number of operations and use for another gear and in the (2), catch by sea bed or boat side is first of all and next bad condition of sea, bad boat operation, over-much fishing, wearing by boat side or drum and size of engine.

As they are considered in the view of every fishing base, on the (1) number or period of operations in Ishinomaki at Miyagi Pref., degree of wear in Funakawa at Akita Pref., Shibayama and Kasumi at Hyôgo Pref. and Koyasu at Kanagawa Pref., weakening in operation in Hiragata at Ibaragi Pref., degree of wear and weakening in operation in Otaru at Hokkaido, Chôshi at Chiba Pref. and Hinase at Okayama Pref. and number or period of operations or weakening in operation in Sakai at Tottori Pref. have weight respectively and on the (2) catch by sea bed or boat side in Otaru at Hokkaido, Funakawa at Akita Pref., Sibayama and Kasumi at Hyôgo Pref. Chôshi at Chiba Pref. Sekimae at Ehime Pref. and Hinase at Okayama Pref., bad condition of sea in Sakai at Tottori Pref., over-much fishing in Ishinomaki at Miyagi Pref. and bad boat operation in Hiragata at Ibaragi Pref. have been thought as serious factor. The differences mentioned above may be occured by the conditions of fishing grounds and the operations in various fishing bases.

Table 1. Investigating bases and outlines of their fisheries.

Symbol	Fishery base	Kind of fisheries	Number of boats investigated	Number of tonnage	Size of gear (length of head line) λ	Fishing season	Sediment
1	Otaru Hokkaido	One boat medium trawl	4	60～84₸	m	9～ 6	S.M
2	Funakawa Akita Pref.	Small trawl	17	19～22		9～ 6	S.M, M.S, M, Sh
3	Shibayama Hyôgo 〃	One boat medieum trawl	10	33～43	50～58	9～ 5	S.M
4	Kasumi 〃 〃	〃	8	30～47	50～58	9～ 6	S.M
5	Sakai Tottori 〃	〃	4	30～40	〃	9～ 5	
6	Ishinomaki Miyagi 〃	〃	1	74	70	9～ 6	
7	Hiragata Ibaragi 〃	〃	22	15～35		2～ 6	
8	Chôshi Chiba 〃	〃	8	25～40	50～55	9～ 6	M.S
9	Koyasu Kanagawa 〃	Small trawl	9	3～ 5		1～12	S.M
10	Sekimae Ehime 〃	〃	4	2～ 4		12～ 6	S.M, M, G
11	Hinase Okayama 〃	〃	3	3～ 4		1～12	M, S.M

Table 2. Various conditions and the ratios relative weight.

Fishery base		The points considered as worthless net and rope for use					The weakening factors in operation						
		Number or period of operations	Degree of wear	Weakening in operation	Use for another gear	The rest	Catch by boat side or sea bed	Bad condition of sea	Bad boat operation	Over-much fishing	By HP of engine	Wear by boat side or drum	The rest
Otaru	Hokkaido	.10	.34	.36	.10	0	.34	.18	.06	.03	.06	.31	02*
Funakawa	Akita Pref.	.24	.31	.22	.09	.14	.47	.12	.36	.03	.13	.18	0
Shibayama	Hyôgo 〃	.26	.50	.12	.11	.01	.37	.14	.05	.05	.09	.26	.04*
Kasumi	〃 〃	.20	.45	.30	.05	0	.41	.36	.04	.05	.04	.10	0
Sakai	Tottori 〃	.36	.22	.36	.05	0	.14	.64	.03	.13	0	.01	.05
Ishinomaki	Miyagi 〃	.50	.25	.25	0	0	.30	.20	0	.50	0	0	0
Hiragata	Ibaragi 〃	.15	.28	.40	.15	.02	.14	.17	.47	.02	.02	.18	0
Chôshi	Chiba 〃	.17	.39	.40	.02	.02	.51	.28	.02	.09	.03	.06	.01
Koyasu	Kanagawa 〃	.16	.44	.27	.09	.04	.31	.49	.05	.02	.03	0	.10*
Sekimae	Ehime 〃						.75	.15	.05	0	0	0	0
Hinase	Okayama 〃	0	.50	.50	0	0	.55	.10		0	0	.30	0
Average		.22	.37	.32	.07	.07	.39	.25	.11	.08	.03	.13	.01

* Insufficient preservation

Fig. 1. Various bases of investigating factors and collecting samples.

marks { 1, 2, ···, Tab 1.
① , ② , ···, Tab. 3
$\overline{1}$, $\overline{2}$, ···, Tab. 7
$\underline{1}$, $\underline{2}$, ···, Tab. 9

II. The properties of net already out of use

The bases of fisheries in which the samples of bottom trawl net were collected indicate in Figure 1 and details of samples, outline of their fisheries and the results measured from the samples are denoted in Tables 3 and 4.

Table 3. Samples of the net-fabrics.

1) Stretched mesh size, 2) Square knot, 3) Trawl knot

Symbol	Fishery base	Name of boat (tonnage)	Kind of fishery	Gear size (length of head line) λ	Net-fabric extracted	Preservatives and number of their times	Portion used	Number of total months
①	Wakkanai Hokkaido	A (85₸)	One boat medium trawl	78.0m	Cotton 20S/90 60[1)]mm S[2)]	Cutch	Cod end	3
	〃 〃	〃	〃	〃	〃 20S/24 60 S	〃	Belley	〃
	〃 〃	〃	〃	〃	〃 20S/75 43 S	〃	End of belley	〃
	〃 〃	〃	〃	〃	〃 20S/45 120 S	〃	Wing	〃
	〃 〃	B (86₸)	〃	73.0	〃 20S/36 60 S	〃 3	Belley	
	〃 〃	〃	〃	〃	〃 20S/45 120 S	〃 2	Wing	4
	〃 〃	〃	〃	〃	〃 20S/75 43 S	〃	Cod end	4
	〃 〃	〃	〃	〃	〃 20S/21 75 S	〃	Belley	6
②	Monbetsu 〃	C (60₸)	〃	68.0	〃 20S/21 75 S	〃 1	Bosom (lower)	
	〃 〃	〃	〃	〃	〃 20S/24 75 S	〃 3	Bosom (upper)	5
	〃 〃	〃	〃	〃	〃 20S/24 75 S	〃	End of belley	5
	〃 〃	〃	〃	〃	〃 20S/21 90 S	〃	Bosom	5
	〃 〃	〃	〃	〃	〃 20S/45 70 S	〃 1	Belley	
	〃 〃	〃	〃	〃	〃 20S/24 120 S	〃	Wing	
	〃 〃	〃	〃	〃	〃 20S/24 70 S	〃 3	Arm	
	〃 〃	〃	〃	〃	〃 20S/24 75 S	〃	Arm (upper)	5
	〃 〃	〃	〃	〃	〃 20S/90 75 S	〃 1	Front of cod end	5
③	Kushiro 〃	D (68₸)	〃	79.0	〃 20S/21 50 S	〃 2	Bosom	3
	〃 〃	〃	〃	〃	〃 20S/24 60 S	〃 1	Wing (float)	3
	〃 〃	〃	〃	〃	〃 20S/24 60 S	〃 2	Wing (foot)	3
	〃 〃	〃	〃	〃	〃 20S/75 60 S	〃 1	Front of Cod end	3
	〃 〃	〃	〃	〃	〃 20S/24 50 S	〃 2	Bosom	3
	〃 〃	〃	〃	〃	〃 20S/24 50 S	〃	Wing (front)	3
	〃 〃	〃	〃	〃	〃 20S/75 60 S	〃 1	Cod end	2
	〃 〃	〃	〃	〃	〃 20S/36 120 S	〃 2	Square	

(Table 3. Continued)

Symbol	Fishery base		Name of boat (tonnage)	Kind of fishery	Gear size (length of head line) λ	Net-fabric extracted	Preservatives and number of their times	Portion used	Number of total months
④	Otaru	Hokkaido	E (64㌧)	One boat med. trawl	56.0 m	Cotton 20*S*/15 43 *S*	Cutch 1	Wing	5.5
	〃	〃	〃	〃	〃	〃 20*S*/24 75 *S*	〃	Bosom	
	〃	〃	〃	〃	〃	〃 20*S*/36 28 *S*	〃	Cod end	5.5
	〃	〃	〃	〃	〃	〃 20*S*/24 60 *S*	〃	Wing	
	〃	〃	〃	〃	〃	〃 20*S*/36 120 *S*	〃	Square	
⑤	Shibayama	Hyôgo Pref.	F (37㌧)	〃	45.0	Kyokurin /18 50 *T*[3)]	〃	Belley	1
⑥	Kasumi	〃	G (43㌧)	〃	57.0	Cotton 20*S*/18 22 *T*	〃	Bag	5.5
	〃	〃	〃	〃	〃	〃 20*S*/21 50 *S*	Coal tar	Belley	3
	〃	〃	〃	〃	〃	〃 20*S*/36 38 *T*	Cutch	Cod end	1
	〃	〃	〃	〃	〃	〃 20*S*/60 75 *T*	〃	Cod end (lower)	4
	〃	〃	H	〃	57.0	Nylon 210*d*/6 22 *T*		Belley (upper)	
	〃	〃	〃	〃	〃	〃		Side	
	〃	〃	〃	〃	〃	〃		Belley (upper)	3
	〃	〃	I (40㌧)	〃	42.4	Nylon 210*d*/9 22 *T*		Side	3
	〃	〃	〃	〃	〃	〃		Tunnel	3
	〃	〃	〃	〃	〃	Nylon 210*d*/15 38 *T*		Flupper	
	〃	〃	〃	〃	〃	〃		Belley (upper)	3
	〃	〃	J (37㌧)	〃	62.0	Cotton 20*S*/18 43 *S*	Cutch	Belley (lower)	3
	〃	〃	〃	〃	〃	〃 20*S*/36 38 *S*	〃	Cod end	2
⑦	Sakai	Tottori Pref.	K (35㌧)	〃	54.0	〃 20*S*/9 23 *S*	〃	Wing	
	〃	〃	〃	〃	〃	〃 20*S*/60 60 *T*	〃	Cod end	1.5
⑧	Shimono-seki	Yamaguchi Pref.	L 〃	Two boat med. trawl	62.0	Cremona 20*S*/74 60 *	Coal tar	Belley	2
⑨	Tobata	Fukuoka Pref.	M 〃	〃	64.4	Manila twine 3.2g/m 60	〃	Front of square	2
	〃	〃	〃	〃	〃	〃 〃 75 *T*	〃	Belley	2
	〃	〃	〃	〃	〃	〃 〃 75 *T*	〃	Flupper	9
⑩	Ishino-maki	Miyagi Pref.	N (74㌧)	One boat med. trawl	70.0	Cotton 20*S*/36 38 *S*	Cutch	Wing	9
	〃	〃	〃	〃	〃	〃 〃 105 *S*	〃	Bag	6

(Table 3. Continued)

Symbol	Fishery base	Name of boat (tonnage)	Kind of fishery	Gear size (length of head line) λ	Net-fabric extracted	Preservatives and number of their times	Portion used	Number of total months
⑪	Katanohara Aichi Pref.	O (74㌧)	One boat med. trawl	53.0 m	Cotton 20S/12 S	Cutch 1		
	〃 〃	〃	〃	〃	〃 〃 S	〃	Flupper	
	〃 〃	〃	〃	〃	〃 〃 S	〃		
	〃 〃	〃	〃	〃	〃 〃 S	〃	Belley	
	〃 〃	〃	〃	〃	〃 〃 S	〃		

Table 4. Values measured on the samples of net-fabrics.

( ) coefficent of variation

Fishery base		Name of boat	λ	D	L	L/L_0	T_u	T_u/T_0	$\frac{T_0-T_u}{n}$	T_u/D
			m	m	m		kg		kg/month	$^{Kg/m}\times 10^3$
Hokkaido	Wakkanai	A	78.0	0.0026	0.049	0.82	49.0	0.75	5.4	18.8
〃	〃	〃	〃	0.0014	0.051	0.85	18.5	0.78	1.7	13.2
〃	〃	〃	〃	0.0026	0.043	0.99	32.0	0.53	9.5	12.3
〃	〃	〃	〃	0.0018	0.105	0.87	29.9	0.78	2.8	17.2
〃	〃	B	73.0	0.0016	0.058	0.93	11.7(18.9)	0.45		7.3
〃	〃	〃	〃	0.0018	0.114	0.90	26.9(11.8)	0.89	2.8	14.8
〃	〃	〃	〃	0.0025	0.038	0.82	41.1(15.7)	0.87	1.1	16.7
〃	〃	〃	〃	0.0012	0.067	0.89	15.3(12.4)	0.87	1.5	12.3
〃	Monbetsu	C	68.0	0.0012	0.071	0.09	5.8(35)	0.33		4.7
〃	〃	〃	〃	0.0013	0.072	0.92	13.1(19.1)	0.76	0.81	10.2
〃	〃	〃	〃	0.0012	0.089	0.95	10.4(8.4)	0.64	1.4	8.4
〃	〃	〃	〃	0.0013	0.088	0.92	7.3(35)	0.42	2.0	5.4
〃	〃	〃	〃	0.0012	0.071	0.98	7.1(15)	0.41		5.8
〃	〃	〃	〃	0.0018	0.116	0.92	25.2(9.6)	0.84		14.3
〃	〃	〃	〃	0.0012	0.069	0.97	11.0(27.9)	0.64	1.3	9.4
〃	〃	〃	〃	0.0014	0.084	0.91	6.6(10)	0.38	2.1	4.8
〃	〃	〃	〃	0.0026	0.068		41.5(9.8)	0.79		16.2
〃	Kushiro	D	79.0	0.0012	0.049	0.92	13.4(13.2)	0.78	1.3	11.0
〃	〃	〃	〃	0.0013	0.057	0.92	14.2(10.5)	0.82	0.99	11.3
〃	〃	〃	〃	0.0012	0.055	0.87	11.7(8.60)	0.68	1.8	9.7
〃	〃	〃	〃	0.0023	0.055	0.85	44.2(9.01)	0.94	1.5	18.3
〃	〃	〃	〃	0.0012	0.049	0.95	12.0(9.62)	0.70	1.7	9.5
〃	〃	〃	〃	0.0013	0.056	0.94	11.6(13.6)	0.67	1.9	9.2
〃	〃	〃	〃	0.0022	0.058	0.86	37.8(11.4)	0.86	4.5	15.8
〃	〃	〃	〃	0.0015	0.113	0.92	19.3(19.4)	0.74		12.5
〃	Otaru	E	56.0	0.0010	0.039	0.89	9.2(13.2)	0.68	0.48	8.9
〃	〃	〃	〃	0.0012	0.073	0.94	5.6(25)	0.33		4.6
〃	〃	〃	〃	0.0015	0.024	0.87	15.4(12.1)	0.59	1.2	9.6
〃	〃	〃	〃	0.0012	0.057	0.91	13.8(14.5)	0.80	0.66	11.4
〃	〃	〃	〃	0.0016	0.133		24.5(8.80)	0.94		15.4

Fishery base	Name of boat	λ	D	L	L/L_0	T_u	T_u/T_0	$\frac{T_0-T_u}{n}$	T_u/D
		m	m	m		kg		kg/month	$^{Kg/m}\times 10^3$
Hyôgo Pref. Shibayama	F	45.0	0.00090	0.049	0.97	13.8(7.62)	0.80	0.31	15.3
〃 Kasumi	G	57.8	0.0012	0.022	0.95	11.4(7.10)	0.71	0.85	9.5
〃 〃	〃	〃	0.0012	0.048	0.87	11.3(2.05)	0.70	1.6	9.4
〃 〃	〃	〃	0.0017	0.039	0.95	19.0(13.1)	0.68	8.8	11.2
〃 〃	〃	〃	0.0019	0.065	0.79	13.9	0.33	7.1	7.3
〃 〃	H	57.0	0.00059	0.020	0.89	6.3(5.1)	0.75		10.7
〃 〃	〃	〃	0.00069	0.021	0.93	8.4(6.4)	1.0		12.2
〃 〃	〃	〃	0.00086	0.046		8.3(7.0)	0.99	0.033	9.7
〃 〃	I	57.0	0.00062	0.022	0.93	6.3(12)	0.51	0.21	10.1
〃 〃	〃	〃	0.00069	0.021	0.92	4.4(10)	0.36	2.6	6.4
〃 〃	〃	〃	0.00056	0.021	0.89	5.7(9.3)	0.25		10.2
〃 〃	〃	〃	0.00065	0.020	0.88	6.8(14)	0.33	4.6	10.4
〃 〃	J	42.4	0.0014			9.0	0.62	1.8	6.4
〃 〃	〃	〃	0.0020			10.8	0.39	8.4	5.4
Tottori Pref. Sakai	K	52.1	0.00075	0.024	0.95	5.6(24)	0.65		7.5
〃 〃	〃	〃	0.0021	0.070	0.85	9.4(15)	0.23		4.5
Yamaguchi Pref. Shimonoseki	L	62.0	0.0028	0.056	0.85	43.8(12.2)	0.89	3.6	15.6
Fukuoka Pref. Tobata	M	64.4	0.0028			39.1(19.0)	0.87	4.9	13.9
〃 〃	〃	〃	0.0030			31.4(27.1)	0.69	7.0	10.1
〃 〃	〃	〃	0.0030			36.9(16.3)	0.82	4.1	12.3
Miyagi Pref. Ishinomaki	N	70.0	0.0015	0.108	0.94	24.2	0.85	0.49	16.0
〃 〃	〃	〃	0.0015	0.038	0.94	16.3	0.58	1.3	10.8
Aichi Pref. Katanohara	O	53.0	0.00089	0.018		3.5(18)	0.35	1.1	3.9
〃 〃	〃	〃	0.00098	0.027	0.027	4.5(18)	0.45		4.5
〃 〃	〃	〃	0.00095	0.030		7.5(10)	0.75		7.9
〃 〃	〃	〃	0.00098	0.029		4.2(32)	0.42		4.2
〃 〃	〃	〃	0.00093	0.026		7.2(7.4)	0.72		7.7

II·1 Varieties of mesh sizes

The mesh size varies in the course of operation. On the design of the gear, it is important matter to decide mesh size of the net suitably for object of catching. It is said that enough catch is not kept up or maintenance of the net form becomes difficult or continuation of fishery fall into a difficult on account of deciding mesh size unsuitably. Accordingly, at the start, with respect to decide the mesh size, it is necessary that we know both the varaieties of mesh sizes during the opperations and the properties of net which is using in future. This change of mesh size may be manifested with some differences by materials of netting threads, portion used, period of operation and fishing grounds.

The ratios of length of mesh sizes measured from the net disused (L) and before use (L_0*) are gathered in Table 5 and as seen in this Table, even cotton,

Table 5. Ratio between the mesh sizes observed before and after the use.

Kind of net	Ratio between before and after the use l/l_0
Cotton net	0.79～0.99
Nylon net	0.88～0.93
Vinylon net	0.85

Table 6. Relation between the sizes of the gears and values of decrement in knot strength.

(Unit kg/month)

		Cotton net			Manila hemp net	Nylon net	Cremona net
Net size λ	Small $\lambda<50m$	8.4 1.8					
	Medieum $50m<\lambda<70m$	0.85 1.6 8.8 7.1 1.1	0.49 1.3 0.48 1.2 0.66	0.81 1.4 2.0 1.3 2.1	4.9 7.0 4.1	0.033 2.1 2.6 4.6	3.6
	Large $70m<\lambda$	5.4 9.5 2.8 1.7	2.8 1.1 1.5 4.5	0.99 1.7 1.8 1.5 1.7 1.9			

* These values told by fishermen as the samples were collected.

nylon, and vinylon net are gradually shrinkaged in the course of operations. That ratio is large and there are exceedingly shrinkaged or almost unshrinkageed nets in the cotton net and too it is the least in nylon net.

II·2 The decrement of net-fabric strength

The degree of decrement in strength of net-fabric used for bottom trawl net during their usage may be varied by the gear size, portion used, period applied, fishing season, management of the gear and conditions of fishing grounds.

The knot strength was adopted, on this occasion, as the measure of net-fabric strength. To determine the knot strength each two of the four arms around a knot were gathered and stretched by a tensile tester.

Differences between initial (T_0) and after their usage (T_u) of knot strength are devided by the total number of months used (n) and then the values of average decrement per month are caluculated. As shown in Table 4, the values of decrement varies evidently by the portion used even with same sort of net. According to the relation between the gear size and the values of decrement in Table 6, that values are various to the net size and so have not fixed tendency. Generally, the decrement values seem low in synthetic net-fabrics.

II·3 Safety limit strength of utlity in net-fabric

Minimum strength allowable for net-fabric which is used for a part of bottom trawl net may be determined by long experience of fishermen under

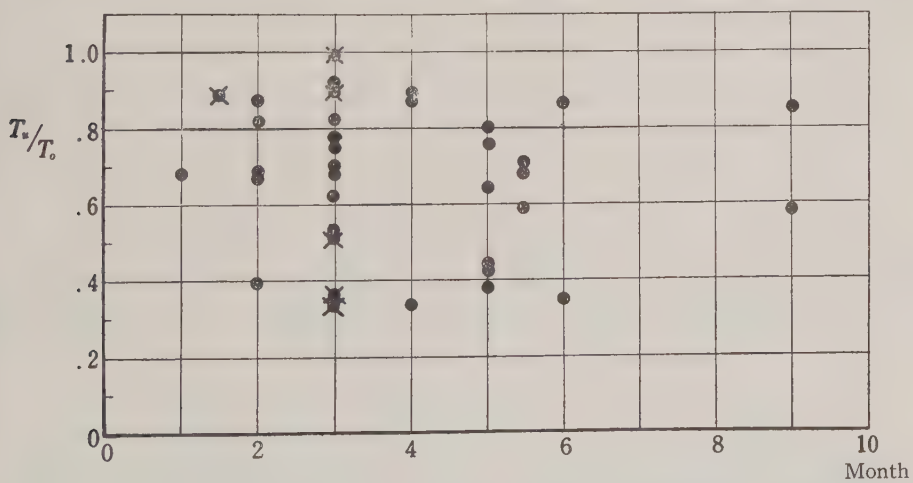

Fig. 2. Relation between T_u/T_0 and total number of months used (abscissa).
×.....Synthetic fiber net.

consideration with the gear size, state of operation, fishes aimed at catch and fishing ground condition respectively.

At first, in order to learn the minimum strength which is able to use for the initial strength, the relation between ratio of strength of disused net (T_u): initial one (T_0) and total number of months used is shown in Figure 2. As shown in this figure, the minimum ratio allowable is deduced by about 35 per cent and we may find a measure of minimum strength of net disused.

In the next place, there are various factors as seen in paragraph I as for becoming them unuseful but the strength remained in disused net is at least required larger than resistance working per unit length of head line in their usual operations.

Namely, in this occasion, size of bottom trawl net expresses the length of float line. If it is denoted by λ, the area of net used is proportioned to λ^2 and resistance λ^2 too. Accordingly, the force working per unit length of float line may be proportioned to λ. Subsequently, when the bottom twawl net is dragged with the velocity v, we get the following equation:

$$R = Kf(D/L)\lambda v^2$$

where the various letters have following meanings respectively: K, constant number; f, changeable coefficent by angle holded between current direction and net plane; D, diameter of netting thread; L, stretched mesh size; R, resistance.

If the net strength is treated as well as the case of fixed set net[1], the relation mentioned above is displayed by the following equation:

$$T_u \geqq K_1 D\lambda v^2$$

where K_1 is constant number. From this equation, measure of the minimum strength of T_u is grasped.

In the case of taking t hour for operating with the gear size λ, if the operation is carried with the same method in each fishing boat, we get the following equation:

$$v \backsim \lambda/t$$

and when the fishes resembled in behaviour are fishing, the operation may be done as t is proportioned to λ. If it is so, there is no relation between v and λ.

On this occasion, we have no data investigated directly with the matter above mentioned but there is no relation between v and λ so that T_u/D is to proportion to λ as considering v is almost the same. From the measurement of samples collected, T_u/D is expressed on each groups of the values and the relation between this group and λ is shown in Figure 3 and let the minimum values of T_u/D be joined in the same values of λ and then we get the next relation:

$$T_u/D \backsim \lambda^2$$

namely,

$$T_u = K_2 D\lambda^2 \quad \cdots\cdots\cdots\cdots\cdots\cdots\cdots\cdots (1)$$

where K_2 is constant number. If T_u denotes in kg. and D and λ in m., K_2 is about 2.80. Consequently, the tension working on netting threads during their operations can not becomes the measure of net strength disused.

Well, the weakening factors effected in the net are mainly catching by sea bed or boat side or bad condition of sea as seen in Paragraph I and then the increment of breaking caused by those matters and at the same time another

various factors may become the measure of net disused. Accordingly, above equation (1) is explained as the case of treating in fixed set net[2].

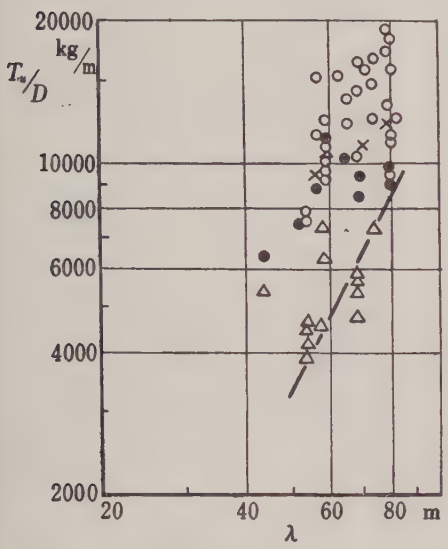

Fig. 3. Relation between T_u/D and λ. $T_u/T_0 \cdots$, ○>.70>●>.60>×>.50>△

III. The properties of rope already out of use

Warps, head lines and foot ropes were investigated as for rope disused in bottom trawl net.

The sources and values measured from samples of warps, head lines and foot ropes in bottom trawl net are shown in Tables 7, 8, and 9.

III·1 The decrement of rope strength

The decrement of rope strength during their usage may be varied by condition of fishing ground, fishing season and state of operation.

In order to examine the outline of decrement of rope strength, on this occasion, differences between initial strength (T_0) and after using (T_u) are devided by the total number of months used(n) and then this obtained values are manifested as for that of average decrement per month and pointed in Table 8. According to it, their values are high with the warps used in Hokkaido district in which the net is comparatively larger than another for period of usage being short. Namely, it is thought that their ropes are weakened sooner than other district.

III·2 Safety limit strength of utility in rope

1) Warp

Minimum strength allowable for ropes used as a part of the gear may have been decided by long experience of the fishermen under consideration with peculiarities in individual fishing ground. In order to examine minimum strength, the relation between ratio of rope strength disused (T_v): initial one (T_0) and total number of months applied is shown in Figure 4. From this Figure, the minimum ratio allowable is presumed by about 50% and then we can find a measure of minimum strength of rope.

Secondary, there are various factors so as to become the net unuseful but the strength kept in rope disused is at least needed larger than the total resistance of the whole net $K(D/L)\lambda^2 v^2$ in their usal dragging net.

Namely,

$$T_v \geqq K(D/L)\lambda^2 v^2 \quad \cdots\cdots\cdots\cdots\cdots\cdots (2)$$

Table 7. Samples of the warps.

Symbol	Fishery base	Fishing boat (tonnage)	Kind of fishery	Gear size (length of head line) λ	Rope extracted		Number of total months used
$\overline{1}$	Kushiro Hokkaido	A (68₸)	One boat medieum trawl	79.5 m	Manila hemp dia.	30 mm	3
$\overline{2}$	Monbetsu 〃	B (60₸)	〃	68.0	〃	28	2
$\overline{3}$	Wakkanai 〃	C (85₸)	〃	78.0	〃	34	3
	〃 〃	〃 (〃 ₸)	〃	〃	〃	30	3
	〃 〃	D	〃	〃	〃	32	3
$\overline{4}$	Kasumi Hyôgo Pref.	E (35₸)	〃	45.0	〃	26	5
	〃 〃	F (39₸)	〃	〃	〃	28	5
	〃 〃	G	〃	48.0	〃	24	6
$\overline{5}$	Sakai Tottori Pref.	H (35₸)	〃	53.0	〃		6
$\overline{6}$	Chôshi Chiba Pref.	I (40₸)	〃	52.0	〃	30	5
	〃 〃	J (35₸)	〃	〃	〃	24	9

Table 8. Values measured on the warps.

Fishery base	Name of boat	λ	L	D	D_1	T_v	Breaking elongation	T_v/T_0	$\frac{T_0-T_v}{n}$	$T_v/(D/L)$
		m	m	m	mm	ton	%		kg/month	kg/m/m $\times 10^4$
Kushiro Hokkaido	A	79.5	0.052	0.0012	31.2	2.56	0.68	0.68	380	11.1
Monbetsu 〃	B	68.0	0.076	0.0015	29.2	3.31	0.88	0.88	220	16.8
Wakkanai 〃	C	78.0	0.076	0.0016	34.0	3.58	0.75	0.75	348	16.9
〃 〃	〃	〃	〃	0.0016	31.4	3.29	0.85	0.85	160	15.6
〃 〃	D	〃	〃	0.0014	31.9	3.04	0.71	0.71	360	17.7
Kasumi Hyôgo Pref.	E	45.0	0.038	0.0012	23.9	1.94	0.72	0.72	201	6.1
〃 〃	F	〃	〃	〃	26.2	2.56	0.81	0.81	80	8.1
〃 〃	G	48.0	0.038	0.00085	24.0	1.36	0.54	0.54	194	6.2
Sakai Tottori Pref.	H	53.0	〃	〃	17.8	0.985	0.49	0.49	172	4.5
Chôshi Chiba Pref.	I	52.0	0.043	0.0012	27.4	1.50	0.39	0.39	310	5.4
〃 〃	J	〃	〃	〃	22.1	1.12	0.44	0.44	156	4.0

Table 9. Samples of the head lines and the foot ropes.

Symbol		Fishery base	Fishing boat (tonnage)	Kind of fishery	Gear size (length of head line) λ	Rope extracted		Number of total months used
Head line	1	Kushiro Hokkaido	A (68₸)	One boat medium trawl	79.5 m	Manila hemp dia.	18 mm	2
	2	Monbetsu 〃	B (60₸)	〃	68.0	〃	20	
	3	Kasumi Hyôgo Pref.	C (43₸)	〃	48.0	〃	12	20
		〃	D (40₸)	〃	〃	〃	12	〃
		〃	E (47₸)	〃	57.6	〃	16	8
Foot rope		Kushiro Hokkaido	A (68₸)	One boat medium trawl	79.5	〃	18	2
		Monbetsn 〃	B (60₸)	〃	68.0	〃	20	
	4	Wakkanai 〃	C (85₸)	〃	78.0	〃	18	
		Kasumi Hyôgo Pref.	D (37₸)	〃	57.6	〃	22	8
	5	Sakai Tottori Pref.	E (35₸)	〃	62.0	〃	16	6
	6	Chôshi Chiba Pref.	F (40₸)	〃	52.0	〃	24	2

Table 10. Values measured on the head lines and the foot ropes.

	Fishery base	Name of boat	λ	L	D	D_1	T_w	Breaking elongation	T_w/T_0	$T_w/(D/L)$
			m	m	m	mm	ton	%		kg/m/m $\times 10^4$
Head line	Kushiro Hokkaido	A	79.5	0.047	0.0012	18.2	2.03	26.5	0.80	7.9
	Monbetsu 〃	B	68.0	0.074	0.0013	19.5	2.38	12.7	0.92	13.2
	Kasumi Hyôgo Pref.	C	48.0	0.038	0.00085	12.4	0.744 (15.1)	27.6	0.77	3.5
	〃 〃	D	〃	0.038	0.00085	12.4	0.672 (11.9)	27.6	0.70	3.0
	〃 〃	E	57.6	0.038	0.00090	16.5	0.808 (6.64)	27.8	0.62	3.4
							T_x		T_x/T_0	$T_x/(D/L)$
Foot rope	Kushiro Hokkaido	A	79.5	0.047	0.0012	14.8	1.09	17.1	0.61	6.6
	Monbetsu 〃	B	68.0	0.074	0.0013	12.9	0.247	17.3	0.34	1.4
	Wakkanai 〃	C	78.0	0.076	0.0016	17.5	1.88	20.5	0.91	8.9
	Kasumi Hyôgo Pref.	D	57.6	0.038	0.00090	20.2	0.653 (16.9)	21.0	0.27	2.8
	Sakai Tottori Pref.	E	62.0	0.038	0.00085	15.9	1.12 (16.4)	29.4	0.67	5.1
	Chôshi Chiba Pref.	F	52.0	0.043	0.0012	21.7	1.31 (8.35)	24.2	0.51	4.7

where various letters mean ; K, constant number ; D, diameter of netting thread ; L, stretched mesh size; λ, gear size and in this occasion length of float line;

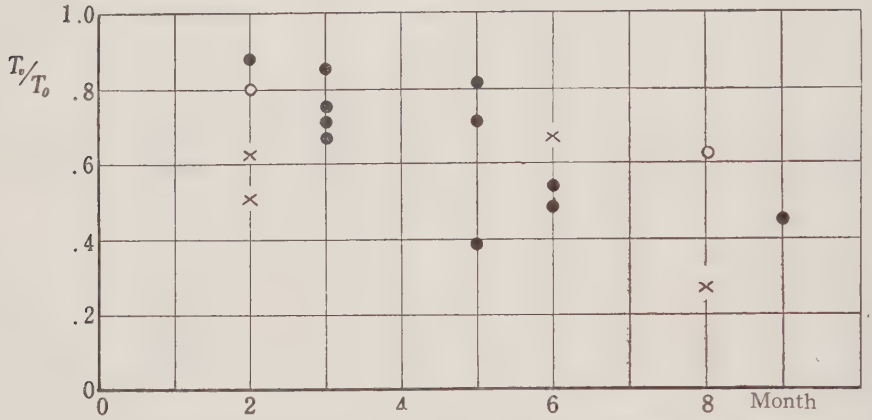

Fig. 4. Relation between T_v/T_0 and total number of months used (abscissa). ●, warp; ○, head line; ×, foot rope

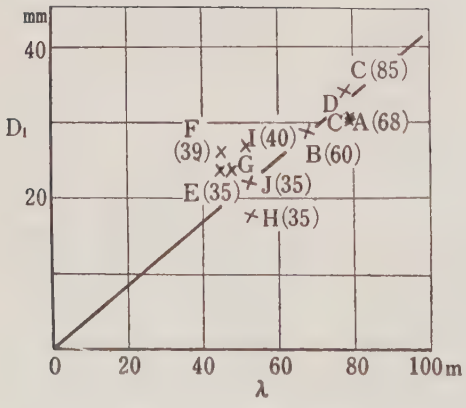

Fig. 5. Relation between diameter of rope D_1 and λ. ( ), tonnage of boat; $A, B, C, \cdots$, name of boat.

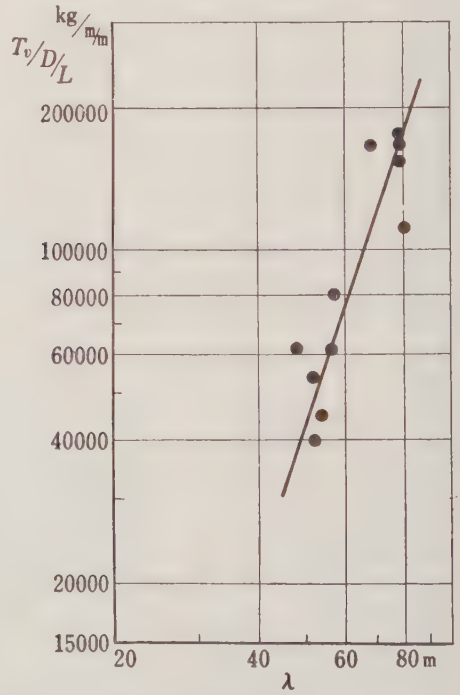

Fig. 6. Relation between $T_v/(D/L)$ and λ.

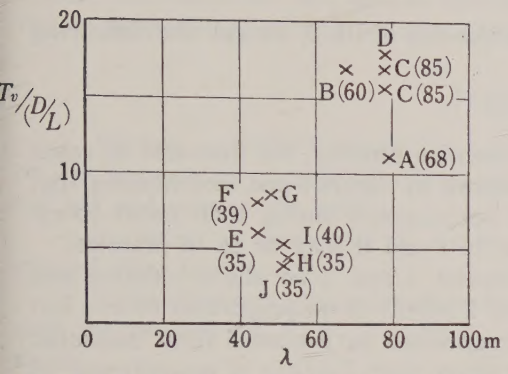

Fig. 7. Relation between $T_v/(D/L)$ and λ. ( ), tonnage of boat; $A, B, C, \cdots$, name of boat.

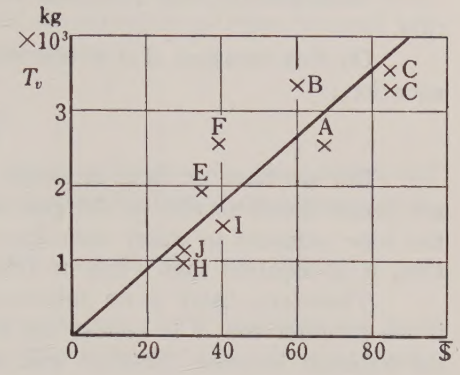

Fig. 8. Relation between T_v and tonnage of boat (abscissa). $A, B, C, \cdots$, name of boat.

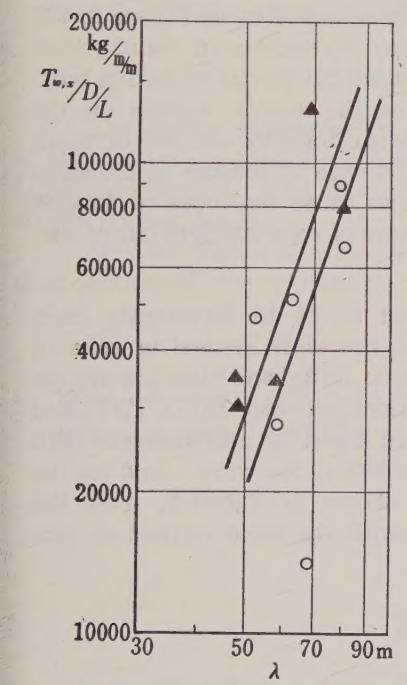

Fig. 9. Relation between $T_w/(D/L)$, $T_x/(D/L)$ and λ. ○, head line; ▲ foot rope.

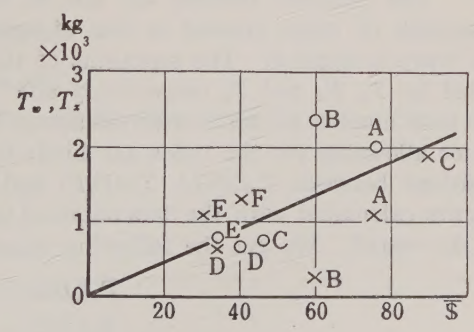

Fig. 10. Relation between T_w, T_x and tonnage of boat (absissa). ○ head line; ×, foot rope; $A, B, C, \cdots$, name of boat.

v, velocity of dragging net.

Subsequently, the minimum strength of T_v is concluded from above equation.

On this occasion, if it is treated by the idea of III. 2, we get the following equation:

$$v \backsim \lambda/t$$

But we have no data collected to examine directly, the diameter of ropes are proportioned to size of the gear as shown in Figure 5 and then in order that the rope balances to water resistance of net accepted during their usual operation, it is required that v has no relation to λ and it may be so in practice.

Therefore, there is no relation between v and λ as above mention and if we consider that v is almost the same, $T_v/(D/L)$ is to proportion to λ^2. But the relation between $T_v/(D/L)$ and λ is expressed in Figure 6 from measured values with data collected and it seems likely that $T_v/(D/L)$ is proportioned to λ^3 and the measure of strength disused is not satisfied even if considering the tention worked on the gear during the operation. On the relation between $T_v/(D/L)$ and λ in Figure 7, the values of $T_v/(D/L)$ are separated to the same values of λ and it is formed that the fishing boat is the larger, its the greater. Accordingly, owing to another treatment, the relation between the strength of rope disused and number of tonnages of fishing boat indicates in Figure 8, the strength kept in rope disused is likely proportioned to number of tonnages of fishing boat. If it is so, the judgement of rope disused due to size of fishing boat. The above fact is explained as the followings; as the tension workes on the warps is inertia of boat stored both when the net is caught by sea bed or there is waves on the sea surface, the force which proportioned to number of tonnages of boat grows repeatedly and then above conditions cause the ropes to fatigue gradually and too this is considered for the measure of rope strength out of use.

2) Head line and foot rope

The samples treated are not so many but so as to investigate their strengths of ropes disused to that of initial ones, the same method in case of the warp is applied. The strengths of the ropes on initial and after use are denoted by T_0, T_w and T_x respectively and the relations between T_w/T_0, T_x/T_0 and the total number of month used are shown in Figure 4 and the minimum strength ratios allowable for the ropes are likely by about 50% in the warp. And too the relations between $T_w/(D/L)$, $T_x/(D/L)$ and λ are shown in Figure 9, from the results calculated with the data obtained treating with the same method in case of the warp*. We get the following equations:

$$T_w/(D/L) = K_1\lambda^3$$
$$T_x/(D/L) = K_2\lambda^3$$

---

* As head line and foot rope accept $1/m$ or $1/n$ of the water resistance of whole net respectively in usual operation, they are expressed as the following equations:

$$T_w \geqq (K/m)(D/L)\lambda^2 v^2 \geqq K_1(D/L)\lambda^2 v^2$$
$$T_x \geqq (K'/n)(D/L)\lambda^2 v^2 \geqq K_2(D/L)\lambda^2 v^2$$

where K_1 and K_2 are constant numbers.

Moreover, the relations between T_w, T_x and number of tonnages of boats display in Figure 10. As seen in this figure, the strengths of ropes disused are nearly proportioned to number of tonnages of boats.

Summery

Various conditions effected in bottom trawl net operation were distincted on the measure of already out of use and the weakening factors during operation for net and rope of the gear.

Varieties of mesh size of cotton, nylon and vinylon net disused were cleared after their usage.

If the minimum strengths allowable for net-fabric, warp, head line and foot rope are denoted by T_u, T_v, T_w and T_x respectively, we get the following equations:

$$T_u = K_u D\lambda^2$$
$$T_v = K_v(D/L)\lambda^3$$
$$T_w = K_w(D/L)\lambda^3$$
$$T_x = K_x(D/L)\lambda^3$$

where K_u, K_v, K_w and K_x are constant numbers.

Acknowledgements

The author expresses his sincere gratitude to emeritus Prof. Dr. M. Tauti of the Tokyo University of Fisheries and Prof. Dr. T. Kawakami of the Kyoto University for their invaluable advices and encouragement throughout the course of the present study.

He also wishes to express his heartily thanks to member of the fishing gear section of this University for their kind help in these experiments.

References

1) HONDA, K. 1958.: Bull. J. Soc. Sci. Fish. **24** (4)

2) HONDA, K. 1960.: Jour. Tokyo Univ. Fish. Special edition **3** (2)